
This manuscript, entitled ***Geochronology and formal stratigraphy of the Sturtian Glaciation in the Adelaide Superbasin***, is a preprint that has not undergone peer-review. It is subject to revision by co-authors and the peer review process. If accepted the final version of this manuscript will be available via the “published version” link at the top of this webpage. Please feel free to contact the main author; we welcome feedback and queries.

Jarred C. Lloyd^{1,2}; Wolfgang V. Preiss^{1,3}; Alan S. Collins¹; Georgina M. Virgo^{2,1}; Morgan L. Blades¹; Sarah E. Gilbert⁴; Darwinaji Subarkah¹, Carmen B.E. Krapf³; Kathryn J. Amos²

- 1 1. Department of Earth Sciences, University of Adelaide, Adelaide, SA 5005, Australia
- 2 2. Australian School of Petroleum and Energy Resources, University of Adelaide, Adelaide, SA 5005,
3 Australia
- 4 3. Department for Energy and Mining, Geological Survey of South Australia, Adelaide, SA 5000,
5 Australia
- 6 4. Adelaide Microscopy, University of Adelaide, Adelaide, SA 5005, Australia

Corresponding author email: jarred.lloyd@adelaide.edu.au

7 Geochronology and formal stratigraphy of the Sturtian 8 Glaciation in the Adelaide Superbasin

9 Jarred C. Lloyd^{1,2}; Wolfgang V. Preiss^{1,3}; Alan S. Collins¹; Georgina M. Virgo^{2,1}; Morgan L.
10 Blades¹; Sarah E. Gilbert⁴; Darwinaji Subarkah¹, Carmen B.E. Krapf³; Kathryn J. Amos²

- 11 1. Department of Earth Sciences, University of Adelaide, Adelaide, SA 5005, Australia
- 12 2. Australian School of Petroleum and Energy Resources, University of Adelaide, Adelaide, SA 5005,
13 Australia
- 14 3. Department for Energy and Mining, Geological Survey of South Australia, Adelaide, SA 5000,
15 Australia
- 16 4. Adelaide Microscopy, University of Adelaide, Adelaide, SA 5005, Australia

17 Abstract

18 The glaciogenic nature of the Yudnamutana Subgroup was first identified over a century ago,
19 and its global significance was recognised shortly after, eventually culminating with the global
20 Sturtian Glaciation and Snowball Earth theory. Much debate on the origin and timing of these
21 rocks, locally and globally, has ensued in the years since. A significant corpus of research on
22 the lithology, sedimentology, geochronology, and formal lithostratigraphy of these sequences
23 globally has attempted to resolve many of these debates. In the type area for the Sturtian
24 Glaciation, South Australia's Adelaide Superbasin, lithostratigraphy and sedimentology have
25 been well understood; however, formal stratigraphic nomenclature has remained complicated
26 and contested. Geochronology has also been extremely sparse in this area. The result of these
27 longstanding issues has been disagreement as to whether the sedimentary rocks of the
28 Yudnamutana Subgroup are truly correlative throughout South Australia, and if they were
29 deposited in the same time window recently defined for Sturtian glacial rocks globally, c. 717
30 Ma to c. 660 Ma. In this study we present a large detrital zircon study, summarise and compile
31 existing global geochronology for the Sturtian Glaciation, and provide an updated formal
32 lithostratigraphy. We show equivalence of the rocks that comprise the revised Sturt Formation
33 of the Yudnamutana Subgroup, and that it was deposited within the time span globally defined
34 for Sturtian Glaciation.

35 1 Introduction

36 The Neoproterozoic is one of the most pivotal times in Earth's history for earth system changes
37 that led to the Phanerozoic world of extensive macroscopic mineralised life, significantly
38 oxygenated atmosphere and hydrosphere, and a buffered climate devoid of whole-planet
39 glaciations (Halverson et al. 2009; Och & Shields-Zhou 2012; Shields et al. 2022; Tostevin &
40 Mills 2020; Wallace et al. 2017). Within the Neoproterozoic, the Cryogenian Period (derived
41 from the Greek: κρύος, meaning cold), is named for the globally distributed, and long-lasting
42 continental glaciations (Plumb 1991; Plumb & James 1986) characteristic of this time. The
43 record of these glaciations is known on every continent except Antarctica (Arnaud et al. 2011),
44 with notably well studied sections in Australia (Le Heron 2012; Preiss et al. 2011; Virgo et al.

45 2021), Canada (Hoffman & Halverson 2011; Macdonald et al. 2010; Macdonald et al. 2018),
46 China (Rooney et al. 2020; Wu et al. 2019; Xiao et al. 2020; Xu et al. 2009; Zhang, Q-R et al.
47 2011; Zhu & Wang 2011), Ethiopia (Park et al. 2019), Namibia (Hoffman et al. 2021; Hoffman
48 et al. 2017b; Nascimento et al. 2017), Scotland (Ali et al. 2018; Fairchild et al. 2018), Siberia
49 (Romanov et al. 2021), Svalbard (Halverson et al. 2017; Halverson et al. 2018), and the USA
50 (Le Heron et al. 2018; Lechte et al. 2018; Link & Christie-Blick 2011; Lund et al. 2011; Mrofka
51 & Kennedy 2011; Petterson et al. 2011). While the concept of a Snowball Earth, and even the
52 glaciogenic nature of these some of these formations remains contentious for some
53 researchers (e.g., Allen & Etienne 2008; Eyles & Januszczak 2004; Le Heron et al. 2020;
54 Williams & Gostin 2019), most authors accept that two major glacial episodes are indicated;
55 an older Sturtian Glaciation, and a younger Marinoan (Elatina) Glaciation (or
56 "cryochron" Hoffman et al. 2017a). These two major glacial events of the Cryogenian have
57 been invoked to be key drivers of nutrient supply into oceans during the interglacial and post-
58 glacial periods, which has been hypothesised as a cause of the subsequent rise of algae and
59 other eukaryotic life, leading to the emergence of animals (Brocks 2018; Brocks et al. 2017;
60 Lechte et al. 2019).

61 Absolute geochronological constraints have become well established in several of these
62 regions (Rooney et al. 2015) and is ever improving across the globe (e.g. MacLennan et al.
63 2018; Nascimento et al. 2017; Park et al. 2019; Rud`ko et al. 2020; Środoń et al. 2022). One
64 notable exception is that of the sequences of Australia where some the thickest and best-
65 preserved Cryogenian glaciogenic formations are found. Until recently (Cox et al. 2018b;
66 Keeman et al. 2020; Lloyd et al. 2020; Rose et al. 2013) radiometric dates of any form for the
67 Cryogenian glaciogenic and interglacial sequences of the Adelaide Superbasin, South
68 Australia, were extremely sparse (Fanning & Link 2006; Ireland et al. 1998; Kendall et al.
69 2006). This is in part due to the dearth of known volcanogenic horizons within the South
70 Australian Cryogenian sequences, the challenges of dating Precambrian sedimentary rocks
71 (Halverson et al. 2018; Shields et al. 2022), and the general lack of geochronological research
72 conducted on the basin since the marked advancement in laser ablation and chemical
73 abrasion geochronological techniques during the mid-2000s (Gehrels et al. 2008; Mattinson
74 2005; Mundil et al. 2004). In this study we address this by presenting a new in-situ Rb–Sr
75 shale age and 1034 new detrital zircon analyses from fifteen samples [Figure 1] of the
76 Yudnamutana Subgroup (Sturtian Glaciation), 59 analyses from the Yancowinna Subgroup of
77 New South Wales (that is interpreted as an equivalent unit), and an additional 56 analyses
78 from the interglacial Serle Conglomerate. The purpose of this paper is not to debate the
79 environmental aspects of this time, but to provide the base of a geochronological framework
80 for the Sturtian glaciogenic rocks of the Adelaide Superbasin, i.e., the true Sturtian.

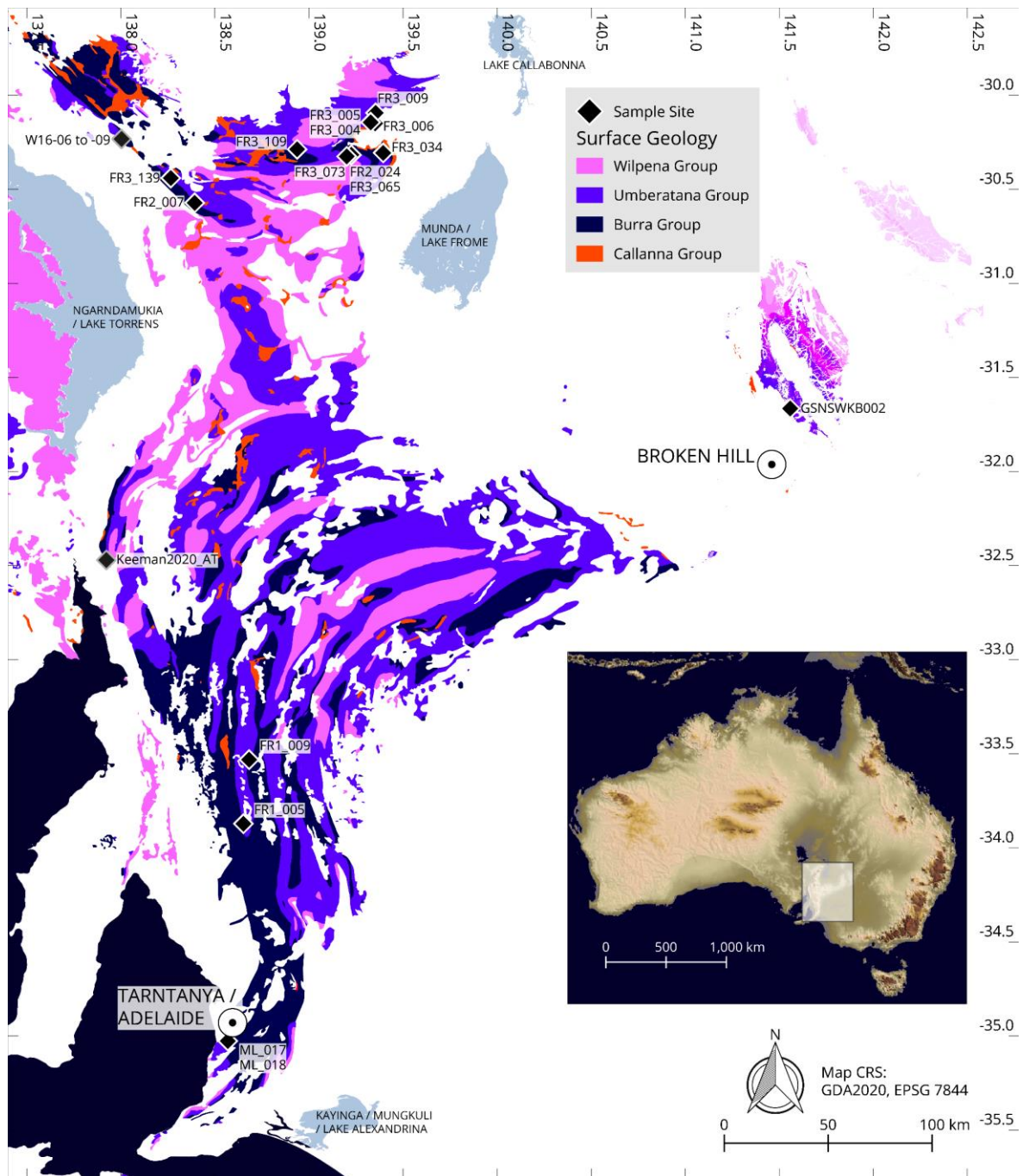


Figure 1 – Sample locality map, showing distribution of Neoproterozoic stratigraphy within the Adelaide Rift Complex of the Adelaide Superbasin. GPS coordinates for samples are provided with the U-Pb data (see data availability).

81 2 Geological Background

82 2.1 Adelaide Superbasin

83 The Adelaide Superbasin (Lloyd et al. 2020) consists of several named basins and sub-basins
 84 that form a large, Neoproterozoic to middle Cambrian sedimentary system at the southeast
 85 margin of Proterozoic Australia. Formation of the Adelaide Superbasin initiated at c. 890–830
 86 Ma as a result of the breakup of the Rodinia supercontinent (Lloyd et al. 2022a; Powell et al.
 87 1994; Preiss 2000). The Adelaide Rift Complex is the largest and oldest of the basins within
 88 the Adelaide Superbasin and includes a number of extensional depocentres, among them the

89 Yudnamutana Trough (northern Flinders Ranges), Baratta Trough (Olary and eastern Flinders
90 Ranges) and Yancowinna Trough of western New South Wales. The rift complex is contiguous
91 with the relatively undeformed rocks of the Torrens Hinge Zone, Stuart Shelf (Sprigg 1952),
92 and Coombalarnie Platform (Callen 1990). Two Cambrian basins, the Arrowie Basin, and the
93 Stansbury Basin, are also considered as part of the Adelaide Superbasin (Lloyd et al. 2020;
94 Preiss et al. 2002). Deposition within the Adelaide Superbasin spans over 300 million years of
95 Earth's history and stretches from the northernmost regions of South Australia to Kangaroo
96 Island in the south, and east into western Victoria and New South Wales. The basin began as
97 an intracontinental rift system that successfully progressed to a passive margin basin in its
98 southeast region, yet remained a failed rift in the north (Lloyd et al. 2022a; 2022b [preprint];
99 Preiss 2000). Deposition within the basin ceased during the Delamerian orogeny c. 514–490
100 Ma (Drexel & Preiss 1995; Foden et al. 2006; Foden et al. 2020; Preiss 2000). Present day
101 exposure of the sedimentary basin is largely restricted to the Flinders and Mount Lofty Ranges
102 of South Australia, and the Barrier Ranges of South Australia and New South Wales. The
103 stratigraphy of the Adelaide Superbasin is divided into three supergroups (Preiss 2000), two
104 for the Neoproterozoic sequences and the third for the Cambrian sequences, with numerous
105 group and subgroup level divisions. The Warrina Supergroup comprises the Callanna, Burra,
106 and Poolamacca Groups, and the Heysen Supergroup contains the Umberatana, Wilpena,
107 Torrowangee, and Farnell Groups. Each of these groups are further divided into numerous
108 subgroups. Here we focus on the Yudnamutana Subgroup [Figure 2, Figure 3], which
109 represents deposits of the Sturtian Glaciation, and present an additional sample from the
110 overlying Nepouie Subgroup; both are constituents of the Umberatana Group. One further
111 sample is presented from the thought to be equivalent Yancowinna Subgroup (NSW). The
112 reader is referred to Preiss (1987), Preiss (2000), Counts (2017), Cowley (2020), Lloyd et al.
113 (2020), and references therein for further detail on the geological history of the Adelaide
114 Superbasin.

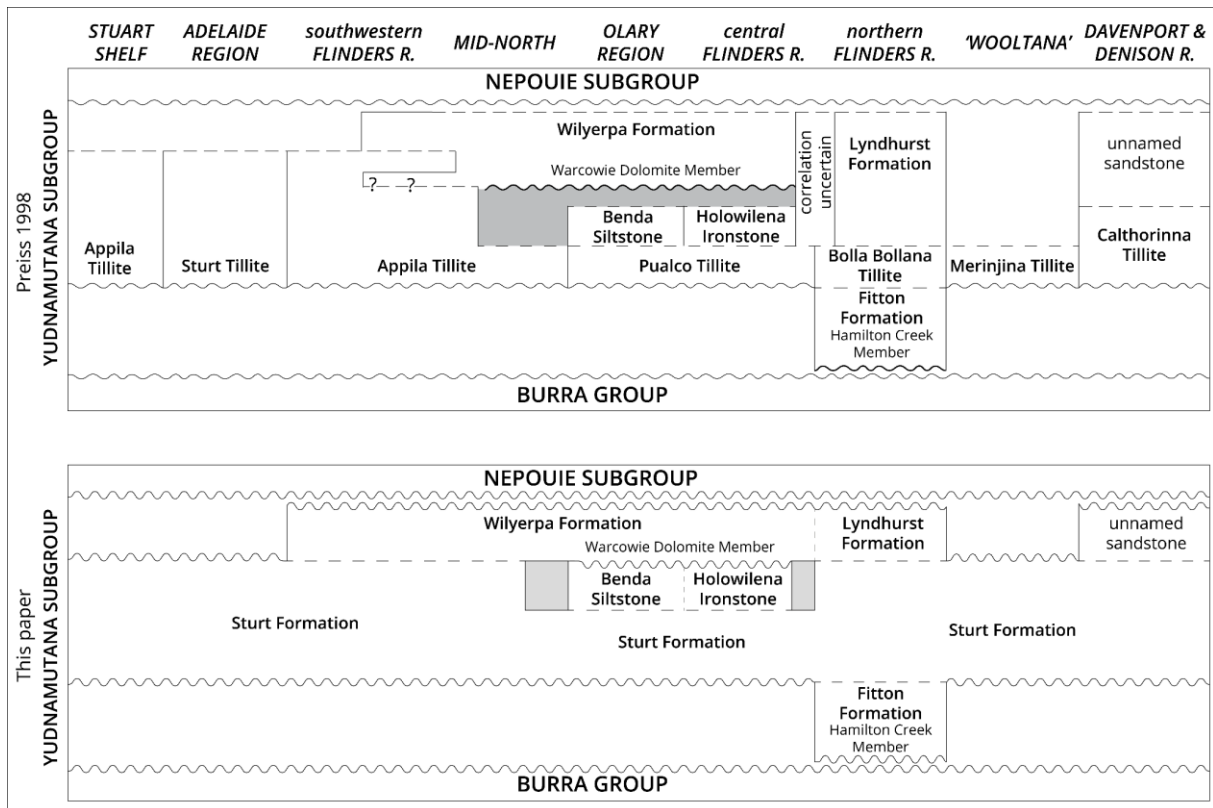


Figure 2 – Stratigraphic table showing past (Preiss et al. 1998) and current correlations (this study) of the Yudnamutana Subgroup.

115 2.1.1 Yudnamutana Subgroup

116 The Yudnamutana Subgroup (Coats & Preiss 1987; Preiss et al. 1998; Thomson et al. 1964) is
 117 the lowermost subdivision of the Umberatana Group and comprises sedimentary rocks that
 118 represent the Sturtian glacial event in South Australia. The glaciogenic nature of these rocks
 119 was first recognised by Howchin (1901), and these were traced during the early 20th century
 120 throughout the Mount Lofty, Flinders, and Olary Ranges (Preiss et al. 2011). A significant
 121 corpus of research has been published of over the past century (e.g., Coats & Forbes 1977;
 122 Conor & Preiss 2019; Cox et al. 2013; Cox et al. 2018b; David 1906; Fanning & Link 2008;
 123 Forbes & Cooper 1976; Howchin 1901; 1904; 1906; 1908; 1920; Le Heron et al. 2014; Le
 124 Heron et al. 2011; Link & Gostin 1981; Mawson & Sprigg 1950; Preiss 1987; 2000; Preiss et al.
 125 1998; Preiss et al. 2011; Preiss et al. 1978; Segnit 1939; Sprigg 1952; Thomson et al. 1964;
 126 Virgo et al. 2021) on the nature of these formations, with the “tillites” quickly rising to
 127 international fame (Cooper, BJ 2010; David 1906; Howchin 1908; and references therein). The
 128 most characteristic lithofacies of the Yudnamutana Subgroup is diamictite, with clasts ranging
 129 in size up to boulders and even megaclasts. The matrix varies from mudstone, through to silty
 130 sandstone, and carbonate is abundant in some places. Siltstone with lonestones and
 131 dropstones are commonly associated with the diamictites, as are sandstones of varying
 132 compositions and grain sizes. Non-diamictite conglomerates are a minor, but locally important
 133 lithofacies of the Yudnamutana Subgroup (Preiss et al. 2011). Sedimentary ironstones are
 134 present but restricted to the Baratta Trough (Preiss 1987; Preiss et al. 2011) in the eastern
 135 portion of the Adelaide Superbasin.

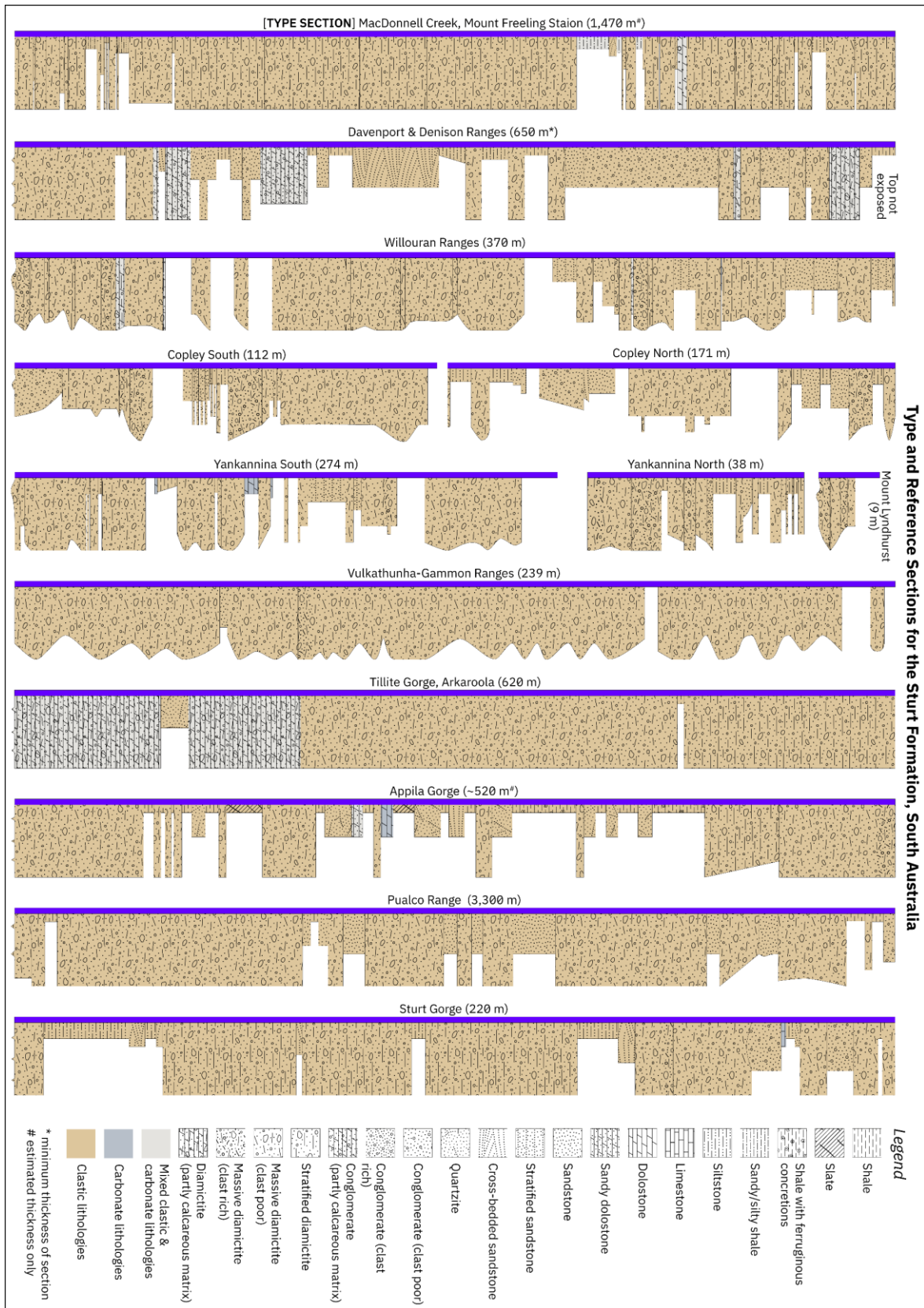


Figure 3 – Generalised stratigraphic logs of the Sturt Formation at its type section, and additional reference sections. For coordinates of locations see the accompanying stratigraphic unit definition (Appendix 1). Copley, Yankannina, Willouran Ranges, and Vulkathuhna-Gammon Ranges sections are from logging done by authors in this study. Type section is based on data from Belperio (1973) and Young and Gostin (1989b). Other sections are compiled from Segnit (1939), Forbes and Cooper (1976), Coats and Preiss (1987), and Link (1977).

137 The Fitton Formation, the lowermost known glaciogenic rock of the Sturtian Glaciation in South
138 Australia, is only present in the Yudnamutana Trough of the northern Flinders Ranges, where it
139 is overlain by the Bolla Bollana Tillite (Preiss et al. 1998; Young & Gostin 1989b). The latter is
140 one of six currently named diamictite/tillite formations that represent the glacial maximum.
141 These are the Appila Tillite (Thomson et al. 1964) (based on the section of Segnit 1939), the
142 Bolla Bollana Tillite (Coats & Forbes 1977; Thomson et al. 1964), the Calthorinna Tillite
143 (Ambrose et al. 1981), the Merinjina Tillite (Coats & Preiss 1987), the Pualco Tillite (Forbes &
144 Cooper 1976), and the Sturt Tillite (Howchin 1920; Mawson & Sprigg 1950). For reasons
145 outlined later in this publication, the formations representative of the glacial maximum are
146 here combined and renamed the Sturt Formation. The Benda Siltstone, Old Boolcoomata
147 Conglomerate and Holowilena Ironstone overlie the Sturt Formation but are limited in
148 distribution to the Baratta Trough (Conor & Preiss 2019; Lechte & Wallace 2015; Preiss 2006).
149 The exact stratigraphic correlation of these units is still uncertain but are likely partial
150 equivalents of both underlying and overlying stratigraphy. The Wilyerpa Formation (Dalgarno &
151 Johnson 1966; Forbes 1971; Thomson et al. 1964) and Lyndhurst Formation (Thomson et al.
152 1964; Young & Gostin 1989b) are the uppermost units of the Yudnamutana Subgroup and
153 represent the waning of the Sturtian glacial event (Preiss 1987; Preiss et al. 1998).

154 2.1.2 Yancowinna Subgroup

155 The Yancowinna Subgroup, Torrowangee Group, of western New South Wales, was defined by
156 Cooper, PF and Tuckwell (1971) presented in further detail by Cooper, PF et al. (1974). It
157 consists of a sequence of coarse poorly sorted and siliciclastics that include arkose, quartzite,
158 sandstone, siltstone, conglomerate, and diamictite (Cooper, PF et al. 1974; Fitzherbert &
159 Downes 2015; Preiss 1987). Diamictite of glacial origin (Tillite) has only been confidently
160 recognised in one area (Cooper, PF 1973), but many of the facies closely resemble probable
161 equivalents in South Australia (Preiss 1987). Its stratigraphic position supports an equivalence
162 with the Yudnamutana Subgroup of South Australia, with the Yancowinna Subgroup overlain by
163 the Euriovie Subgroup (inter-glacial) that is in turn overlain by the Teamsters Creek Subgroup,
164 which is thought to represent the Marinoan (Elatina) glacial event (Fitzherbert & Downes 2015;
165 Preiss 1987). Aside from detailed mapping and the original sedimentological work, there is
166 extraordinarily little research on these sequences, and no geochronology has been published
167 to date. As such the correlations are likely, but uncertain and not yet confirmed by
168 geochronology.

169 2.1.3 Nepouie Subgroup

170 The inter-glacial Nepouie Subgroup (Preiss et al. 1998) most notably includes the basin-wide
171 Tapley Hill Formation. Other formations in the Nepouie Subgroup are the basal Serle
172 Conglomerate, and the Brighton Limestone and Balcanoona Formation at the top, with the
173 latter two overlying and interfingering with Tapley Hill Formation. The Balcanoona Formation is
174 coeval with the upper Tapley Hill Formation, forming large palaeo-reef systems above it and
175 passing laterally into it (Wallace et al. 2015). The Tapley Hill Formation itself is primarily
176 composed of well sorted, commonly carbonaceous, calcareous, or dolomitic siltstone, with
177 pyritic shale and dolostone at the base. While extensive in both distribution (basin-wide) and
178 uniformity, there are several minor lithofacies variations within the Tapley Hill Formation,
179 including arkose, greywacke, siltstone, dolostone, and lenticular conglomerate beds. The latter

180 is attributed to debris flows reworking the underlying glaciogenic sequences (Preiss 1987).
181 The only formation of the Nepouie Subgroup with a still somewhat uncertain stratigraphic
182 position is the Serle Conglomerate, however a position conformably below the Tapley Hill
183 Formation seems likely (Dyson 1996; 2004; Preiss et al. 1998; Young & Gostin 1989a). The
184 Serle Conglomerate is thought to be deposited as part of a submarine fan complex (Young &
185 Gostin 1989a).

186 2.2 Sturtian Glaciation

187 The term Sturtian was originally defined as a chronostratigraphic unit (Series) in South
188 Australia (Mawson & Sprigg 1950) and was later proposed for use as a global
189 chronostratigraphic division by Dunn et al. (1971). However, this has since been superseded
190 by international nomenclature (Gradstein et al. 2005; Knoll et al. 2006; Lloyd et al. 2020;
191 Plumb 1991; Preiss et al. 2011; Shields-Zhou et al. 2016; Shields et al. 2022) with the Sturtian
192 Glaciation wholly encompassed within the Cryogenian Period (Plumb 1991; Shields-Zhou et al.
193 2016). At present, Sturtian is informally used by the international community as the name for
194 the older of two global (or near-global) glacial events (Fairchild & Kennedy 2007; Hoffman et
195 al. 2017a; Hoffman et al. 1998; Hoffman & Schrag 2002) proposed to have occurred during
196 the Cryogenian. In a split from the growing consensus, Le Heron et al. (2020) have advocated
197 that the name “Laurentian Neoproterozoic Glacial Interval” be used in favour of the Sturtian,
198 and Sturtian be restricted to the formations in Australia, a concept we are not in favour of and
199 will discuss later.

200 The global distribution of Precambrian glacial sequences, in particular those now attributed to
201 the Sturtian Glaciation, was recognised nearly a century ago (Hoffman 2011; Hoffman et al.
202 2017a, and references therein); however, their synchronicity was long debated until the advent
203 of reliable and precise geochronology within the past two decades (e.g., Cox et al. 2018b;
204 Dempster et al. 2002; Hoffman et al. 2017a; Keeman et al. 2020; Kendall et al. 2006; Lamothe
205 et al. 2019; Lloyd et al. 2020; Macdonald et al. 2010; Miller 2013; Park et al. 2019; Rooney et
206 al. 2014; Rooney et al. 2015; Rooney et al. 2020; Shields et al. 2018; Xu et al. 2009). The
207 recognition of global time equivalence led Hoffman et al. (2017a) to propose calling the
208 Cryogenian glacial periods ‘cryochrons’. Advancements in the application of geochronology
209 and mass spectrometry have led to tight constraints on the global major onset of glaciation
210 and deglaciation c. 717 Ma and c. 660 Ma respectively (Hoffman et al. 2017a; Rooney et al.
211 2015). Many of the thickest glacial successions are found in extensional basins associated
212 with the break-up of Rodinia; the very thick Sturt Formation deposits in the Baratta,
213 Yudnamutana, and Yancowinna troughs of the Adelaide Superbasin are typical of these.

214 3 Methods

215 3.1 Detrital zircon U–Pb geochronology

216 Fifteen samples [Figure 1] from the Yudnamutana Subgroup (FR1_005_02, FR1_009_01,
217 FR2_007_01, FR2_024_01, FR3_005, FR3_006, FR3_009, FR3_034, FR3_065, FR3_073,
218 FR3_084a, FR3_109, FR3_139, ML_017, & ML_018), one sample from the equivalent
219 Yancowinna Subgroup (GSNSWK002), and one sample from the lowermost Nepouie
220 Subgroup (FR3_004), were analysed for detrital zircon geochronology.

221 Rock samples were prepared for detrital zircon analysis by crushing, sieving, panning and,
222 where necessary due to low zircon yield, heavy liquid separation. Any grain that remotely
223 resembled a zircon was picked to minimise human bias, an issue highlighted by Sláma and
224 Košler (2012) and Dröllner et al. (2021). Where permitted by zircon yields, at least 300 zircons
225 were picked per sample, otherwise all zircons in the sample were picked.
226 Cathodoluminescence images were obtained on either a FEI Quanta 600 scanning electron
227 microscope (for zircon analysed in 2020) or a Cameca SXFive Electron Microprobe (for zircon
228 analysed in 2021). The zircons were analysed using Laser Ablation Inductively Coupled
229 Plasma Mass Spectrometry (LA-ICP-MS) to obtain a suite of elemental data for U–Pb
230 geochronology and rare earth element (REE) analysis. All zircons were analysed using a
231 RESOLution-LR 193 nm ArF excimer laser ablation system coupled with an Agilent 7900x
232 inductively coupled plasma mass spectrometer. All analytical instruments used are housed at
233 Adelaide Microscopy, University of Adelaide, Australia.

234 GJ-1 (Horstwood et al. 2016; Jackson et al. 2004), was used as the primary calibration
235 reference material for U–Pb ratios and NIST610 (Jochum et al. 2011) was used as the primary
236 calibration reference material for Pb isotope ratios and trace element data. The internal
237 standard element for trace element data was ^{91}Zr with a value of 431,400 ppm (43.14 wt%)
238 assigned to unknowns. Plešovice (Horstwood et al. 2016; Sláma et al. 2008) and 91500
239 (Horstwood et al. 2016; Wiedenbeck et al. 1995; Wiedenbeck et al. 2004) were used as
240 validation reference materials to check accuracy. Unknowns were bracketed by two analyses
241 of GJ-1, followed by a combined two to three analyses of Plešovice and 91500, and two
242 analyses of NIST610 every 20–30 unknowns. A 30 second gas blank followed by either a 40
243 second or 30 second ablation (session on 2021-03-30) time was used with a laser repetition
244 rate of 5 Hz. A spot size of 29 μm and a nominal fluence of 2 Jcm^{-2} was used for zircon, and a
245 spot size of 43 μm using a nominal fluence of 3.5 Jcm^{-2} was used for NIST610. Data were
246 processed using LADR (Norris & Danyushevsky 2018), version 1.1.06 and output as “Full
247 Analytical Uncertainty”. No common Pb corrections were applied to the data. Reference
248 material ratios used for GJ-1, Plešovice, and 91500 were the Chemical Abrasion Isotope
249 Dilution Thermal Ionisation Mass Spectrometry (CA-ID-TIMS) values (uncorrected for thorium
250 disequilibria and common-Pb) of Horstwood et al. (2016). Weighted averages and dispersion
251 statistics for all standards are available from the link in data availability.

252 Statistical analysis of the zircon U–Pb data follows the method of Lloyd et al. (2020). Data are
253 considered concordant if within $\pm 10\%$, and a “meaningful” age if the two-standard error (2SE)
254 uncertainty is $\leq 10\%$ —if a datum satisfies both parameters it is termed a *Filtered Age*.
255 Maximum depositional ages are determined from a stricter 2% concordance filter and use the
256 older age of the three isotope ratios ($^{207}\text{Pb}/^{235}\text{U}$, $^{206}\text{Pb}/^{238}\text{U}$, $^{207}\text{Pb}/^{206}\text{Pb}$) for a conservative
257 estimate of the youngest single concordant grain. All uncertainties are quoted at 2SE level.
258 Kernel density estimates (KDEs), and multidimensional scaling plots (MDS) were generated
259 using IsoplotR (Vermeesch 2018). Key zircon trace element data are presented graphically
260 using methods following Verdel et al. (2021) and additionally lanthanoid data are represented
261 using violin plots and lambda representation (Anenburg 2020; O’Neill 2016).

262 Metadata for the LA-ICP-MS sessions, data for all analyses, cathodoluminescence images, and
263 R code used to generate plots are available from the links in data and code availability.

264 3.2 In-situ Rb–Sr geochronology

265 Two siltstone/shale samples (3404236 & 3404235) were acquired for in-situ Rb–Sr
266 geochronology from the Sturt Formation within drillhole SR13/2 located on the north-eastern
267 margin of the Stuart Shelf, South Australia.

268 Polished rock blocks in 25mm round epoxy mounts were analysed using an Agilent 8900x ICP-
269 MS/MS coupled to a RESolution-LR 193 nm ArF excimer LA system house at Adelaide
270 Microscopy, the University of Adelaide. Methods follow Redaa et al. (2021) and Subarkah et al.
271 (2021). Briefly, N₂O was used as the reaction gas to mass separate ⁸⁷Sr from ⁸⁷Rb with Sr
272 measured as the reacted ⁸⁷Sr¹⁶O product ion mass at 103. A nominal fluence of 3.5 J cm⁻² with
273 a 67 μm circular spot, a 5 Hz repetition rate, and 40 second ablation time preceded by a 30
274 second gas blank were used. NIST610 glass (Jochum et al. 2011) was used as the primary
275 calibration reference material for Sr isotope ratios, and the Mica-Mg (Govindaraju 1995)
276 pressed nanopowder pellet was used as the primary calibration reference material for Rb–Sr
277 ratios. Accuracy was checked by analysing MDC (crystalline phlogopite) and Högsbo
278 (crystalline muscovite) (Hogmalm et al. 2017; Redaa et al. 2021) as validation reference
279 materials. Unknowns were bracketed by two analyses of NIST610 and three analyses of Mica-
280 Mg every thirty unknowns.

281 Data were reduced in LADR (Norris & Danyushevsky 2018) version 1.1.07 and output as “Full
282 Analytical Uncertainty”. Isochrons were calculated using IsoplotR (Vermeesch 2018) using a
283 ⁸⁷Rb decay constant (λ) of $(1.3972 \pm 0.0045) \times 10^{-11} \text{ a}^{-1}$ (Villa et al. 2015). Error correlations (ρ)
284 were calculated in LADR by using a workaround to proxy the Rb–Sr data as U–Pb data. Except
285 for translating headers using a cross-platform PowerShell module from Rb to U and Sr to Pb,
286 all other parameters are the same resulting in identical ratio outputs but allowing for
287 calculation of error correlations. Uncertainties are quoted at 2SE level initially without decay
288 constant uncertainty propagation. The decay constant uncertainty is propagated into the
289 quoted uncertainty during the discussion when comparing to other geochronometric systems.

290 4 Results

291 4.1 Detrital zircon geochronology

292 4.1.1 Fitton Formation

293 A cumulative total of 124 analyses, with 95 analyses passing filtering parameters, were
294 conducted for samples FR3_065 (92/74), FR3_009 (9/1), and FR2_024_01 (23/20). The data
295 for these samples are combined as only two samples yield more than one filtered analysis.
296 These two samples are ~200 m apart (geographically), all three samples are from the broader
297 local area [Figure 1], and there are no discernible differences in the age spectra. Ages range
298 from $1134 \pm 24 \text{ Ma}$ to $2458 \pm 37 \text{ Ma}$, with as primarily population peak c. 1580 Ma, and a
299 secondary peak c. 1160 Ma [Figure 4].

300 4.1.2 Sturt Formation and equivalents

301 A cumulative total of 162 analyses, with 107 analyses passing filtering parameters, were
302 conducted on zircon from samples ML_017 (117/93) and ML_018 (45/14), South Mount Lofty
303 Ranges (Sturt Gorge, Adelaide). Data from these samples are combined as the two sampling
304 sites are ~60 m apart (geographically) [Figure 1] and there are no discernible differences in the
305 age spectra. Ages range from 930 ± 16 Ma to 2933 ± 34 Ma, with a primary population peak c.
306 1840 Ma, tailing towards 1560 Ma. An additional minor population peak is present c. 1100 Ma
307 [Figure 4].

308 A total of 178 zircons were analysed from
309 sample FR1_009_01, North Mount Lofty
310 Ranges (Spalding area) [Figure 1], with 98
311 passing filtering parameters. Ages range
312 from 1501 ± 48 Ma to 3374 ± 32 Ma, with
313 a single population peak c. 1790 Ma
314 [Figure 4].

315 A cumulative total of 81 analyses, with 77
316 analyses passing filtering parameters,
317 were conducted on zircon from samples
318 FR2_007_01 (31/28) and FR3_139
319 (50/49), North Flinders Ranges (Copley
320 area) [Figure 1]. Data from these samples
321 are combined as they were sampled from
322 the same stratigraphic interval at
323 approximately the same stratigraphic
324 height. Ages range from 663 ± 11 Ma to
325 2718 ± 21 Ma, with a primary population
326 peak c. 1740 Ma and secondary population
327 peaks c. 1580 Ma, 1180 Ma, and 1050 Ma
328 [Figure 4].

329 A cumulative total of 52 analyses, with 46
330 analysed passing filtering parameters were
331 conducted on zircon from FR3_084a
332 (10/9) and FR3_109 (42/37), North
333 Flinders Ranges (Yankaninna area). Data
334 from these two samples are combined as
335 they are sampled from within 30 metres of
336 each other in the same interval of outcrop
337 [Figure 1]. Ages range from 1042 ± 19 Ma
338 to 2514 ± 48 Ma, with a single primary
339 population peak c. 1640 Ma [Figure 4].

340 A total of 118 zircons were analysed from
341 sample FR3_073, North Flinders Ranges
342 (Vulkathuhna-Gammon Ranges) [Figure 1],

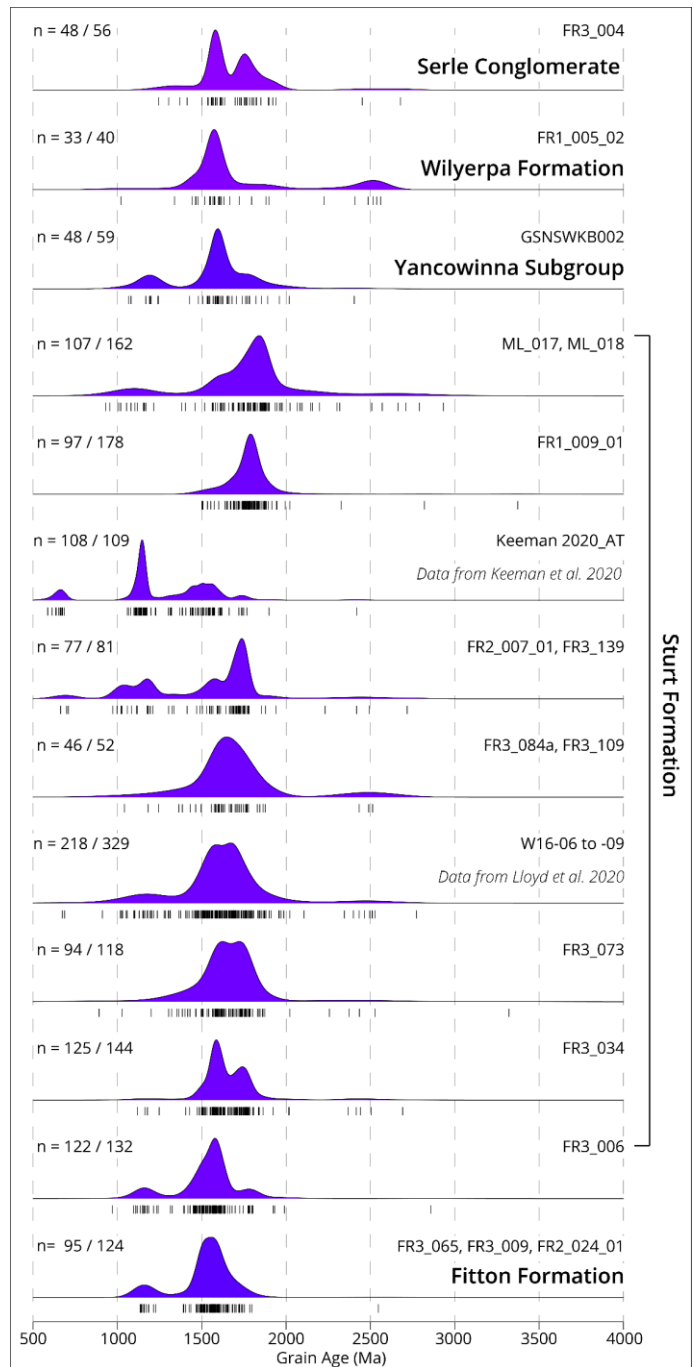


Figure 4 – Kernel density estimates [KDEs] of detrital zircon populations from Yudnamutana, Yancowinna and Nepouie Subgroup samples. Data are from this study unless otherwise denoted. Tick marks below each plot represent an analysis. n = filtered analyses / total analyses. Generated using IsoplotR (Vermeesch 2018).

343 with 94 passing filtering parameters. Ages range from 891 ± 15 Ma to 3322 ± 35 Ma, with a
344 single broad, and slightly bimodal population peak range of c. 1740 Ma to c. 1620 Ma [Figure
345 4].

346 A total of 144 zircons were analysed from sample FR3_034, North Flinders Ranges (Stubbs
347 Waterhole, Arkaroola), with 125 passing filtering parameters. Ages range from 1117 ± 34 Ma
348 to 2691 ± 42 Ma, with a primary population peak c. 1590 Ma, and a secondary population
349 peak c. 1750 Ma [Figure 4].

350 A total of 132 zircons were analysed from sample FR3_006, North Flinders Ranges (Stanley
351 Mine, Arkaroola) [Figure 1], with 122 passing filtering parameters. Ages range from 969 ± 16
352 Ma to 2858 ± 47 Ma, with a primary population peak c. 1580 Ma, and secondary population
353 peaks c. 1790 Ma and 1160 Ma [Figure 4].

354 A total of 59 zircons were analysed from sample GSNSWKB002, Yancowinna Subgroup, Barrier
355 Ranges (New South Wales) [Figure 1], with 48 passing filtering parameters. Ages range from
356 1065 ± 18 Ma to 2404 ± 37 Ma [Figure 4].

357 4.1.3 Lyndhurst and Wilyerpa Formations

358 Sample FR3_005, Lyndhurst Formation, had extremely low zircon yield with only three zircons
359 obtained and analysed. Of those, only two passed filtering parameters, with ages of 1532 ± 24
360 Ma and 1174 ± 19 Ma [Figure 4].

361 A total of 40 zircons were analysed from sample FR1_005_02, Wilyerpa Formation, North
362 Mount Lofty Ranges [Figure 1]. Of these, 33 passed filtering parameters with ages ranging from
363 1020 ± 19 Ma to 2560 ± 79 Ma, with a primary population peak c. 1580 Ma and a secondary
364 population c. 2500 Ma [Figure 4].

365 4.1.4 Serle Conglomerate

366 A total of 56 zircons were analysed from
367 sample FR3_004, Serle Conglomerate,
368 with 48 passing filtering parameters. Ages
369 range from 1246 ± 24 Ma to 2679 ± 65 Ma,
370 with a primary population peak c. 1590
371 Ma, and a secondary population peak c.
372 1760 Ma [Figure 4].

373 4.2 Zircon trace element 374 geochemistry

375 Most analyses resolved lanthanoid
376 concentrations that are typical for zircons,
377 with several orders-of-magnitude increase
378 in concentration from light to heavy
379 elements, a slight negative deviation in
380 europium (Eu), and a positive deviation in
381 cerium (Ce) [Figure 5]. However, two

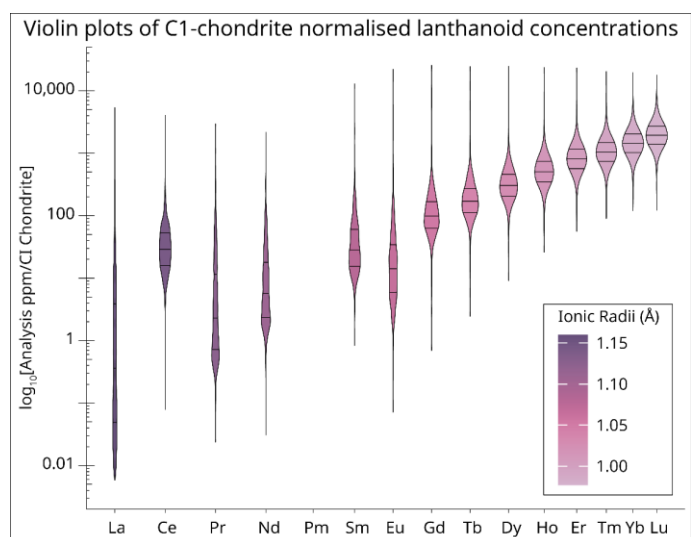


Figure 5 – Violin plots of CI chondrite (O'Neill 2016) normalised lanthanoids for all filtered zircon analysed in this study. X-axis is spaced by ionic radii (Shannon 1976) and ordered by atomic number. Black lines across the fill of each plot represent the 0.25, 0.5, and 0.75 quantiles. Bandwidth of the density estimates is calculated using the Botev algorithm from the Provenance package (Vermeesch et al. 2016).

382 analyses (FR1_009_01b – 057, and FR1_009_01 - 044) have lanthanoid concentrations
 383 atypical of zircon, with overall positive (based on ionic radii) slopes (λ_1 of +7.14, and +1.06)
 384 due to highly elevated light lanthanoids (La to Nd). Overall, the lanthanoid pattern for both
 385 analyses have a concave-up shape with heavy lanthanoid concentration increasing as would
 386 normally occur in zircon. Major element percentages, ~14.4 wt% and ~15.6 wt% silicon,
 387 suggest these two analyses are zircon, and CL images also support this, although show patchy
 388 textures. The ages for these are at the limit of discordance acceptance (90%). It is likely these
 389 two analyses have gone through complicated zones of inclusions, altered metamict zones,
 390 and/or mineral overgrowths.

391 4.3 In-situ Rb–Sr Geochronology

392 Of the two siltstone/shale samples analysed for Rb–Sr geochronology, 3404236 (upper Sturt
 393 Formation) and 3404235 (lower Sturt Formation), only the latter sample yielded a meaningful
 394 result. The analyses on sample 3404236, n = 60, had little spread in Rb/Sr ratios and a low
 395 percentage of radiogenic Sr ($^{87}\text{Sr}/^{86}\text{Sr} < 0.8$), nonetheless a date of 839 ± 235 Ma was obtained
 396 with an initial $^{87}\text{Sr}/^{86}\text{Sr}$ of 0.7030 ± 0.0127 [Figure 6]. For sample 3404235, n = 51, there was
 397 reasonable spread in Rb/Sr ratios and a date of 684 ± 37 Ma with an initial $^{87}\text{Sr}/^{86}\text{Sr}$ of 0.7204
 398 ± 0.0054 was obtained [Figure 6].

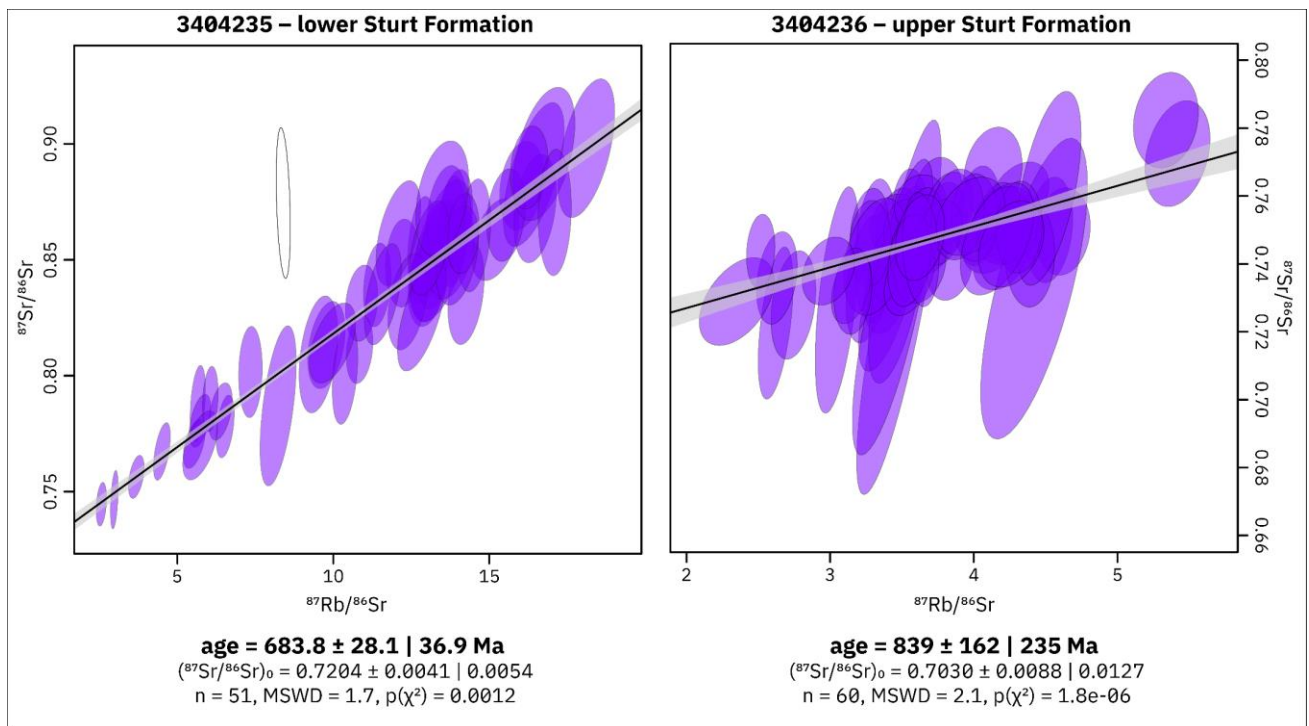


Figure 6 – Rb–Sr isochrons of the two shale/siltstone samples from the Sturt Formation in drillhole SR13/2 analysed in this study. Quoted uncertainty and ellipses are two standard error (2SE). The second uncertainty term accounts for overdispersion. Generated using IsoplotR (Vermeesch 2018), without the decay constant uncertainty propagated. ^{87}Rb decay constant used = $(1.3972 \pm 0.0045) \times 10^{-11} \text{ a}^{-1}$.

400 5 Discussion

401 5.1 Zircon trace element geochemistry

402 Zircons analysed in this study mostly show
403 affinity to generation in continental crust
404 with only a small number of zircons
405 potentially of oceanic affinity [Figure 7], as
406 inferred by the U/Yb against Y plot (Grimes
407 et al. 2007; Grimes et al. 2015). Almost all
408 zircons have a Th/U ratio >0.07 and are
409 inferred to be generated as magmatic
410 rather than metamorphic zircon (Collins et
411 al. 2004; Rubatto 2002). C1 chondrite
412 normalised (O'Neill 2016) lanthanoids
413 concentrations are generally typical for
414 zircon [Figure 5] with a positive pattern
415 slope (increasingly negative λ_1 values)
416 from light to heavy lanthanoids, a positive
417 Ce anomaly, and negative Eu anomaly
418 (Hoskin & Ireland 2000; Hoskin &
419 Schaltegger 2003). There is no apparent
420 trend in lanthanoid pattern slope or
421 curvature [Figure 8], denoted as λ_1 (linear
422 slope), λ_2 (quadratic slope), and λ_3 (cubic
423 slope) (Anenburg 2020), with time or
424 sample. Both Eu and Ce anomalies
425 (denoted by Eu* and Ce*) show a significant
426 spread through time. The youngest few zircons
427 c. 670 Ma, although limited in number, have
428 out of phase Eu* (low) and Ce* (high) anomalies
429 suggestive of growth in competition with plagioclase, and not reflective of magma oxidation state (Verdel et al. 2021).

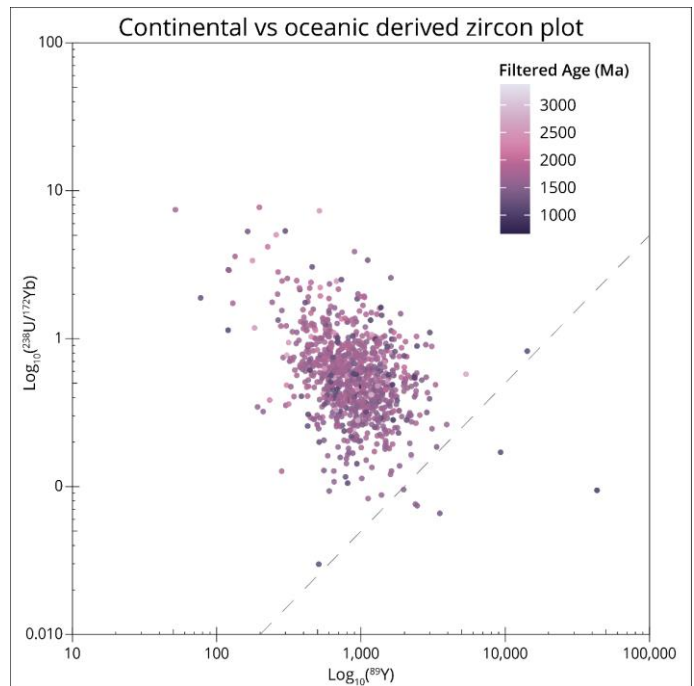


Figure 7 – Plot based on Grimes et al. (2007) used as an indicator of zircon crustal origin. This plots Y against U/Yb, with the dashed reference line dividing the “oceanic” (below line) and “continental” (above line) fields. Most data plot above the reference line, suggesting zircon formation mostly in crust of continental affinity. Coloured by filtered age where light is older and darker is younger.

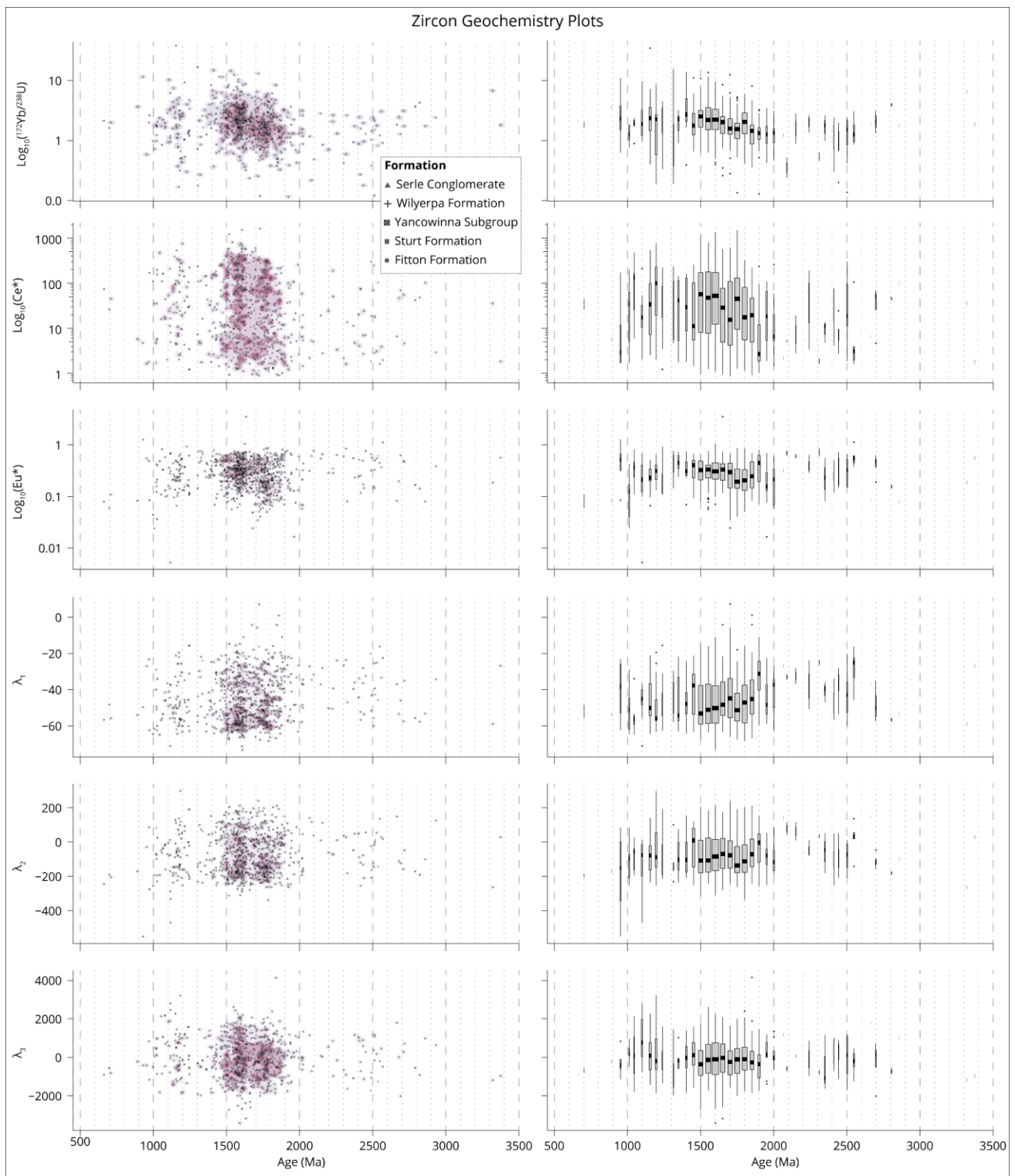


Figure 8 – Key zircon geochemistry plots for zircon analysed in this study. Left: Scatter plots underlain with 2D density estimation. Right: 50-million-year binned boxplots with width scaled by the count of values in the bin. Top to bottom: Yb/U, Ce*, Eu* and λ_{1-3} . λ_{1-3} are measures of lanthanoid pattern shapes, with λ_{1-3} representing the linear slope, quadratic slope and cubic slope respectively. Ce*, Eu* and λ_{1-3} are calculated using BLambdaR (Anenburg & Williams 2021).

431 5.2 Provenance and maximum depositional ages

432 5.2.1 Maximum depositional ages

433 The older limit of expected depositional age for samples in this study is constrained by two
434 detrital zircon MDAs from the underlying Belair Subgroup, namely the Gilbert Range Quartzite
435 (731 ± 34 Ma, Keeman et al. 2020; Lloyd et al. 2020) and Mitcham Quartzite (c. 730 Ma, Lloyd
436 et al. 2022b [preprint]; van der Wolff 2020). The younger age limit for deposition of the
437 Yudnamutana Subgroup is constrained by a 663.03 ± 0.76 Ma tuff in the Wilyerpa Formation
438 (Cox et al., 2018). The Serle Conglomerate is older than the c. 642 Ma Tapley Hill Shale (Re–Os
439 shale, Kendall et al. 2006) that it is interpreted to underlie.

440 A maximum depositional age (MDA) of 1162 ± 49 Ma was obtained for the combined Fitton
441 Formation samples. This is significantly older than the expected depositional age c. 663–730
442 Ma.

443 Maximum depositional ages for each of the Sturt Formation samples are presented here
444 according to the combinations outlined in 4.1.2.

- 445 • South Mount Lofty Ranges (Sturt Gorge, Adelaide): 1007 ± 14 Ma
- 446 • North Mount Lofty Ranges (Clare Valley): 1774 ± 39 Ma
- 447 • North Flinders Ranges (Copley area): 666 ± 25 Ma
- 448 • North Flinders Ranges (Yankaninna area): 1186 ± 50 Ma
- 449 • North Flinders Ranges (Vulkathuhna-Gammon Ranges): 891 ± 15 Ma
- 450 • North Flinders Ranges (Stubbs Waterhole, Arkaroola): 1188 ± 51 Ma
- 451 • North Flinders Ranges (Stanley Mine, Arkaroola): 1118 ± 48 Ma

452 Previous MDAs obtained from detrital zircon studies (Keeman et al. 2020; Lloyd et al. 2020) on
453 the Sturt Formation are:

- 454 • South Mount Lofty Ranges (Sturt Gorge, Adelaide): 714 ± 28 Ma
- 455 • South Flinders Ranges (Pichi Richi Pass): 667 ± 6 Ma
- 456 • North Flinders Ranges (Willouran Ranges): 673 ± 19 Ma

457 There is significant scatter in the MDAs of individual samples; however, population spectra are
458 similar [Figure 4, Figure 9] across all samples (spanning more than 500 km north–south,
459 Figure 1), and three independent sets of samples over a distance of ~250 km north–south,
460 have MDAs within uncertainty of each other. While detrital zircon population spectra variations
461 occur locally, as is expected across a large basin, and with significant recycling of underlying
462 stratigraphy in glacially derived sediment, the remarkable similarity of most samples' spectra
463 [Figure 4, Figure 9] adds support to unit equivalence, as is strongly suggested by previous
464 mapping of the lithostratigraphy. The variation in MDAs also highlights the main challenge in
465 determining depositional ages via detrital zircon studies as it is entirely possible for the MDA to
466 be significantly older than the true age of deposition. This is both a factor of chance (sampling)
467 and dependant on original sediment input—if no zircon of syndepositional ages are present in
468 the detritus being fed into the depocentre, the true age of deposition cannot be determined by
469 this method, hence the need to treat these as maximum depositional ages only. In addition,
470 many workers have noted that the Sturtian Glaciation deposits often consist of two diamictite
471 packages separated by an argillaceous or arenaceous sequence (Lechte & Wallace 2015; Virgo

472 et al. 2021). It is likely the different regions preserve deposits from different parts of the
473 Sturtian cryochron. The two diamictites may represent different periods of glacial advance, or
474 different phases of the glaciation (Lechte & Wallace 2015; Lechte et al. 2018), which would
475 mean in both cases that they were deposited at different times and therefore may well
476 preserve different MDAs. Chronological constraints for the Sturt Formation had been almost
477 non-existent up until recently but are now (Cox et al. 2018b; Fanning & Link 2008; Keeman et
478 al. 2020; Lloyd et al. 2022b [preprint]; van der Wolff 2020) robust enough to bracket
479 deposition of the Sturt Formation to between 663.03 ± 0.76 Ma and c. 730 Ma. Because the
480 older age limit itself is a maximum depositional age for the unconformably underlying Belair
481 Subgroup, the MDA of c. 666 ± 25 Ma is likely close to the true depositional age for the
482 terminal deposits (upper portion) of the Sturt Formation as a whole.

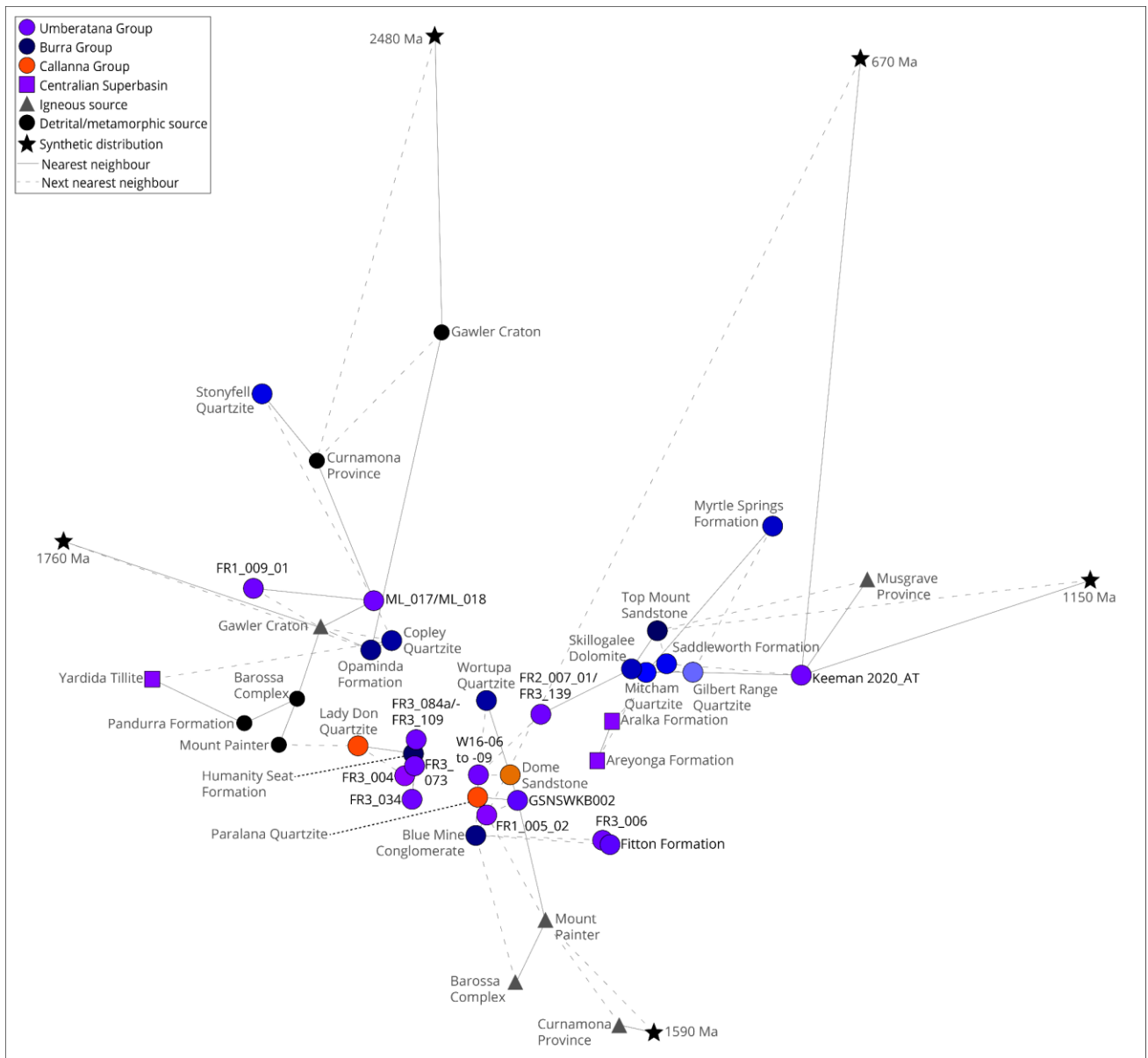


Figure 9 – Non-metric multidimensional scaling plot of samples analysed ($n > 30$) in this study (purple circles) with data from potential correlative formations of the Centralian Superbasin (purple squares), potential source regions (black and grey circles and triangles), and synthetic distributions (black stars) generated from the primary and secondary peaks of a KDE that combines all new data in this study. This plot shows relative similarity of all data to each other and are intended as a visual guide. Points that closer together suggest greater similarity. Axes are omitted as the algorithm used produces normalised values with no physical meaning and can be safely removed. Produced using IsoplotR (Vermeesch 2018).

483

484 GSNSWKB002 is a reconnaissance sample collected from undifferentiated Yancowinna
 485 Subgroup in the Barrier Ranges of New South Wales to test the general correlation with the
 486 Yudnamutana Subgroup of South Australia. This area is the easternmost known extension of
 487 the Adelaide Superbasin during the Neoproterozoic (Cooper, PF 1973; Cooper, PF & Tuckwell
 488 1971; Fitzherbert & Downes 2015; Lloyd et al. 2020; Preiss 1987). The sample is from a highly
 489 weathered diamictite with clasts ranging up to pebble size, and a silty to fine sand matrix. An
 490 MDA of 1075 ± 40 Ma was obtained from the sample, with a detrital zircon population
 491 spectrum similar to that of the likely correlatives in South Australia [Figure 4, Figure 9]. This
 492 provides limited, but supporting evidence of a shared detrital source and that these two
 493 subgroups are correlative as is indicated by the existing lithostratigraphic framework (Lloyd et

494 al. 2020).

495 An MDA of 1502 ± 70 Ma was obtained from the Wilyerpa Formation (FR1_005_02) sampled
496 in the Clare Valley. This is significantly older than the expected depositional age (i.e. c. 663 Ma)
497 and may be a factor of low zircon yield and/or no zircon close to depositional age being present
498 in the sample.

499 An MDA of 1291 ± 50 Ma was obtained from the Serle Conglomerate sample (FR3_004).
500 Again, this is significantly older than true depositional age that is expected to be between c.
501 663 Ma and c. 642 Ma. The detrital zircon population spectrum somewhat differs [Figure 4,
502 Figure 9] from the nearby Sturt Formation sample (FR3_006), although this may partially be an
503 artifact of the much lower zircon yield from the Serle Conglomerate sample.

504 5.2.2 Provenance

505 Two detrital zircon populations, c. 1840–1790 Ma and c. 1640–1580 Ma, form major peaks in
506 virtually all samples. The exact age positions and magnitude of the population peaks varies
507 slightly by sample, with broad north–south and east–west variations, generally trending to
508 older Palaeoproterozoic age populations in the west and south. It is likely that there is
509 significant recycling of the unconformably underlying stratigraphy due to sub-glacial erosion
510 (Young & Gostin 1989b). The similarity of the detrital zircon spectra within the samples of this
511 study to each other, and to earlier rocks of the Adelaide Superbasin [Figure 9], suggests
512 homogenisation of detrital material over a large area, potentially with extra-basin material, and
513 also supports the notion of intra-basin recycling occurring from sub-glacial erosion of earlier
514 stratigraphy.

515 Zircons with ages greater than ~1400 Ma are likely sourced locally, from the Gawler Craton,
516 Barossa Complex, and Curnamona Province that record numerous zircon generation events
517 and sedimentary sequences known to hold zircon of these ages (Barovich & Hand 2008;
518 Belousova et al. 2009; Conor & Preiss 2008; Fanning et al. 2007; Fraser et al. 2010; Fraser &
519 Neumann 2010; Jagodzinski & Fricke 2010; Jagodzinski & McAvaney 2017; Jagodzinski et al.
520 2020; Kromkhun et al. 2013; McAvaney 2012; Meaney 2012; 2017; Morrissey et al. 2019;
521 Morrissey et al. 2018; Morrissey et al. 2013; Reid et al. 2019; Reid & Hand 2012; Reid et al.
522 2008; Reid et al. 2014a; Reid et al. 2014b; Reid et al. 2017; Reid & Payne 2017; Reid et al.
523 2021; Stevens et al. 2008; Swain et al. 2005; Wade, CE 2011). The southernmost samples
524 from Sturt Gorge are dominated by c. 1840 Ma zircons, and northward progression generally
525 sees a shift in dominance of the c. 1840 Ma population to the younger c. 1590 Ma. This
526 observation is likely a result of the variation in local basement geology of the Gawler Craton
527 and Curnamona Province near the sample sites.

528 The generally minor Stenian population of zircon at c. 1160 Ma is suggestive of provenance
529 from the Musgrave Province (Smithies et al. 2008; Smithies et al. 2011; Smits et al. 2014;
530 Wade, BP et al. 2008), but as noted in Lloyd et al. (2022a) they may be sourced from an as yet
531 undiscovered but inferred late Mesoproterozoic (c. 1300–1000 Ma) source to the east
532 (Fergusson et al. 2007; Korsch et al. 2012; Mackay 2011; Wysoczanski & Allibone 2004). This
533 population is generally more abundant in samples closer to the eastern and western margins
534 of the basin [Figure 4, Figure 1]. Alternative sources of these late Mesoproterozoic zircon could
535 be the South Tasman Rise (Fioretti et al. 2005), Coompana Province (Pawley et al. 2020) or

536 far-field transport across Antarctica from the Tonian Oceanic Arc Super Terrane (Jacobs et al.
537 2015). Again, recycling of underlying stratigraphy is a likely source of some of these zircons.

538 Neoproterozoic zircons with ages between c. 900 Ma and c. 780 Ma are feasibly attributed to
539 early known magmatism in the Adelaide Superbasin (Lloyd et al. 2020); however, those
540 younger than 780 Ma are much more difficult to reconcile. It is apparent that some zircon-
541 bearing magmatic crystallisation of zircon was occurring c. 700 Ma to c. 660 Ma, and that
542 these were in the sediment supply of the Sturt Formation. While a 663.03 ± 0.76 Ma tuff has
543 been dated (Cox et al. 2018b) from within the Wilyerpa Formation immediately post-dating
544 deposition of the Sturt Formation, the site of the volcanic centre for the ashfall is unknown.
545 Additionally, zircon of this age range (c. 700–660 Ma), within the Sturt Formation has so far,
546 only been found on the far western margin of the Adelaide Rift Complex within the Adelaide
547 Superbasin [Figure 10], potentially suggesting this magmatic source was to the west of, or on
548 the western margin of the basin.

549 Comparison is made with three correlatives (Edgoose 2013; Kruse et al. 2013; Normington &
550 Donnellan 2020) from the Centralian Superbasin, the syn-glacial Yardida Tillite and Areyonga
551 Formation, and the post-glacial Aralka Formation (Preiss et al. 1978). Interestingly, the detrital
552 zircon age spectra of the Yardida Tillite (Georgina Basin, Northern Territory/Queensland) which
553 is likely to be a time correlative of the Sturt Formation, is very similar [Figure 9] to the local
554 basement of South Australia (e.g. Gawler Craton). This is explained by its proximity to the
555 Mount Isa and Aileron Provinces, suggested to be the primary zircon source for the Yardida
556 Tillite (Verdel et al. 2021). These provinces host abundant c. 1640-1850 Ma zircon that are
557 also found in the Gawler Craton and Curnamona Province. In addition, palaeomagnetic and
558 geological reconstructions for the time suggest that the South Australian Craton may have
559 been rotated closer to the Georgina Basin at that time (Li, Z-X & Evans 2010; Lloyd et al.
560 2020). The age spectra in the Areyonga Formation and Aralka Formations (Amadeus Basin,
561 Northern Territory/Western Australia) are similar to the Burra Group and Sturt Formation
562 samples from the western margin of the Adelaide Rift Complex. All of these aforementioned
563 formations are suggested to ultimately source zircon from the Musgrave Province where
564 Stenian-aged zircons are abundant, and both basins have abundant nearby sources of pre-
565 Stenian aged zircon. Notably though no zircon younger than c. 800 Ma has been found in the
566 Areyonga and Aralka formations to date.

567

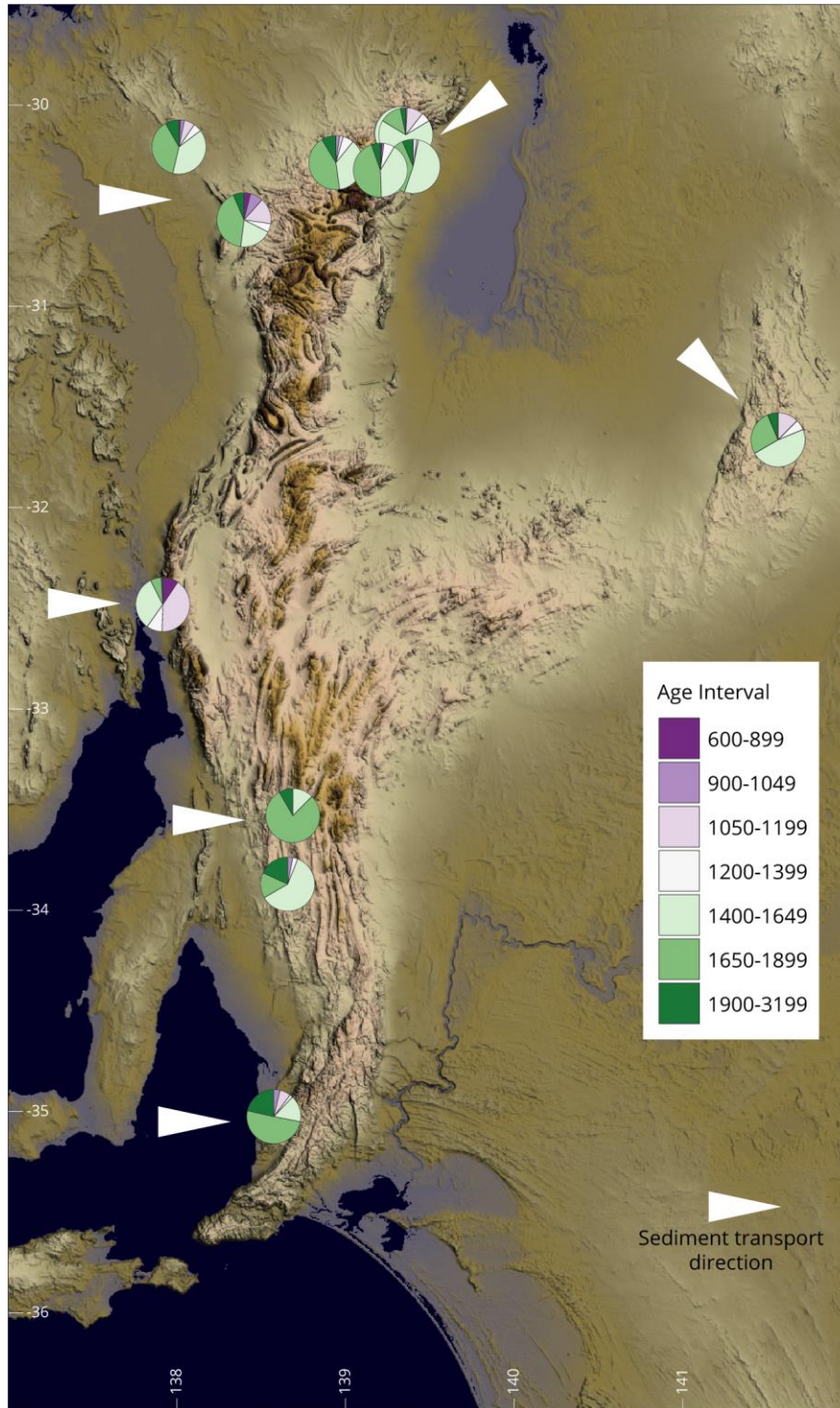


Figure 10 – Schematic map with pie charts at samples locations to highlight the changes in zircon population spectra relative to geographic location. Arrows are generalised schematic indicators of palaeo-sediment transport direction.

568

569 5.2.3 Comparison to Palaeocurrent data

570 Observations drawn in this study from detrital zircon are generally supportive of existing
 571 palaeocurrent data (Link & Gostin 1981; Young & Gostin 1989b; 1991). Palaeocurrent data
 572 from the Yudnamutana Subgroup suggest a westerly transport direction in the Mount Painter

573 area and along the Paralana fault system, northerly transport on the northern side of the
574 Gammon syncline and Yankaninna anticline, and north-easterly transport along the western
575 edge of the Adelaide Rift Complex (Copley area, south-eastern Willouran Ranges). It is likely
576 that underlying strata have been recycled by sub-glacial erosion, making the use of detrital
577 zircon spectra for determining palaeo-transport paths difficult; however, the only area in which
578 the detrital data from this study might potentially differ in transport direction from the existing
579 palaeocurrent data is the Vulkathuhna-Gammon Ranges. Our data (Figure 4: FR3_073, Fitton
580 Formation samples) suggest a south, or south-westerly sediment transport [Figure 10]
581 direction as the detrital zircon populations are similar to the older stratigraphy of the basin,
582 and to the local basement sources located to the northeast [Figure 9, Figure 1].

583 5.3 Rb–Sr geochronology

584 In-situ Rb–Sr geochronology is a rapidly developing technique that, when applied to shales,
585 can provide information about depositional ages or early diagenetic illite formation (Subarkah
586 et al. 2021). While a powerful although imprecise technique, in shales the Rb–Sr isotopic
587 system is susceptible to low–moderate temperature hydrothermal alteration (Subarkah et al.
588 2022) and can be influenced by detrital input. These complications mean careful assessment
589 must be done before assigning geological significance to obtained dates. For the two samples
590 analysed in this study, the obtained dates must be between 730 and 663 Ma for them to be
591 representative of depositional age. Uncertainties quoted in this section include propagation of
592 the decay constant uncertainty on ^{87}Rb ($\sim 0.32\%$, Villa et al. 2015) to allow for comparison to
593 other geochronometric systems (e.g. U–Pb).

594 The date obtained for sample 3404236, 839 ± 241 Ma [Figure 6], is not a meaningful date due
595 to large uncertainty and it likely comprises a significant detrital component pushing the date
596 older than the constraints for the Sturt Formation. These reservations also apply to the former
597 attempts to date the overlying Tapley Hill Formation via traditional whole rock Rb–Sr methods
598 (Webb 1980; Webb et al. 1983). The 684 ± 37 Ma [Figure 6] date obtained for sample
599 3404235 is consistent with the constrained depositional age for the Sturt Formation and can
600 be considered a meaningful age representing a syn-depositional constraint.

601 5.4 Tectonic and palaeogeographic implications

602 While the dataset needs to be expanded in future to cover more of the basin, particularly to the
603 east (Olary area, and New South Wales) and far northwest (Davenport and Denison Ranges),
604 some points can be made regarding the palaeogeography and tectonics of the Adelaide
605 Superbasin during the Sturtian Glaciation. Firstly, it is apparent that the detrital zircon
606 spectrum of each sample is highly dependent on local geology, commonly recycling the
607 underlying stratigraphy and/or from the nearby basement geology. This supports the common
608 observation of clasts in diamictites that can be identified as derived from the Burra Group and,
609 locally, the Callanna Group. This finding suggests that the far-field sediment supply to the
610 Burra Group was shut off during deposition of the Yudnamutana Subgroup, with locally derived
611 detritus becoming much more prominent (Lloyd et al. 2020; Preiss 2014). Secondly, active
612 zircon-bearing magmatism occurred at c. 700–660 Ma, although the location and volume of
613 this magmatism remains unknown. The spatial distribution of the samples containing
614 Cryogenian zircon [Figure 10] suggests that the source was to the west, or along the western

615 margin, of the basin. Of note, there is a basalt conglomerate at the base of the Sturt Formation
616 at the central-western margin (Depot Creek) of the Adelaide Rift Complex (Hopton 1983);
617 however, its origin and age remain enigmatic. Thirdly, the detrital zircon spectrum of the
618 Yancowinna Subgroup sample supports a shared sediment supply for it and the Sturt
619 Formation samples in the northeast of the basin, consistent with earlier palaeographic
620 interpretations that the Curnamona Province was a topographic high between these two areas
621 that was shedding detrital material to both sides. The data presented here also add support to
622 the Yancowinna Subgroup being an equivalent of the Yudnamutana Subgroup, as is suggested
623 by the current stratigraphic framework (Cooper, PF 1973; Cooper, PF & Tuckwell 1971;
624 Fitzherbert & Downes 2015; Lloyd et al. 2020; Preiss 1987). In combination with glacial
625 scouring, it is clear that active tectonics played a significant control on the dramatic thickness
626 variations of the Yudnamutana Subgroup sedimentary rocks (Le Heron 2012; Le Heron et al.
627 2014; Preiss et al. 2011; Young & Gostin 1991). The Yudnamutana, Baratta, and Yancowinna
628 troughs are major extensional sub-basins bounded by mappable normal growth faults (Preiss
629 1985; Preiss & Conor 2001; Preiss et al. 2011). This has been interpreted as the last phase of
630 rifting associated with continental separation (Preiss 2000), although Merdith et al. (2017)
631 considered that the rift-drift transition of the Australia–Laurentia margin occurred earlier at c.
632 780 Ma.

633 5.5 Sturtian nomenclature

634 5.5.1 South Australian Formal Stratigraphy

635 Correlations of the ‘older’ glacial units across southern Australia (e.g. Sturt Tillite, Appila
636 Tillite) were originally argued to represent either one or two separate glacial intervals (Coats &
637 Forbes 1977; Coats & Preiss 1987). Subsequent work showed that they were all consistent
638 with only one glacial event (Murrell et al. 1977; Preiss 1993; 2000; Preiss et al. 1998) but
639 representing ice sheet advance-retreat cycles (Le Heron 2012). No significant lithological
640 differentiation (in the sense of formal stratigraphy) can be made to distinguish them from each
641 other (Preiss et al. 1998; Preiss et al. 2011), and both stratigraphic position and
642 geochronology support their equivalence (this study, Cox et al. 2018b; Keeman et al. 2020;
643 Lloyd et al. 2020; Preiss et al. 1998; Young & Gostin 1989b). Considering this knowledge, we
644 redefine and combine the stratigraphic nomenclature for the outcrops that represent the
645 glacial maximum (e.g. Appila Tillite, Bolla Bollana Tillite, Sturt Tillite) as the Sturt Formation
646 [Figure 2]. Sturt is retained as the first diamictite formally named was the Sturtian tillite
647 (Howchin 1920; Mawson & Sprigg 1950), and as such it takes precedence over all other
648 equivalent formation names, and it has become internationally synonymous with the Sturtian
649 Glaciation. Tillite has been dropped in favour of Formation as, while diamictite is the most
650 distinctive lithology, it is not necessarily exclusively of glacial origin, and is not the most
651 volumetrically abundant rock type in all areas (Preiss et al. 2011). Instead, the Sturt Formation
652 comprises numerous lithologies that were deposited under general glacial conditions (Link
653 1977; Link & Gostin 1981; Preiss 1987; 2000; Preiss et al. 2011). This argument in favour of
654 Formation instead of Tillite was made prior by Murrell et al. (1977) and it follows the
655 international stratigraphic guide. A formal definition card accompanies this paper as Appendix
656 1, with the generalised stratigraphic logs of the type and reference sections presented in
657 Figure 3. An additional stratigraphic log from drillhole SR13/2 on the Stuart Shelf is provided in

658 supplementary figure S1.

659 5.5.2 Sturtian Glaciation (Cryochron)/Laurentian Neoproterozoic Glacial Interval

660 Le Heron et al. (2020) proposed that the name “Laurentian Neoproterozoic Glacial Interval” be
661 used in favour of the Sturtian, with the latter name used exclusively for Australian strata. They
662 highlight the issue of interpreting results in a model-led approach, a point we agree on, but
663 primarily base this on their interpretation that most Sturtian rocks of Australia
664 chronometrically lie outside of the Sturtian glacial interval, c. 717–660 Ma, defined by Rooney
665 et al. (2015). Only the tuff from near the base of the Wilyerpa Formation (663.03 ± 0.76 Ma,
666 Cox et al. 2018b) was considered to be within this time interval, and this point was reiterated
667 by Kennedy et al. (2020). However, we argue that this interpretation is incorrect, as the
668 interpretation by Le Heron et al. (2020) appears to hinge on the previous lack of data from the
669 South Australian Sturtian glacial (Yudnamutana Subgroup) and pre-glacial (Burra Group)
670 sequences. Since publication, even with the challenges associated with constraining
671 deposition by detrital zircon studies, two studies (Keeman et al. 2020; Lloyd et al. 2020) have
672 provided maximum depositional age constraints from the Sturt Formation: South Mount Lofty
673 Ranges, 714 ± 28 Ma; South Flinders Ranges, 667 ± 6 Ma; North Flinders Ranges, 673 ± 19
674 Ma. This study presents a further ten detrital zircon samples, with FR3_139 yielding an MDA of
675 666 ± 25 Ma, and a new in-situ Rb–Sr age from the Sturt Formation of 684 ± 37 Ma.
676 Importantly, detrital zircon MDA constraints from the underlying Belair Subgroup, namely the
677 Gilbert Range Quartzite (731 ± 34 Ma, Keeman et al. 2020; Lloyd et al. 2020) and Mitcham
678 Quartzite (c. 730 Ma, Lloyd et al. 2022b [preprint]; van der Wolff 2020) provide the maximum
679 age estimations for which final deposition occurred within the upper Burra Group. Le Heron et
680 al. (2020) treat the Cox et al. (2018b) tuff age (Wilyerpa Formation, AUS) as a maximum
681 depositional age; however, both Fanning and Link (2006) and Cox et al. (2018b) demonstrate
682 that the tuff age is syndepositional, with their age dating volcanism coeval with deglaciation. It
683 provides neither a maximum nor minimum age limit for the entire Wilyerpa Formation as it
684 occurs part way up section with ~50 additional stratigraphic metres overlying the tuff to the
685 base of the Tapley Hill Formation. However, this age provides a robust minimum age constraint
686 for the underlying diamictite. Thus, these two bracketing constraints require that the Sturtian
687 glaciogenic rocks of South Australia (Sturt Formation, Fitton Formation) are deposited c. ≤ 730
688 Ma and $\geq 663 \pm 0.76$ Ma, thereby constraining the age of the true Sturtian (*sensu stricto*) to this
689 time bracket. The initiation of final deglaciation can also be constrained by the data presented
690 here, albeit loosely to between 666 ± 25 Ma and 663.03 ± 0.76 Ma, as samples FR3_139 and
691 FR2_007_01 come from the same stratigraphic interval as the tuff from the Wilyerpa
692 Formation. This independently aligns with the current definition for global timing of the
693 Sturtian Glaciation, c. 717–660 Ma [Figure 11] (Rooney et al. 2015).

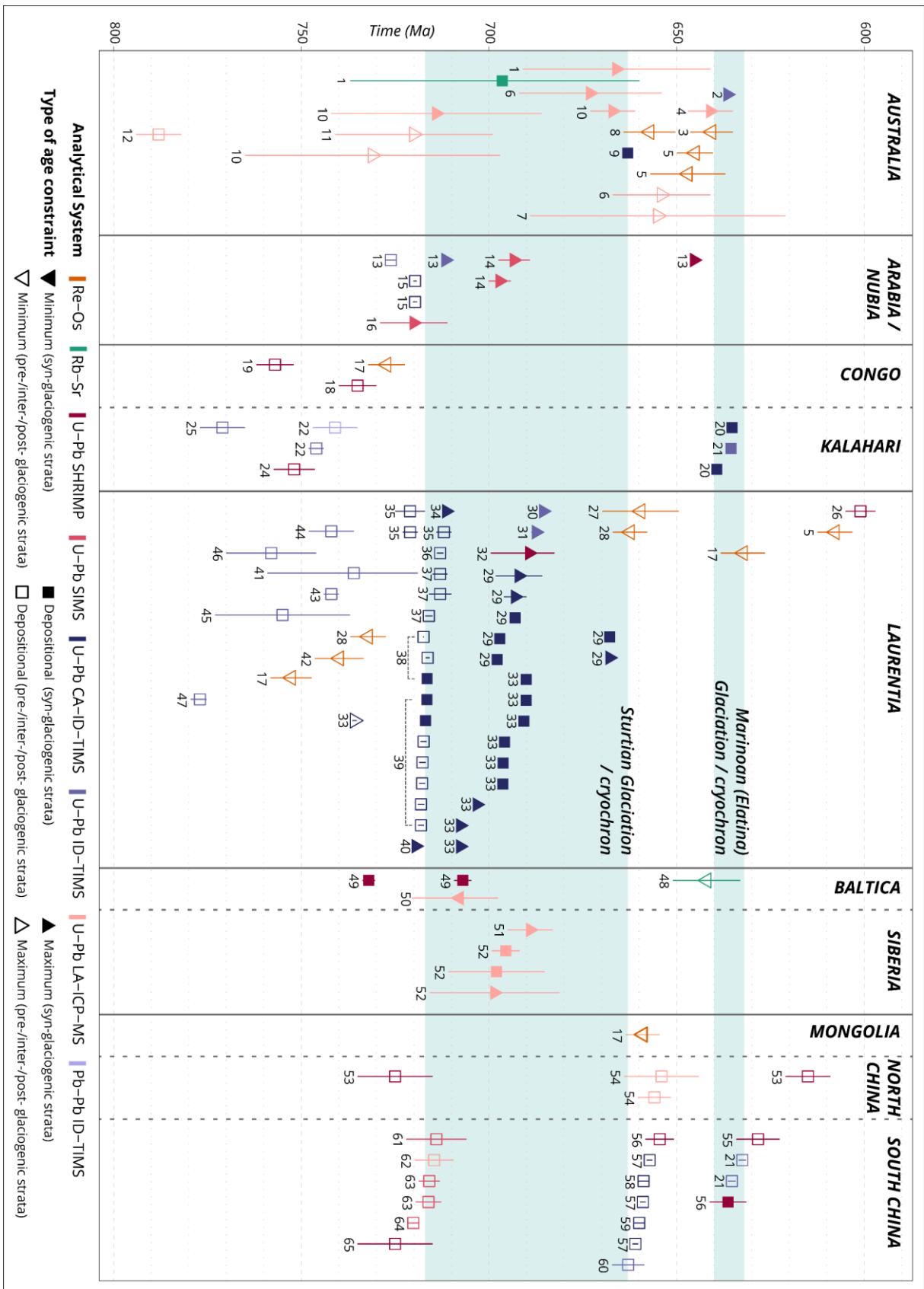


Figure 11 – Compilation of global geochronologic data for the Sturtian and *Marinoan* glaciations. Symbols are colour coded to reflect analytical method (see figure legend for details). Open symbols are data from pre-, inter-, and post-glaciogenic strata, and closed symbols denote data from syn-glaciogenic strata. Shapes signify age type where squares are considered syn-depositional ages, and triangles denote minimum (tip points older) or maximum (tip points younger) depositional ages. Data sources: **AUSTRALIA:** (1) This study; (2) Calver et al. (2013); (3) Kendall et al. (2009); Rose et al. (2013); (5) Kendall et al. (2004); (6) Lloyd et al. (2020); (7) Ireland et al. (1998); (8) Kendall et al. (2006); (9) Cox et al. (2018b); (10) Keeman et al. (2020); (11) van der Wolff (2020); (12) Armistead et al. (2020). **ARABIA/NUBIA:** (13) Bowring et al. (2007); (14) Abd El-Rahman et al. (2020); (15) MacLennan et al. (2018); (16) Li, XH et al. (2018). **CONGO:** (17) Rooney et al. (2015); (18) Key et al. (2001); (19) Nascimento et al. (2016). **KALAHARI:** (20) Prave et al. (2016); (21) Schmitz (2012); (22) Frimmel et al. (1996); (23) Hoffman et al. (1996); (24) Borg et al. (2003); (25) Frimmel et al. (2001). **LAURENTIA:** (5) Kendall et al. (2004); (17) Rooney et al. (2015); (26) Dempster et al. (2002); (27) Rooney et al. (2011); (28) Rooney et al. (2014); (29) Isakson (2017); (30) Keeley et al. (2013); (31) Condon and Bowring (2011); (32) Lund et al. (2003); (33) Eyster et al. (2018); (34) Baldwin et al. (2016); (35) Denyszyn et al. (2009b); (36) Cox et al. (2018a); (37) Denyszyn et al. (2009a); (38) Macdonald et al. (2010); (39) Macdonald et al. (2018); (40) Cox et al. (2015); (41) McDonough and Parrish (1991); (42) Strauss et al. (2014); (43) Fetter and Goldberg (1995); (44) Karlstrom et al. (2000); (45) Ross and Villeneuve (1997); (46) Aleinikoff et al. (1995); (47) Jefferson and Parrish (1989). **BALTICA:** (48) Zaitseva et al. (2019); (49) Krasnobaev et al. (2019); (50) Środoń et al. (2022) **SIBERIA:** (51) Kochnev et al. (2015); (52) Rud`ko et al. (2020). **MONGOLIA:** (17) Rooney et al. (2015). **NORTH CHINA:** (53) Xu et al. (2009); (54) He et al. (2014). **SOUTH CHINA:** (21) Schmitz (2012); (55) Chongyu et al. (2005); (56) Zhang, S et al. (2005); (57) Rooney et al. (2020); (58) Zhou, C et al. (2019); (59) Zhou, C-M et al. (2020); (60) Zhou, C et al. (2004); (61) Lan et al. (2015); (62) Song et al. (2017); (63) Lan et al. (2014); (64) Lan et al. (2020); (65) Zhang, Q-R et al. (2008)

695

696 By contrast Le Heron et al. (2020) treat the reworked tuff age from the Pocatello Formation,
 697 USA (Fanning & Link 2004), as a minimum age estimate. This reworked tuff of Fanning and Link
 698 (2004) from the “upper diamictite” (Isakson 2017) of the Pocatello Formation has been re-
 699 evaluated as a maximum depositional age and may actually be a *Marinoan* glacial sequence,
 700 unconformably overlying a non-glacial sequence that in turn unconformably overlies a lower
 701 Sturtian sequence (Isakson 2017). Isakson (2017) had also revised several of the igneous
 702 ages presented in the Le Heron et al. (2020) compilation, notably a syn-Sturtian age from the
 703 Hogback Rhyolite from 684 ± 4 Ma (Lund et al. 2010; Lund et al. 2003) to 693.03 ± 0.73 Ma.
 704 This author also presented two additional ages from volcanics in the lower Scout Mountain
 705 Member of the Pocatello Formation of c. 697 Ma, previously interpreted to be 686 ± 4 Ma
 706 (Fanning & Link 2008). The data of Keeley et al. (2013) from the lower Scout Mountain
 707 member (685 ± 0.4 Ma) are presented as a depositional age by Le Heron et al. (2020), rather
 708 than as a maximum depositional age as the original authors and Isakson (2017) present.

709 Additionally, data from our study refute the Le Heron et al. (2020) suggestion of a short, 2.4
 710 million year, Sturtian glacial, 659.6 ± 10.2 Ma to 657.2 ± 5.4 Ma, based on Re–Os ages from
 711 the Aralka Formation (Kendall et al. 2006), and Ballachulish Slate (Rooney et al. 2011), as the
 712 Australian Sturtian deposits are now constrained to be older than this proposed interval, there
 713 is an erosional unconformity between the Yudnamutana Subgroup rocks and the overlying
 714 post-glacial transgressive sequences, and the Aralka Formation is demonstrably post-glacial.

715 Considering the above, we disagree with the proposal of Le Heron et al. (2020) that the use of
 716 Sturtian to refer to a globally distributed glaciation can no longer be justified. The available
 717 geochronology [Figure 11] suggests that deposition of the Neoproterozoic glaciogenic rocks, in
 718 at least, Australia (Keeman et al. 2020; Lloyd et al. 2020), Arabia/Nubia (MacLennan et al.
 719 2018; Park et al. 2019), Baltica (Środoń et al. 2022), Laurentia (Isakson 2017; Macdonald et
 720 al. 2018), South China (Lan et al. 2020; Rooney et al. 2020; Song et al. 2017; Wang et al.
 721 2019), and Siberia (Rud`ko et al. 2020) occurred globally within the c. 717–665 Ma interval.
 722 This certainly does not discount the possibility of different times for the onset of glaciation, or
 723 the presence of glacial advance and retreats. Final deglaciation appears to be relatively
 724 synchronous globally at c. 665 Ma [Figure 11]. However, it must be noted, that while Figure 11

725 and the equivalent diagram in Le Heron et al. (2020) provide brevity for visualisation and
726 assessment of the expanding global geochronologic datasets for the Cryogenian, they lack
727 detailed stratigraphic context and methodology. This is an unavoidable limitation of this style
728 of diagram, with size, legibility, and accessibility considerations (e.g., Crameri et al. 2020) all
729 contributing to this. The ideal, and more accurate representation of all these data globally,
730 would be detailed stratigraphic logs of each section with accompanying regional correlations
731 and detailed geochronometric methodology and results. At present, in some regions this
732 information is either unavailable, unreliable, or limited. It would also require significant space
733 and would be best attempted in a global review. To highlight this point, the apparent
734 diachroneity of glacial onset present in Laurentia may in part be a result of complexity in
735 zircons (post crystallisation Pb loss) that may be slightly older than current determinations
736 suggest, as hinted at by Isakson (2017), and that these dates are from within glaciogenic
737 strata with both over, and underlying portions of glaciogenic strata. The volcanogenic strata
738 and corresponding dates provide a maximum age for the mid- to upper portions of the
739 glaciogenic formation and do not preclude slightly earlier initiation. Eyster et al. (2018) also
740 highlights how this type of ambiguous interpretation was used to argue for a diachroneity of
741 onset (Baldwin et al. 2016).

742 Careful scrutiny of geochronologic data, particularly detrital zircon data, as a maximum age
743 constraint rather than as depositional age, stratigraphic position and relationships, and
744 carefully considering the limitations of geochronologic studies and methods, is essential as
745 misinterpretations of either can lead to spurious conclusions e.g. “the Kaigas Formation was
746 previously miscorrelated with glaciogenic strata of the Numees Formation” (Rooney et al.
747 2015).

748 6 Conclusions

749 This research provides an updated chronostratigraphic framework for the Yudnamutana
750 Subgroup of South Australia, i.e., the true Sturtian Glaciation. Additionally, the
751 lithostratigraphy representing the glacial maximum of the Sturtian Glaciation in South
752 Australia is consolidated and redefined as the Sturt Formation.

753 Key findings of this research are:

- 754 • An MDA for the (upper) Sturt Formation in the Copley area of 666 ± 25 Ma, providing
755 independent support for MDAs obtained by Keeman et al. (2020) and Lloyd et al.
756 (2020) elsewhere in the Adelaide Superbasin.
- 757 • An in-situ Rb–Sr age from the lower Sturt Formation of 683.8 ± 36.9 | 37.1 Ma (without
758 λ_{SE} | with λ_{SE}), interpreted to be a syn-depositional age.
- 759 • Broadly equivalent detrital zircon spectra of all samples, with local variation, and
760 similarity to underlying Burra and Callanna Group rocks suggests recycling of
761 underlying stratigraphy and sourcing of detritus from local basement rocks consistent
762 with the common occurrence of clasts derived from the underlying geology.
- 763 • Detrital zircon spectra support lithostratigraphic correlation of Yancowinna Subgroup
764 (New South Wales) with the Yudnamutana Subgroup (South Australia).
- 765 • Support for the continued use of Sturtian Glaciation or *cryochron* globally.

766 Funding

767 The Geological Survey of South Australia and the MinEx CRC funded this research. This
768 research was supported by an Australian Government Research Training Program (RTP)
769 Scholarship awarded to JCL.

770 Data Availability

771 Complete data for this publication are freely available for download from figshare at the
772 following links. These datasets contain all the U–Pb geochronology data, trace element data,
773 Rb–Sr geochronology data, and basic sample metadata.

774 Zircon and NIST standards data for all analytical sessions:

775 <https://doi.org/10.6084/m9.figshare.18131432>

776 Yudnamutana Subgroup detrital zircon data (this study):

777 <https://doi.org/10.6084/m9.figshare.19181144>

778 Zircon CL images: <https://doi.org/10.6084/m9.figshare.19181024>

779 Shale Rb–Sr data: <https://doi.org/10.6084/m9.figshare.21624162>

780 Code Availability

781 R code used to generate the zircon geochemistry plots is available on GitHub at

782 <https://github.com/jarredclloyd/zircon-trace-element-plots>

783 PowerShell module used to adjust headers for rho calculation is available on GitHub at

784 https://github.com/jarredclloyd/PowerShell_LADR_errorcorrelation_workaround

785 CRediT author statement

786 **Jarred C. Lloyd:** Conceptualisation, investigation, writing - original draft, writing - review &
787 editing, methodology, formal analysis, data curation, visualisation. **Wolfgang V. Preiss:**
788 Investigation, writing – review and editing. **Alan S. Collins:** Conceptualisation, funding
789 acquisition, supervision, investigation, writing - review & editing. **Georgina M. Virgo:**
790 Investigation, writing – review and editing. **Morgan L. Blades:** Investigation, writing - review &
791 editing. **Sarah E. Gilbert:** Formal analysis, methodology, investigation, writing - review &
792 editing. **Darwinaji Subarkah:** Investigation, writing - review & editing. **Carmen B. E. Krapf:**
793 Investigation, writing - review & editing, funding acquisition. **Kathryn J. Amos:**
794 Conceptualisation, supervision, writing - review & editing.

795 Acknowledgements

796 We acknowledge the Adnyamathanha, Arabana, Banggarla, Kurna, Kokatha, Kuyani, Ngadjuri
797 and Nukunu Peoples as the Traditional Owners and Custodians of the land on which this
798 research was conducted. We acknowledge and respect their deep feelings of attachment and
799 spiritual relationship to Country, and that their cultural and heritage beliefs are still as
800 important to the living people today.

801 The authors acknowledge the instruments and scientific and technical assistance of
802 Microscopy Australia at Adelaide Microscopy, The University of Adelaide, a facility that is
803 funded by the University, and State and Federal Governments. Particular thanks to Aoife
804 McFadden for their assistance with SEM-CL imaging.

805 We also thank James Nankivell (University of Adelaide) for their assistance with fieldwork, and
806 the Geological Survey of South Australia and MinEx CRC for funding the research. Chris Folkes
807 (Geological Survey of New South Wales) and John Greenfield (formerly GSNSW) are thanked
808 for their expertise on the New South Wales sequences. Arkaroola Wilderness Sanctuary and
809 Operation Flinders (Yankaninna Station) are thanked for their generous hospitality during
810 fieldwork on their properties.

811 This work is conducted with the relevant permissions and scientific permits from the relevant
812 stakeholders. This publication forms MinEx CRC output #XXXX

813 References

- 814 Abd El-Rahman, Y, Gutzmer, J, Li, X-H, Seifert, T, Li, C-F, Ling, X-X & Li, J 2020, 'Not all Neoproterozoic iron
815 formations are glaciogenic: Sturtian-aged non-Rapitan exhalative iron formations from the Arabian–
816 Nubian Shield', *Mineralium Deposita*, vol. 55, no. 3, pp. 577-596. doi:10.1007/s00126-019-00898-
817 0.
- 818 Aleinikoff, JN, Zartman, RE, Walter, M, Rankin, DW, Lyttle, PT & Burton, WC 1995, 'U-Pb ages of metarhyolites
819 of the Catoctin and Mount Rogers formations, Central and Southern Appalachians; evidence for two
820 pulses of Iapetan rifting', *American Journal of Science*, vol. 295, no. 4, p. 428.
821 doi:10.2475/ajs.295.4.428.
- 822 Ali, DO, Spencer, AM, Fairchild, IJ, Chew, KJ, Anderton, R, Levell, BK, Hambrey, MJ, Dove, D & Le Heron, DP
823 2018, 'Indicators of relative completeness of the glacial record of the Port Askaig Formation,
824 Garvellach Islands, Scotland', *Precambrian Research*, vol. 319, pp. 65-78.
825 doi:10.1016/j.precamres.2017.12.005.
- 826 Allen, PA & Etienne, JL 2008, 'Sedimentary challenge to Snowball Earth', *Nature Geoscience*, vol. 1, no. 12,
827 pp. 817-825. doi:10.1038/ngeo355.
- 828 Ambrose, GJ, Flint, RB & Webb, AW 1981, *Precambrian and Palaeozoic Geology of the Peake and Denison*
829 *Ranges*, Bulletin, 50, Geological Survey of South Australia, Adelaide, South Australia.
- 830 Anenburg, M 2020, 'Rare earth mineral diversity controlled by REE pattern shapes', *Mineralogical Magazine*,
831 vol. 84, no. 5, pp. 629-639. doi:10.1180/mgm.2020.70.
- 832 Anenburg, M & Williams, MJ 2021, 'Quantifying the Tetrad Effect, Shape Components, and Ce–Eu–Gd
833 Anomalies in Rare Earth Element Patterns', *Mathematical Geosciences*. doi:10.1007/s11004-021-
834 09959-5.
- 835 Armistead, SE, Collins, AS, Buckman, S & Atkins, R 2020, 'Age and geochemistry of the Boucaut Volcanics in
836 the Neoproterozoic Adelaide Rift Complex, South Australia', *Australian Journal of Earth Sciences*, pp.
837 1-10. doi:10.1080/08120099.2021.1840435.
- 838 Arnaud, E, Halverson, GP & Shields-Zhou, GA (eds) 2011, *The Geological Record of Neoproterozoic*
839 *Glaciations*, Memoirs, 36, Geological Society, London.
- 840 Baldwin, GJ, Turner, EC & Kamber, BS 2016, 'Tectonic controls on distribution and stratigraphy of the
841 Cryogenian Rapitan iron formation, northwestern Canada', *Precambrian Research*, vol. 278, pp. 303-
842 322. doi:10.1016/j.precamres.2016.03.014.
- 843 Barovich, KM & Hand, M 2008, 'Tectonic setting and provenance of the Paleoproterozoic Willyama
844 Supergroup, Curnamona Province, Australia: Geochemical and Nd isotopic constraints on contrasting
845 source terrain components', *Precambrian Research*, vol. 166, no. 1, pp. 318-337.
846 doi:10.1016/j.precamres.2007.06.024.
- 847 Belousova, EA, Reid, AJ, Griffin, WL & O'Reilly, SY 2009, 'Rejuvenation vs. recycling of Archean crust in the
848 Gawler Craton, South Australia: Evidence from U–Pb and Hf isotopes in detrital zircon', *Lithos*, vol.
849 113, no. 3-4, pp. 570-582. doi:10.1016/j.lithos.2009.06.028.
- 850 Belperio, AP 1973, 'The stratigraphy and facies of the Late Precambrian Lower Glacial sequence, Mt Painter,
851 South Australia', Department of Geology, Honours Thesis, Bachelor of Science (Honours), University
852 of Adelaide, Adelaide, South Australia, <<https://hdl.handle.net/2440/131123>>.
- 853 Borg, G, Kärner, K, Buxton, M, Armstrong, R & Merwe, SWvd 2003, 'Geology of the Skorpion Supergene Zinc
854 Deposit, Southern Namibia', *Economic Geology*, vol. 98, no. 4, pp. 749-771.
855 doi:10.2113/gsecongeo.98.4.749.

- 856 Bowring, SA, Grotzinger, JP, Condon, DJ, Ramezani, J, Newall, MJ & Allen, PA 2007, 'Geochronologic
857 constraints on the chronostratigraphic framework of the Neoproterozoic Huqf Supergroup, Sultanate
858 of Oman', *American Journal of Science*, vol. 307, no. 10, pp. 1097-1145. doi:10.2475/10.2007.01.
- 859 Brocks, JJ 2018, 'The transition from a cyanobacterial to algal world and the emergence of animals',
860 *Emerging Topics in Life Sciences*, vol. 2, no. 2, pp. 181-190. doi:10.1042/etls20180039.
- 861 Brocks, JJ, Jarrett, AJM, Sirantoine, E, Hallmann, C, Hoshino, Y & Liyanage, T 2017, 'The rise of algae in
862 Cryogenian oceans and the emergence of animals', *Nature*, vol. 548, no. 7669, pp. 578-581.
863 doi:10.1038/nature23457.
- 864 Callen, RA 1990, *Curnamona*, 1:250 000 Geological Series—Explanatory Notes, Department of Mines and
865 Energy, Adelaide, South Australia.
- 866 Calver, CR, Crowley, JL, Wingate, MTD, Evans, DAD, Raub, TD & Schmitz, MD 2013, 'Globally synchronous
867 Marinoan deglaciation indicated by U-Pb geochronology of the Cottons Breccia, Tasmania, Australia',
868 *Geology*, vol. 41, no. 10, pp. 1127-1130. doi:10.1130/g34568.1.
- 869 Chongyu, Y, Feng, T, Liu, Y, Gao, L, Yang, Z, Wang, Z, Liu 刘鹏举, P, Xing, YZ & Song, B 2005, 'New U-Pb zircon
870 ages from the Ediacaran (Sinian) System in the Yangtze Gorges: Constraint on the age of Miaohu
871 biota and Marinoan glaciation', *Geological Bulletin of China*, vol. 24, pp. 393-400.
- 872 Coats, RP & Forbes, BG 1977, 'Evidence for two Sturtian Glaciations in South Australia', *Quarterly Geological
873 Notes*, vol. 64, pp. 19-20.
874 [https://sarigbasis.pir.sa.gov.au/WebtopEw/ws/samref/sarig1/wci/Record?r=0&m=1&w=catno=2041
875 398.](https://sarigbasis.pir.sa.gov.au/WebtopEw/ws/samref/sarig1/wci/Record?r=0&m=1&w=catno=2041398)
- 876 Coats, RP & Preiss, WV 1987, 'Stratigraphy of the Umberatana Group', in WV Preiss (ed.), *Adelaide
877 Geosyncline—late Proterozoic stratigraphy, sedimentation, palaeontology and tectonics*, Geological
878 Survey of South Australia, Adelaide, South Australia, pp. 125-211.
- 879 Collins, AS, Reddy, SM, Buchan, C & Mruma, A 2004, 'Temporal constraints on Palaeoproterozoic eclogite
880 formation and exhumation (Usagaran Orogen, Tanzania)', *Earth and Planetary Science Letters*, vol.
881 224, no. 1, pp. 175-192. doi:10.1016/j.epsl.2004.04.027.
- 882 Condon, DJ & Bowring, SA 2011, 'A user's guide to Neoproterozoic geochronology', in E Arnaud, GP
883 Halverson & GA Shields-Zhou (eds), *The Geological Record of Neoproterozoic Glaciations*, Geological
884 Society, London, pp. 135-149.
- 885 Conor, CHH & Preiss, WV 2008, 'Understanding the 1720–1640Ma Palaeoproterozoic Willyama Supergroup,
886 Curnamona Province, Southeastern Australia: Implications for tectonics, basin evolution and ore
887 genesis', *Precambrian Research*, vol. 166, no. 1, pp. 297-317.
888 doi:10.1016/j.precamres.2007.08.020.
- 889 Conor, CHH & Preiss, WV 2019, 'Cryogenian glaciomarine megaclasts of the MacDonald Corridor, Bimbowrie
890 Conservation Park, Olary Region, South Australia', *Australian Journal of Earth Sciences*, vol. 67, no. 6,
891 pp. 857-872. doi:10.1080/08120099.2018.1553206.
- 892 Cooper, BJ 2010, '“Snowball Earth”: The Early Contribution from South Australia', *Earth Sciences History*, vol.
893 29, no. 1, pp. 121-145. doi:10.17704/eshi.29.1.j8874825610u68w5.
- 894 Cooper, PF 1973, 'Striated Pebbles from the Late Precambrian Adelaidean', *Quarterly Notes - Geological
895 Survey of New South Wales*, vol. 11, pp. 13-15.
- 896 Cooper, PF & Tuckwell, KD 1971, 'The upper Precambrian Adelaidean of the Broken Hill area—a new
897 subdivision', *Quarterly Notes - Geological Survey of New South Wales*, vol. 3, pp. 8-16.

- 898 Cooper, PF, Tuckwell, KD, Gilligan, LB & Meares, RMD 1974, *Geology of the Torrowangee and Fowlers Gap*
899 *1:100,000 Sheets*, Geological Survey of New South Wales, Department of Mines, Sydney, New South
900 Wales.
- 901 Counts, JW 2017, *The Adelaide Rift Complex in the Flinders Ranges: geologic history, past investigations and*
902 *relevant analogues*, Report Book, no. 2017/00016, Geological Survey of South Australia,
903 Department of Premier and Cabinet, Adelaide, South Australia,
904 <[https://sarigbasis.pir.sa.gov.au/WebtopEw/ws/samref/sarig1/wcir/Record?r=0&m=1&w=catno=20](https://sarigbasis.pir.sa.gov.au/WebtopEw/ws/samref/sarig1/wcir/Record?r=0&m=1&w=catno=2039731)
905 [39731](https://sarigbasis.pir.sa.gov.au/WebtopEw/ws/samref/sarig1/wcir/Record?r=0&m=1&w=catno=2039731)>.
- 906 Cowley, WM 2020, 'Geological setting of exceptional geological features of the Flinders Ranges', *Australian*
907 *Journal of Earth Sciences*, vol. 67, no. 6, pp. 763-785. doi:10.1080/08120099.2020.1748109.
- 908 Cox, GM, Halverson, GP, Denyszyn, S, Foden, J & Macdonald, FA 2018a, 'Cryogenian magmatism along the
909 north-western margin of Laurentia: Plume or rift?', *Precambrian Research*, vol. 319, pp. 144-157.
910 doi:10.1016/j.precamres.2017.09.025.
- 911 Cox, GM, Halverson, GP, Minarik, WG, Le Heron, DP, Macdonald, FA, Bellefroid, EJ & Strauss, JV 2013,
912 'Neoproterozoic iron formation: An evaluation of its temporal, environmental and tectonic
913 significance', *Chemical Geology*, vol. 362, pp. 232-249. doi:10.1016/j.chemgeo.2013.08.002.
- 914 Cox, GM, Isakson, V, Hoffman, PF, Gernon, TM, Schmitz, MD, Shahin, S, Collins, AS, Preiss, WV, Blades, ML,
915 Mitchell, RN & Nordsvan, A 2018b, 'South Australian U-Pb zircon (CA-ID-TIMS) age supports globally
916 synchronous Sturtian deglaciation', *Precambrian Research*, vol. 315, pp. 257-263.
917 doi:10.1016/j.precamres.2018.07.007.
- 918 Cox, GM, Strauss, JV, Halverson, GP, Schmitz, MD, McClelland, WC, Stevenson, RS & Macdonald, FA 2015,
919 'Kikiktat volcanics of Arctic Alaska—Melting of harzburgitic mantle associated with the Franklin large
920 igneous province', *Lithosphere*, vol. 7, no. 3, pp. 275-295. doi:10.1130/l435.1.
- 921 Crameri, F, Shephard, GE & Heron, PJ 2020, 'The misuse of colour in science communication', *Nature*
922 *Communications*, vol. 11, no. 1, p. 5444. doi:10.1038/s41467-020-19160-7.
- 923 Dalgarno, CR & Johnson, JE 1966, *Parachilna map sheet SH54-13*, 1st edn, Geological Atlas of South
924 Australia, 1:250 000 series, Geological Survey of South Australia, Adelaide, South Australia.
- 925 David, TWE 1906, 'Australis: les conditions du climat aux époques géologiques', in *10th International*
926 *Geological Congress*, Mexico.
- 927 Dempster, TJ, Rogers, G, Tanner, PWG, Bluck, BJ, Muir, RJ, Redwood, SD, Ireland, TR & Paterson, BA 2002,
928 'Timing of deposition, orogenesis and glaciation within the Dalradian rocks of Scotland: constraints
929 from U–Pb zircon ages', *Journal of the Geological Society*, vol. 159, no. 1, pp. 83-94.
930 doi:10.1144/0016-764901061.
- 931 Denyszyn, SW, Davis, DW & Halls, HC 2009a, 'Paleomagnetism and U–Pb geochronology of the Clarence
932 Head dykes, Arctic Canada: orthogonal emplacement of mafic dykes in a large igneous province',
933 *Canadian Journal of Earth Sciences*, vol. 46, no. 3, pp. 155-167. doi:10.1139/E09-011.
- 934 Denyszyn, SW, Halls, HC, Davis, DW & Evans, DAD 2009b, 'Paleomagnetism and U–Pb geochronology of
935 Franklin dykes in High Arctic Canada and Greenland: a revised age and paleomagnetic pole
936 constraining block rotations in the Nares Strait region', *Canadian Journal of Earth Sciences*, vol. 46,
937 no. 9, pp. 689-705. doi:10.1139/E09-042.
- 938 Drexel, JF & Preiss, WV (eds) 1995, *The geology of South Australia*, vol. 2, The Phanerozoic, Bulletin, 54,
939 Geological Survey of South Australia, South Australia.

- 940 Dröllner, M, Barham, M, Kirkland, CL & Ware, B 2021, 'Every zircon deserves a date: selection bias in detrital
941 geochronology', *Geological Magazine*, vol. 158, no. 6, pp. 1135-1142.
942 doi:10.1017/s0016756821000145.
- 943 Dunn, PR, Thomson, BP & Rankama, K 1971, 'Late Pre-Cambrian Glaciation in Australia as a Stratigraphic
944 Boundary', *Nature*, vol. 231, no. 5304, pp. 498-502. doi:10.1038/231498a0.
- 945 Dyson, IA 1996, 'Stratigraphy of the Burra and Umberatana Groups in the Willippa Anticline, central Flinders
946 Ranges', *Quarterly Geological Notes*, vol. 129, pp. 10-26.
- 947 Dyson, IA 2004, 'Geology of the eastern Willouran Ranges - evidence for earliest onset of salt tectonics in the
948 Adelaide Geosyncline', *MESA Journal*, vol. 35, pp. 46-56.
949 [https://sarigbasis.pir.sa.gov.au/WebtopEw/ws/samref/sarig1/wci/Record?r=0&m=1&w=catno=2023](https://sarigbasis.pir.sa.gov.au/WebtopEw/ws/samref/sarig1/wci/Record?r=0&m=1&w=catno=2023965)
950 [965.](https://sarigbasis.pir.sa.gov.au/WebtopEw/ws/samref/sarig1/wci/Record?r=0&m=1&w=catno=2023965)
- 951 Edgoose, CJ 2013, 'Chapter 23: Amadeus Basin', in M Ahmad & TJ Munson (eds), *Geology and mineral*
952 *resources of the Northern Territory*, Northern Territory Geological Survey, Northern Territory.
- 953 Eyles, N & Januszczak, N 2004, 'Zipper-rift': a tectonic model for Neoproterozoic glaciations during the
954 breakup of Rodinia after 750 Ma', *Earth-Science Reviews*, vol. 65, no. 1-2, pp. 1-73.
955 doi:10.1016/s0012-8252(03)00080-1.
- 956 Eyster, A, Ferri, F, Schmitz, MD & Macdonald, FA 2018, 'One diamictite and two rifts: Stratigraphy and
957 geochronology of the Gataga Mountain of northern British Columbia', *American Journal of Science*,
958 vol. 318, no. 2, pp. 167-207. doi:10.2475/02.2018.1.
- 959 Fairchild, IJ & Kennedy, MJ 2007, 'Neoproterozoic glaciation in the Earth System', *Journal of the Geological*
960 *Society*, vol. 164, no. 5, pp. 895-921. doi:10.1144/0016-76492006-191.
- 961 Fairchild, IJ, Spencer, AM, Ali, DO, Anderson, RP, Anderton, R, Boomer, I, Dove, D, Evans, JD, Hambrey, MJ,
962 Howe, J, Sawaki, Y, Shields, GA, Skelton, A, Tucker, ME, Wang, Z & Zhou, Y 2018, 'Tonian-Cryogenian
963 boundary sections of Argyll, Scotland', *Precambrian Research*, vol. 319, pp. 37-64.
964 doi:10.1016/j.precamres.2017.09.020.
- 965 Fanning, CM & Link, PK 2004, 'U-Pb SHRIMP ages of Neoproterozoic (Sturtian) glaciogenic Pocatello
966 Formation, southeastern Idaho', *Geology*, vol. 32, no. 10, pp. 881-884. doi:10.1130/G20609.1.
- 967 Fanning, CM & Link, PK 2006, 'Constraints on the timing of the Sturtian Glaciation from Southern Australia; IE
968 for the true Sturtian', in *2006 Philadelphia Annual Meeting*, vol. 7, Geological Society of America,
969 Pennsylvania, p. 115.
- 970 Fanning, CM & Link, PK 2008, 'Age constraints for the Sturtian Glaciation; data from the Adelaide
971 Geosyncline, South Australia and Pocatello Formation, Idaho, USA', in SJ Gallagher & MW Wallace
972 (eds), *Neoproterozoic extreme climates and the origin of early metazoan life, Selwyn Symposium of the*
973 *GSA Victoria Division*, Geological Society of Australia, The University of Melbourne, vol. 91, pp. 57-
974 62.
- 975 Fanning, CM, Reid, AJ & Teale, GS 2007, *A geochronological framework for the Gawler Craton, South*
976 *Australia*, Bulletin, 55, Geological Survey of South Australia, Adelaide, South Australia.
- 977 Fergusson, CL, Henderson, RA, Fanning, CM & Withnall, IW 2007, 'Detrital zircon ages in Neoproterozoic to
978 Ordovician siliciclastic rocks, northeastern Australia: implications for the tectonic history of the East
979 Gondwana continental margin', *Journal of the Geological Society*, vol. 164, no. 1, pp. 215-225.
980 doi:10.1144/0016-76492005-136.
- 981 Fetter, AH & Goldberg, SA 1995, 'Age and Geochemical Characteristics of Bimodal Magmatism in the
982 Neoproterozoic Grandfather Mountain Rift Basin', *The Journal of Geology*, vol. 103, no. 3, pp. 313-
983 326. doi:10.1086/629749.

- 984 Fioretti, AM, Black, LP, Foden, J & Visonà, D 2005, 'Grenville-age magmatism at the South Tasman Rise
985 (Australia): A new piercing point for the reconstruction of Rodinia', *Geology*, vol. 33, no. 10, pp. 769-
986 772. doi:10.1130/G21671.1.
- 987 Fitzherbert, JA & Downes, PM 2015, 'A concise geological history of the Broken Hill region', *Quarterly Notes -
988 Geological Survey of New South Wales*, vol. 143, no. 2, pp. 29-43.
- 989 Foden, JD, Elburg, MA, Dougherty-Page, J & Burt, A 2006, 'The timing and duration of the Delamerian
990 orogeny: Correlation with the Ross Orogen and implications for Gondwana assembly', *Journal of
991 Geology*, vol. 114, no. 2, pp. 189-210. doi:10.1086/499570.
- 992 Foden, JD, Elburg, MA, Turner, S, Clark, C, Blades, ML, Cox, G, Collins, AS, Wolff, K & George, C 2020,
993 'Cambro-Ordovician magmatism in the Delamerian orogeny: Implications for tectonic development
994 of the southern Gondwanan margin', *Gondwana Research*, vol. 81, pp. 490-521.
995 doi:10.1016/j.gr.2019.12.006.
- 996 Forbes, BG 1971, *Parachilna*, 1:250 000 Geological Series—Explanatory Notes, Department of Mines South
997 Australia, Adelaide, South Australia.
- 998 Forbes, BG & Cooper, RS 1976, 'The Pualco Tillite of the Olary Region, South Australia', *Quarterly Geological
999 Notes*, vol. 60, pp. 2-5.
- 1000 Fraser, GL, McAvaney, S, Neumann, NL, Szpunar, M & Reid, A 2010, 'Discovery of early Mesoarchean crust in
1001 the eastern Gawler Craton, South Australia', *Precambrian Research*, vol. 179, no. 1, pp. 1-21.
1002 doi:10.1016/j.precamres.2010.02.008.
- 1003 Fraser, GL & Neumann, NL 2010, *New SHRIMP U-Pb Zircon Ages from the Gawler Craton and Curnamona
1004 Province, South Australia, 2008 - 2010*, Record, no. 2010/16, Geoscience Australia, G Australia,
1005 Canberra, <<http://pid.geoscience.gov.au/dataset/ga/70348>>.
- 1006 Frimmel, HE, Klötzli, US & Siegfried, PR 1996, 'New Pb-Pb Single Zircon Age Constraints on the Timing of
1007 Neoproterozoic Glaciation and Continental Break-up in Namibia', *The Journal of Geology*, vol. 104,
1008 pp. 459-469. doi:10.1086/629839.
- 1009 Frimmel, HE, Zartman, RE & Späth, A 2001, 'The Richtersveld Igneous Complex, South Africa: U-Pb Zircon
1010 and Geochemical Evidence for the Beginning of Neoproterozoic Continental Breakup', *The Journal of
1011 Geology*, vol. 109, pp. 493-508. doi:10.1086/320795.
- 1012 Gehrels, GE, Valencia, VA & Ruiz, J 2008, 'Enhanced precision, accuracy, efficiency, and spatial resolution of
1013 U-Pb ages by laser ablation-multicollector-inductively coupled plasma-mass spectrometry',
1014 *Geochemistry, Geophysics, Geosystems*, vol. 9, no. 3. doi:10.1029/2007gc001805.
- 1015 Govindaraju, K 1995, '1995 WORKING VALUES WITH CONFIDENCE LIMITS FOR TWENTY-SIX CRPG, ANRT
1016 AND IWG-GIT GEOSTANDARDS', *Geostandards Newsletter*, vol. 19, no. s1, pp. 1-32.
1017 doi:10.1111/j.1751-908X.1995.tb00164.x.
- 1018 Gradstein, FM, Ogg, JG & Smith, AG (eds) 2005, *A Geologic Time Scale 2004*, Cambridge University Press,
1019 Cambridge.
- 1020 Grimes, CB, John, BE, Kelemen, PB, Mazdab, FK, Wooden, JL, Cheadle, MJ, Hanghøj, K & Schwartz, JJ 2007,
1021 'Trace element chemistry of zircons from oceanic crust: A method for distinguishing detrital zircon
1022 provenance', *Geology*, vol. 35, no. 7, pp. 643-646. doi:10.1130/G23603A.1.
- 1023 Grimes, CB, Wooden, JL, Cheadle, MJ & John, BE 2015, "'Fingerprinting" tectono-magmatic provenance
1024 using trace elements in igneous zircon', *Contributions to Mineralogy and Petrology*, vol. 170, no. 5, p.
1025 46. doi:10.1007/s00410-015-1199-3.

- 1026 Halverson, GP, Hurtgen, MT, Porter, SM & Collins, AS 2009, 'Neoproterozoic-Cambrian Biogeochemical
1027 Evolution', in C Gaucher, AN Sial, HE Frimmel & GP Halverson (eds), *Developments in Precambrian
1028 Geology*, vol. 16, Elsevier, pp. 351-365.
- 1029 Halverson, GP, Kunzmann, M, Strauss, JV & Maloof, AC 2017, 'The Tonian-Cryogenian transition in
1030 Northeastern Svalbard', *Precambrian Research*, vol. 319, pp. 79-95.
1031 doi:10.1016/j.precamres.2017.12.010.
- 1032 Halverson, GP, Porter, SM & Gibson, TM 2018, 'Dating the late Proterozoic stratigraphic record', *Emerging
1033 Topics in Life Sciences*, vol. 2, no. 2, pp. 137-147. doi:10.1042/etls20170167.
- 1034 He, J, Zhu, W & Ge, R 2014, 'New age constraints on Neoproterozoic diamictites in Kuruktag, NW China and
1035 Precambrian crustal evolution of the Tarim Craton', *Precambrian Research*, vol. 241, pp. 44-60.
1036 doi:10.1016/j.precamres.2013.11.005.
- 1037 Hoffman, PF 2011, 'A history of Neoproterozoic glacial geology, 1871–1997', in E Arnaud, GP Halverson & GA
1038 Shields-Zhou (eds), *The Geological Record of Neoproterozoic Glaciations*, Geological Society, London,
1039 pp. 17-37.
- 1040 Hoffman, PF, Abbot, DS, Ashkenazy, Y, Benn, DI, Brocks, JJ, Cohen, PA, Cox, GM, Creveling, JR, Donnadieu, Y,
1041 Erwin, DH, Fairchild, IJ, Ferreira, D, Goodman, JC, Halverson, GP, Jansen, MF, Le Hir, G, Love, GD,
1042 Macdonald, FA, Maloof, AC, Partin, CA, Ramstein, G, Rose, BEJ, Rose, CV, Sadler, PM, Tziperman, E,
1043 Voigt, A & Warren, SG 2017a, 'Snowball Earth climate dynamics and Cryogenian geology-geobiology',
1044 *Science Advances*, vol. 3, no. 11, p. e1600983. doi:10.1126/sciadv.1600983.
- 1045 Hoffman, PF & Halverson, GP 2011, 'Neoproterozoic glacial record in the Mackenzie Mountains, northern
1046 Canadian Cordillera', in E Arnaud, GP Halverson & GA Shields-Zhou (eds), *The Geological Record of
1047 Neoproterozoic Glaciations*, Geological Society, London, pp. 397-412.
- 1048 Hoffman, PF, Halverson, GP, Schrag, DP, Higgins, JA, Domack, EW, Macdonald, FA, Pruss, SB, Blättler, CL,
1049 Crockford, PW, Hodgkin, EB, Bellefroid, EJ, Johnson, BW, Hodgskiss, MSW, Lamothe, KG, LoBianco,
1050 SJC, Busch, JF, Howes, BJ, Greenman, JW & Nelson, LL 2021, 'Snowballs in Africa: sectioning a long-
1051 lived Neoproterozoic carbonate platform and its bathyal foreslope (NW Namibia)', *Earth-Science
1052 Reviews*, vol. 219. doi:10.1016/j.earscirev.2021.103616.
- 1053 Hoffman, PF, Hawkins, D, Isachsen, C & Bowring, SA 1996, 'Precise U–Pb zircon ages for early Damaran
1054 magmatism in the Summas Mountains and Welwitschia Inlier, northern Damara belt, Namibia',
1055 *Communications of the geological survey of Namibia*, vol. 11, pp. 47-52.
- 1056 Hoffman, PF, Kaufman, AJ, Halverson, GP & Schrag, DP 1998, 'A Neoproterozoic Snowball Earth', *Science*,
1057 vol. 281, no. 5381, p. 1342. doi:10.1126/science.281.5381.1342.
- 1058 Hoffman, PF, Lamothe, KG, LoBianco, SJC, Hodgskiss, MSW, Bellefroid, EJ, Johnson, BW, Hodgkin, EB &
1059 Halverson, GP 2017b, 'Sedimentary depocenters on Snowball Earth: Case studies from the Sturtian
1060 Chuos Formation in northern Namibia', *Geosphere*, vol. 13, no. 3, pp. 811-837.
1061 doi:10.1130/ges01457.1.
- 1062 Hoffman, PF & Schrag, DP 2002, 'The snowball Earth hypothesis: testing the limits of global change', *Terra
1063 Nova*, vol. 14, no. 3, pp. 129-155. doi:10.1046/j.1365-3121.2002.00408.x.
- 1064 Hogmalm, KJ, Zack, T, Karlsson, AKO, Sjöqvist, ASL & Garbe-Schönberg, D 2017, 'In situ Rb–Sr and K–Ca
1065 dating by LA-ICP-MS/MS: an evaluation of N₂O and SF₆ as reaction gases', *Journal of Analytical
1066 Atomic Spectrometry*, vol. 32, no. 2, pp. 305-313. doi:10.1039/c6ja00362a.
- 1067 Hopton, DL 1983, 'Environmental analysis of the Late Precambrian Appila Tillite equivalent at Depot Flat,
1068 southern Flinders Ranges, South Australia', Department of Geology and Mineralogy, Honours Thesis,
1069 Bachelor of Science (Honours), University of Adelaide, Adelaide, South Australia,
1070 <<https://hdl.handle.net/2440/131612>>.

- 1071 Horstwood, MSA, Košler, J, Gehrels, GE, Jackson, SE, McLean, NM, Paton, C, Pearson, NJ, Sircombe, KN,
1072 Sylvester, P, Vermeesch, P, Bowring, JF, Condon, DJ & Schoene, B 2016, 'Community-Derived
1073 Standards for LA-ICP-MS U-(Th-)Pb Geochronology - Uncertainty Propagation, Age Interpretation
1074 and Data Reporting', *Geostandards and Geoanalytical Research*, vol. 40, no. 3, pp. 311-332.
1075 doi:10.1111/j.1751-908X.2016.00379.x.
- 1076 Hoskin, PWO & Ireland, TR 2000, 'Rare earth element chemistry of zircon and its use as a provenance
1077 indicator', *Geology*, vol. 28, no. 7, pp. 627-630. doi:10.1130/0091-
1078 7613(2000)28<627:REECOZ>2.0.CO;2.
- 1079 Hoskin, PWO & Schaltegger, U 2003, 'The composition of zircon and igneous and metamorphic petrogenesis',
1080 *Reviews in Mineralogy and Geochemistry*, vol. 53, no. 1, pp. 27-62. doi:10.2113/0530027.
- 1081 Howchin, W 1901, 'Preliminary Note on the Existence of Glacial Beds of Cambrian Age in South Australia',
1082 *Transactions of the Royal Society of South Australia*, vol. 25, pp. 10-13.
- 1083 Howchin, W 1904, 'The geology of the Mount Lofty Ranges: Part I', *Transactions of the Royal Society of South
1084 Australia*, vol. 28, pp. 253-280.
- 1085 Howchin, W 1906, 'The geology of the Mount Lofty Ranges: Part II', *Transactions of the Royal Society of South
1086 Australia*, vol. 30, pp. 227-262.
- 1087 Howchin, W 1908, 'Glacial Beds of Cambrian Age in South Australia', *Quarterly Journal of the Geological
1088 Society*, vol. 64, no. 1-4, p. 234. doi:10.1144/GSL.JGS.1908.064.01-04.13.
- 1089 Howchin, W 1920, 'Past Glacial Action in Australia', in ABo Statistics (ed.), *Year Book*, vol. 13, Australian
1090 Bureau of Statistics, Australia, pp. 1133-1146.
- 1091 Ireland, TR, Flöttmann, T, Fanning, CM, Gibson, GM & Preiss, WV 1998, 'Development of the early Paleozoic
1092 Pacific margin of Gondwana from detrital-zircon ages across the Delamerian orogen', *Geology*, vol.
1093 26, no. 3, pp. 243-246. doi:10.1130/0091-7613(1998)026<0243:Dotepp>2.3.Co;2.
- 1094 Isakson, VH 2017, 'Geochronology of the Tectonic, Stratigraphic, and Magmatic Evolution of Neoproterozoic
1095 to Early Paleozoic, North American Cordillera and Cryogenian Glaciation', Department of Geoscience,
1096 Dissertation, Doctor of Philosophy, Boise State University, Boise, Idaho, USA.
- 1097 Jackson, SE, Pearson, NJ, Griffin, WL & Belousova, EA 2004, 'The application of laser ablation-inductively
1098 coupled plasma-mass spectrometry to in situ U-Pb zircon geochronology', *Chemical Geology*, vol.
1099 211, no. 1-2, pp. 47-69. doi:10.1016/j.chemgeo.2004.06.017.
- 1100 Jacobs, J, Elburg, MA, Läufer, A, Kleinhanns, IC, Henjes-Kunst, F, Estrada, S, Ruppel, AS, Damaske, D,
1101 Montero, P & Bea, F 2015, 'Two distinct Late Mesoproterozoic/Early Neoproterozoic basement
1102 provinces in central/eastern Dronning Maud Land, East Antarctica: The missing link, 15–21°E',
1103 *Precambrian Research*, vol. 265, pp. 249-272. doi:10.1016/j.precamres.2015.05.003.
- 1104 Jagodzinski, EA & Fricke, CE 2010, *Compilation of new SHRIMP U-Pb geochronological data for the Southern
1105 Curnamona Province, South Australia, 2010*, Report Book, no. 2010/00014, Geological Survey of
1106 South Australia, Department of Primary Industries and Resources, Adelaide, South Australia.
- 1107 Jagodzinski, EA & McAvaney, SO 2017, *SHRIMP U-Pb geochronology data for northern Eyre Peninsula, 2014–
1108 2016*, Report Book, no. 2016/00001, Geological Survey of South Australia, Department of Premier
1109 and Cabinet, Adelaide, South Australia,
1110 <[https://sarigbasis.pir.sa.gov.au/WebtopEw/ws/samref/sarig1/wci/Record?r=0&m=1&w=catno=203
1111 9475](https://sarigbasis.pir.sa.gov.au/WebtopEw/ws/samref/sarig1/wci/Record?r=0&m=1&w=catno=2039475)>.
- 1112 Jagodzinski, EA, Werner, M, Curtis, S, Fabris, A, Pawley, M & Krapf, C 2020, *SHRIMP Geochronology of the Mt
1113 Double area, Southern Gawler Ranges margin*, Report Book, no. 2020/00006, Geological Survey of
1114 South Australia, Department for Energy and Mining, South Australia.

- 1115 Jefferson, CW & Parrish, RR 1989, 'Late Proterozoic stratigraphy, U–Pb zircon ages, and rift tectonics,
1116 Mackenzie Mountains, northwestern Canada', *Canadian Journal of Earth Sciences*, vol. 26, no. 9, pp.
1117 1784-1801. doi:10.1139/e89-151.
- 1118 Jochum, KP, Weis, U, Stoll, B, Kuzmin, D, Yang, Q, Raczek, I, Jacob, DE, Stracke, A, Birbaum, K, Frick, DA,
1119 Günther, D & Enzweiler, J 2011, 'Determination of Reference Values for NIST SRM 610–617 Glasses
1120 Following ISO Guidelines', *Geostandards and Geoanalytical Research*, vol. 35, no. 4, pp. 397-429.
1121 doi:10.1111/j.1751-908X.2011.00120.x.
- 1122 Karlstrom, KE, Bowring, SA, Dehler, CM, Knoll, AH, Porter, SM, Marais, DJD, Weil, AB, Sharp, ZD, Geissman,
1123 JW, Elrick, MB, Timmons, JM, Crossey, LJ & Davidek, KL 2000, 'Chuar Group of the Grand Canyon:
1124 Record of breakup of Rodinia, associated change in the global carbon cycle, and ecosystem
1125 expansion by 740 Ma', *Geology*, vol. 28, no. 7, pp. 619-622. doi:10.1130/0091-
1126 7613(2000)28<619:CGOTGC>2.0.CO;2.
- 1127 Keeley, JA, Link, PK, Fanning, CM & Schmitz, MD 2013, 'Pre- to synglacial rift-related volcanism in the
1128 Neoproterozoic (Cryogenian) Pocatello Formation, SE Idaho: New SHRIMP and CA-ID-TIMS
1129 constraints', *Lithosphere*, vol. 5, no. 1, pp. 128-150. doi:10.1130/L226.1.
- 1130 Keeman, J, Turner, S, Haines, PW, Belousova, E, Ireland, T, Brouwer, P, Foden, J & Wörner, G 2020, 'New UPb,
1131 Hf and O isotope constraints on the provenance of sediments from the Adelaide Rift Complex –
1132 Documenting the key Neoproterozoic to early Cambrian succession', *Gondwana Research*, vol. 83,
1133 pp. 248-278. doi:10.1016/j.gr.2020.02.005.
- 1134 Kendall, BS, Creaser, RA, Calver, CR, Raub, TD & Evans, DAD 2009, 'Correlation of Sturtian diamictite
1135 successions in southern Australia and northwestern Tasmania by Re–Os black shale geochronology
1136 and the ambiguity of “Sturtian”-type diamictite–cap carbonate pairs as chronostratigraphic marker
1137 horizons', *Precambrian Research*, vol. 172, no. 3-4, pp. 301-310.
1138 doi:10.1016/j.precamres.2009.05.001.
- 1139 Kendall, BS, Creaser, RA, Ross, GM & Selby, D 2004, 'Constraints on the timing of Marinoan “Snowball Earth”
1140 glaciation by 187Re–187Os dating of a Neoproterozoic, post-glacial black shale in Western Canada',
1141 *Earth and Planetary Science Letters*, vol. 222, no. 3, pp. 729-740. doi:10.1016/j.epsl.2004.04.004.
- 1142 Kendall, BS, Creaser, RA & Selby, D 2006, 'Re–Os geochronology of postglacial black shales in Australia:
1143 Constraints on the timing of “Sturtian” glaciation', *Geology*, vol. 34, no. 9, pp. 729-732.
1144 doi:10.1130/g22775.1.
- 1145 Kennedy, K, Eyles, N & McArthur, A 2020, 'Syn-rift mass flow generated ‘tectonofacies’ and
1146 ‘tectonosequences’ of the Kingston Peak Formation, Death Valley, California, and their bearing on
1147 supposed Neoproterozoic panglacial climates', *Sedimentology*, vol. 68, no. 1, pp. 352-381.
1148 doi:10.1111/sed.12781.
- 1149 Key, RM, Liyungu, AK, Njamu, FM, Somwe, V, Banda, J, Mosley, PN & Armstrong, RA 2001, 'The western arm
1150 of the Lufilian Arc in NW Zambia and its potential for copper mineralization', *Journal of African Earth
1151 Sciences*, vol. 33, no. 3, pp. 503-528. doi:10.1016/S0899-5362(01)00098-7.
- 1152 Knoll, AH, Walter, MR, Narbonne, GM & Christie-Blick, N 2006, 'The Ediacaran Period: a new addition to the
1153 geologic time scale', *Lethaia*, vol. 39, no. 1, pp. 13-30. doi:10.1080/00241160500409223.
- 1154 Kochnev, BB, Pokrovskii, BG & Proshenkin, AI 2015, 'The Upper Neoproterozoic glacial complex in central
1155 areas of the Siberian platform', *Doklady Earth Sciences*, vol. 464, no. 2, pp. 1001-1004.
1156 doi:10.1134/s1028334x15100049.

- 1157 Korsch, RJ, Huston, DL, Henderson, RA, Blewett, RS, Withnall, IW, Fergusson, CL, Collins, WJ, Saygin, E,
1158 Kositcin, N, Meixner, AJ, Chopping, R, Henson, PA, Champion, DC, Hutton, LJ, Wormald, R,
1159 Holzschuh, J & Costelloe, RD 2012, 'Crustal architecture and geodynamics of North Queensland,
1160 Australia: Insights from deep seismic reflection profiling', *Tectonophysics*, vol. 572-573, pp. 76-99.
1161 doi:10.1016/j.tecto.2012.02.022.
- 1162 Krasnobaev, AA, Puchkov, VN, Sergeeva, ND & Busharina, SV 2019, 'Nature of zircon clastics in the Riphean
1163 and Vendian sandstones of the Southern Urals', *Georesursy*, vol. 21, no. 1, pp. 15-25.
1164 doi:10.18599/grs.2019.1.15-25.
- 1165 Kromkhun, K, Foden, JD, Hore, SB & Baines, G 2013, 'Geochronology and Hf isotopes of the bimodal mafic-
1166 felsic high heat producing igneous suite from Mt Painter Province, South Australia', *Gondwana
1167 Research*, vol. 24, no. 3-4, pp. 1067-1079. doi:10.1016/j.gr.2013.01.011.
- 1168 Kruse, PD, Dunster, JN & Munson, TJ 2013, 'Chapter 28: Georgina Basin', in M Ahmad & TJ Munson (eds),
1169 *Geology and mineral resources of the Northern Territory*, Northern Territory Geological Survey,
1170 Northern Territory.
- 1171 Lamothe, KG, Hoffman, PF, Greenman, JW & Halverson, GP 2019, 'Stratigraphy and isotope geochemistry of
1172 the pre-Sturtian Ugab Subgroup, Otavi/Swakop Group, northwestern Namibia', *Precambrian
1173 Research*, vol. 332, p. 105387. doi:10.1016/j.precamres.2019.105387.
- 1174 Lan, Z, Huyskens, MH, Lu, K, Li, X-H, Zhang, G, Lu, D & Yin, Q-Z 2020, 'Toward refining the onset age of
1175 Sturtian glaciation in South China', *Precambrian Research*, vol. 338.
1176 doi:10.1016/j.precamres.2019.105555.
- 1177 Lan, Z, Li, X-H, Zhu, M, Zhang, Q & Li, Q-L 2015, 'Revisiting the Liantuo Formation in Yangtze Block, South
1178 China: SIMS U-Pb zircon age constraints and regional and global significance', *Precambrian
1179 Research*, vol. 263, pp. 123-141. doi:10.1016/j.precamres.2015.03.012.
- 1180 Lan, Z, Li, X, Zhu, M, Chen, Z-Q, Zhang, Q, Li, Q, Lu, D, Liu, Y & Tang, G 2014, 'A rapid and synchronous
1181 initiation of the wide spread Cryogenian glaciations', *Precambrian Research*, vol. 255, pp. 401-411.
1182 doi:10.1016/j.precamres.2014.10.015.
- 1183 Le Heron, DP 2012, 'The Cryogenian record of glaciation and deglaciation in South Australia', *Sedimentary
1184 Geology*, vol. 243-244, pp. 57-69. doi:10.1016/j.sedgeo.2011.09.013.
- 1185 Le Heron, DP, Busfield, ME, Ali, DO, Al Tofaif, S & Vandyk, TM 2018, 'The Cryogenian record in the southern
1186 Kingston Range, California: The thickest Death Valley succession in the hunt for a GSSP',
1187 *Precambrian Research*, vol. 319, pp. 158-172. doi:10.1016/j.precamres.2017.07.017.
- 1188 Le Heron, DP, Busfield, ME & Collins, AS 2014, 'Bolla Bollana boulder beds: A Neoproterozoic trough mouth
1189 fan in South Australia?', *Sedimentology*, vol. 61, no. 4, pp. 978-995. doi:10.1111/sed.12082.
- 1190 Le Heron, DP, Cox, GM, Trundle, A & Collins, AS 2011, 'Two Cryogenian glacial successions compared:
1191 Aspects of the Sturt and Elatina sediment records of South Australia', *Precambrian Research*, vol.
1192 186, no. 1, pp. 147-168. doi:10.1016/j.precamres.2011.01.014.
- 1193 Le Heron, DP, Eyles, N & Busfield, ME 2020, 'The Laurentian Neoproterozoic Glacial Interval: reappraising the
1194 extent and timing of glaciation', *Austrian Journal of Earth Sciences*, vol. 113, no. 1, pp. 59-70.
1195 doi:10.17738/ajes.2020.0004.
- 1196 Lechte, MA & Wallace, MW 2015, 'Sedimentary and tectonic history of the Holowilena Ironstone, a
1197 Neoproterozoic iron formation in South Australia', *Sedimentary Geology*, vol. 329, pp. 211-224.
1198 doi:10.1016/j.sedgeo.2015.09.014.

- 1199 Lechte, MA, Wallace, MW, Hood, AvS, Li, W, Jiang, G, Halverson, GP, Asael, D, McColl, SL & Planavsky, NJ
1200 2019, 'Subglacial meltwater supported aerobic marine habitats during Snowball Earth', *Proc Natl*
1201 *Acad Sci U S A*, vol. 116, no. 51, pp. 25478-25483. doi:10.1073/pnas.1909165116.
- 1202 Lechte, MA, Wallace, MW, Hood, AvS & Planavsky, N 2018, 'Cryogenian iron formations in the glaciogenic
1203 Kingston Peak Formation, California', *Precambrian Research*, vol. 310, pp. 443-462.
1204 doi:10.1016/j.precamres.2018.04.003.
- 1205 Li, XH, Abd El-Rahman, Y, Abu Anbar, M, Li, J, Ling, XX, Wu, LG & Masoud, AE 2018, 'Old Continental Crust
1206 Underlying Juvenile Oceanic Arc: Evidence From Northern Arabian-Nubian Shield, Egypt',
1207 *Geophysical Research Letters*, vol. 45, no. 7, pp. 3001-3008. doi:10.1002/2018gl077121.
- 1208 Li, Z-X & Evans, DAD 2010, 'Late Neoproterozoic 40° intraplate rotation within Australia allows for a tighter-
1209 fitting and longer-lasting Rodinia', *Geology*, vol. 39, no. 1, pp. 39-42. doi:10.1130/g31461.1.
- 1210 Link, PK 1977, 'Facies and palaeogeography of Late Precambrian Sturtian glacial sediments, Copley area,
1211 northern Flinders Ranges and in the Sturt Gorge near Adelaide, South Australia', Department of
1212 Geology and Mineralogy, Honours Thesis, Bachelor of Science (Honours), University of Adelaide,
1213 Adelaide, <<https://hdl.handle.net/2440/131122>>.
- 1214 Link, PK & Christie-Blick, N 2011, 'Neoproterozoic strata of southeastern Idaho and Utah: record of
1215 Cryogenian rifting and glaciation', in E Arnaud, GP Halverson & GA Shields-Zhou (eds), *The Geological*
1216 *Record of Neoproterozoic Glaciations*, Geological Society, London, pp. 425-436.
- 1217 Link, PK & Gostin, VA 1981, 'Facies and paleogeography of Sturtian glacial strata (late Precambrian), South
1218 Australia', *American Journal of Science*, vol. 281, no. 4, p. 353. doi:10.2475/ajs.281.4.353.
- 1219 Lloyd, JC, Blades, ML, Counts, JW, Collins, AS, Amos, KJ, Wade, BP, Hall, JW, Hore, S, Ball, AL, Shahin, S &
1220 Drabsch, M 2020, 'Neoproterozoic geochronology and provenance of the Adelaide Superbasin',
1221 *Precambrian Research*, vol. 350, p. 105849. doi:10.1016/j.precamres.2020.105849.
- 1222 Lloyd, JC, Collins, AS, Blades, ML, Gilbert, SE & Amos, KJ 2022a, 'Early evolution of the Adelaide Superbasin',
1223 *Geosciences*, vol. 12, no. 4, p. 154. doi:10.3390/geosciences12040154.
- 1224 [Preprint] Lloyd, JC, Collins, AS, Blades, ML, Gilbert, SE & Amos, KJ 2022b, 'Late Tonian development of the
1225 Adelaide Superbasin', *EarthArXiv*. doi:10.31223/X5N63H.
- 1226 Lund, K, Aleinikoff, JN & Evans, KV 2011, 'The Edwardsburg Formation and related rocks, Windermere
1227 Supergroup, central Idaho, USA', in E Arnaud, GP Halverson & GA Shields-Zhou (eds), *The Geological*
1228 *Record of Neoproterozoic Glaciations*, Geological Society, London, pp. 437-448.
- 1229 Lund, K, Aleinikoff, JN, Evans, KV, duBray, EA, Dewitt, EH & Unruh, DM 2010, 'SHRIMP U-Pb dating of
1230 recurrent Cryogenian and Late Cambrian–Early Ordovician alkalic magmatism in central Idaho:
1231 Implications for Rodinian rift tectonics', *GSA Bulletin*, vol. 122, no. 3-4, pp. 430-453.
1232 doi:10.1130/B26565.1.
- 1233 Lund, K, Aleinikoff, JN, Evans, KV & Fanning, CM 2003, 'SHRIMP U-Pb geochronology of Neoproterozoic
1234 Windermere Supergroup, central Idaho: Implications for rifting of western Laurentia and
1235 synchronicity of Sturtian glacial deposits', *GSA Bulletin*, vol. 115, no. 3, pp. 349-372.
1236 doi:10.1130/0016-7606(2003)115<0349:SUPGON>2.0.CO;2.
- 1237 Macdonald, FA, Schmitz, MD, Crowley, JL, Roots, CF, Jones, DS, Maloof, AC, Strauss, JV, Cohen, PA, Johnston,
1238 DT & Schrag, DP 2010, 'Calibrating the Cryogenian', *Science*, vol. 327, no. 5970, pp. 1241-1243.
1239 doi:10.1126/science.1183325.
- 1240 Macdonald, FA, Schmitz, MD, Strauss, JV, Halverson, GP, Gibson, TM, Eyster, A, Cox, G, Mamrol, P & Crowley,
1241 JL 2018, 'Cryogenian of Yukon', *Precambrian Research*, vol. 319, pp. 114-143.
1242 doi:10.1016/j.precamres.2017.08.015.

- 1243 Mackay, WG 2011, 'Structure and sedimentology of the Curdimurka Subgroup, northern Adelaide Fold Belt,
1244 South Australia', Doctoral Thesis, Doctor of Philosophy, University of Tasmania, Hobart, Tasmania,
1245 <<https://eprints.utas.edu.au/12486/>>.
- 1246 MacLennan, S, Park, Y, Swanson-Hysell, N, Maloof, A, Schoene, B, Gebreslassie, M, Antilla, E, Tesema, T,
1247 Alene, M & Haileab, B 2018, 'The arc of the Snowball: U-Pb dates constrain the Islay anomaly and
1248 the initiation of the Sturtian glaciation', *Geology*, vol. 46, no. 6, pp. 539-542. doi:10.1130/G40171.1.
- 1249 Mattinson, JM 2005, 'Zircon U-Pb chemical abrasion ("CA-TIMS") method: Combined annealing and multi-
1250 step partial dissolution analysis for improved precision and accuracy of zircon ages', *Chemical
1251 Geology*, vol. 220, no. 1-2, pp. 47-66. doi:10.1016/j.chemgeo.2005.03.011.
- 1252 Mawson, D & Sprigg, RC 1950, 'Subdivision of the Adelaide System', *Australian Journal of Science*, vol. 13,
1253 no. 3, pp. 69-72.
- 1254 McAvaney, SO 2012, 'The Cooyerdoo Granite: Paleo- and Mesoarchean basement of the Gawler Craton',
1255 *MESA Journal*, vol. 65, pp. 31-40.
1256 [https://sarigbasis.pir.sa.gov.au/WebtopEw/ws/samref/sarig1/wci/Record?r=0&m=1&w=catno=2035
1257 289](https://sarigbasis.pir.sa.gov.au/WebtopEw/ws/samref/sarig1/wci/Record?r=0&m=1&w=catno=2035289).
- 1258 McDonough, MR & Parrish, RR 1991, 'Proterozoic gneisses of the Malton Complex, near Valemount, British
1259 Columbia: U-Pb ages and Nd isotopic signatures', *Canadian Journal of Earth Sciences*, vol. 28, no. 8,
1260 pp. 1202-1216. doi:10.1139/e91-108.
- 1261 Meaney, KJ 2012, 'The geochronology and structural evolution of the Warren Inlier and Springfield
1262 Sequence, Mt. Lofty Ranges: Implications for Proterozoic paleogeographic reconstructions', School of
1263 Earth and Environmental Sciences, Honours Thesis, Bachelor of Science (Honours), University of
1264 Adelaide, Adelaide, South Australia, <<https://hdl.handle.net/2440/95177>>.
- 1265 Meaney, KJ 2017, 'Proterozoic crustal growth in the southeastern Gawler Craton: the development of the
1266 Barossa Complex, and an assessment of the detrital zircon method', Department of Geology and
1267 Geophysics, Doctoral Thesis, Doctor of Philosophy, University of Adelaide, Adelaide, South Australia,
1268 <<https://hdl.handle.net/2440/114255>>.
- 1269 Merdith, AS, Williams, SE, Müller, RD & Collins, AS 2017, 'Kinematic constraints on the Rodinia to Gondwana
1270 transition', *Precambrian Research*, vol. 299, pp. 132-150. doi:10.1016/j.precamres.2017.07.013.
- 1271 Miller, RM 2013, 'Comparative Stratigraphic and Geochronological Evolution of the Northern Damara
1272 Supergroup in Namibia and the Katanga Supergroup in the Lufilian Arc of Central Africa', *Geoscience
1273 Canada*, vol. 40, no. 2, pp. 118 - 140. doi:10.12789/geocanj.2013.40.007.
- 1274 Morrissey, LJ, Barovich, KM, Hand, M, Howard, KE & Payne, JL 2019, 'Magmatism and metamorphism at ca.
1275 1.45 Ga in the northern Gawler Craton: The Australian record of rifting within Nuna (Columbia)',
1276 *Geoscience Frontiers*, vol. 10, no. 1, pp. 175-194. doi:10.1016/j.gsf.2018.07.006.
- 1277 Morrissey, LJ, Barovich, KM, Hand, M, Howard, KE, Payne, JL & Reid, AJ 2018, 'The final event in the long
1278 evolution of the Gawler Craton: new constraints on 1450 Ma metamorphism and magmatism', *MESA
1279 Journal*, vol. 88, no. 3, pp. 4-11.
1280 <https://sarigbasis.pir.sa.gov.au/WebtopEw/ws/samref/sarig1/image/DDD/MESAJ088004-011.pdf>.
- 1281 Morrissey, LJ, Hand, M, Wade, BP & Szpunar, MA 2013, 'Early Mesoproterozoic metamorphism in the Barossa
1282 Complex, South Australia: links with the eastern margin of Proterozoic Australia', *Australian Journal
1283 of Earth Sciences*, vol. 60, no. 8, pp. 769-795. doi:10.1080/08120099.2013.860623.
- 1284 Mrofka, D & Kennedy, M 2011, 'The Kingston Peak Formation in the eastern Death Valley region', in E Arnaud,
1285 GP Halverson & GA Shields-Zhou (eds), *The Geological Record of Neoproterozoic Glaciations*,
1286 Geological Society, London, pp. 449-458.

- 1287 Mundil, R, Ludwig, KR, Metcalfe, I & Renne, PR 2004, 'Age and timing of the Permian mass extinctions: U/Pb
1288 dating of closed-system zircons', *Science*, vol. 305, no. 5691, pp. 1760-1763.
1289 doi:10.1126/science.1101012.
- 1290 Murrell, B, Link, PK & Gostin, VA 1977, 'Evidence for only one Sturtian Glacial Period in the Copley map area',
1291 *Quarterly Geological Notes*, vol. 64, pp. 16-19.
1292 [https://sarigbasis.pir.sa.gov.au/WebtopEw/ws/samref/sarig1/wci/Record?r=0&m=1&w=catno=2041](https://sarigbasis.pir.sa.gov.au/WebtopEw/ws/samref/sarig1/wci/Record?r=0&m=1&w=catno=2041398)
1293 [398](https://sarigbasis.pir.sa.gov.au/WebtopEw/ws/samref/sarig1/wci/Record?r=0&m=1&w=catno=2041398).
- 1294 Nascimento, DB, Ribeiro, A, Trouw, RAJ, Schmitt, RS & Passchier, CW 2016, 'Stratigraphy of the
1295 Neoproterozoic Damara Sequence in northwest Namibia: Slope to basin sub-marine mass-transport
1296 deposits and olistolith fields', *Precambrian Research*, vol. 278, pp. 108-125.
1297 doi:10.1016/j.precamres.2016.03.005.
- 1298 Nascimento, DB, Schmitt, RS, Ribeiro, A, Trouw, RAJ, Passchier, CW & Basei, MAS 2017, 'Depositional ages
1299 and provenance of the Neoproterozoic Damara Supergroup (northwest Namibia): Implications for the
1300 Angola-Congo and Kalahari cratons connection', *Gondwana Research*, vol. 52, pp. 153-171.
1301 doi:10.1016/j.gr.2017.09.006.
- 1302 Normington, VJ & Donnellan, NC 2020, *Characterisation of the Neoproterozoic succession of the northeastern*
1303 *Amadeus Basin, Northern Territory*, Record, no. 2020-010, Northern Territory Geological Survey,
1304 <<https://geoscience.nt.gov.au/gemis/ntgsjspui/handle/1/90622>>.
- 1305 Norris, A & Danyushevsky, L 2018, 'Towards Estimating the Complete Uncertainty Budget of Quantified
1306 Results Measured by LA-ICP-MS', in *Goldschmidt*, Norris Scientific, Boston.
- 1307 O'Neill, HSC 2016, 'The Smoothness and Shapes of Chondrite-normalized Rare Earth Element Patterns in
1308 Basalts', *Journal of Petrology*, vol. 57, no. 8, pp. 1463-1508. doi:10.1093/petrology/egw047.
- 1309 Och, LM & Shields-Zhou, GA 2012, 'The Neoproterozoic oxygenation event: Environmental perturbations and
1310 biogeochemical cycling', *Earth-Science Reviews*, vol. 110, no. 1, pp. 26-57.
1311 doi:10.1016/j.earscirev.2011.09.004.
- 1312 Park, Y, Swanson-Hysell, NL, MacLennan, SA, Maloof, AC, Gebreslassie, M, Tremblay, MM, Schoene, B, Alene,
1313 M, Anttila, ESC, Tesema, T & Haileab, B 2019, 'The lead-up to the Sturtian Snowball Earth:
1314 Neoproterozoic chemostratigraphy time-calibrated by the Tambien Group of Ethiopia', *GSA Bulletin*,
1315 vol. 132, no. 5-6, pp. 1119-1149. doi:10.1130/B35178.1.
- 1316 Pawley, MJ, Dutch, RA & Wise, TW 2020, 'The Relationship Between Crustal Architecture, Deformation, and
1317 Magmatism in the Coompana Province, Australia', *Tectonics*, vol. 39, no. 12.
1318 doi:10.1029/2019tc005593.
- 1319 Petterson, R, Prave, AR & Wernicke, BP 2011, 'Glaciogenic and related strata of the Neoproterozoic Kingston
1320 Peak Formation in the Panamint Range, Death Valley region, California', in E Arnaud, GP Halverson &
1321 GA Shields-Zhou (eds), *The Geological Record of Neoproterozoic Glaciations*, Geological Society,
1322 London, pp. 459-465.
- 1323 Plumb, KA 1991, 'New Precambrian time scale', *International Union of Geological Sciences*, vol. 14, no. 2, pp.
1324 139-140. doi:10.18814/epiugs/1991/v14i2/005.
- 1325 Plumb, KA & James, HL 1986, 'Subdivision of precambrian time: recommendations and suggestions by the
1326 subcommission on precambrian stratigraphy', *Precambrian Research*, vol. 32, no. 1, pp. 65-92.
1327 doi:10.1016/0301-9268(86)90031-8.
- 1328 Powell, CM, Preiss, WV, Gatehouse, CG, Krapez, B & Li, Z-X 1994, 'South Australian record of a Rodinian
1329 epicontinental basin and its mid-neoproterozoic breakup (~700 Ma) to form the Palaeo-Pacific
1330 Ocean', *Tectonophysics*, vol. 237, no. 3-4, pp. 113-140. doi:10.1016/0040-1951(94)90250-x.

- 1331 Prave, AR, Condon, DJ, Hoffmann, KH, Tapster, S & Fallick, AE 2016, 'Duration and nature of the end-
1332 Cryogenian (Marinoan) glaciation', *Geology*, vol. 44, no. 8, pp. 631-634. doi:10.1130/G38089.1.
- 1333 Preiss, WV 1985, *Stratigraphy and Tectonics of the Worumba Anticline and Associated Intrusive Breccias*,
1334 Bulletin, 52, Geological Survey of South Australia, South Australia.
- 1335 Preiss, WV 1987, *Adelaide Geosyncline—late Proterozoic stratigraphy, sedimentation, palaeontology and*
1336 *tectonics*, Bulletin, 53, Geological Survey of South Australia, Adelaide, South Australia.
- 1337 Preiss, WV 1993, 'Neoproterozoic', in JF Drexel, WV Preiss & AJ Parker (eds), *The geology of South Australia*,
1338 vol. 1 The Precambrian, Geological Survey of South Australia, South Australia, pp. 171-204.
- 1339 Preiss, WV 2000, 'The Adelaide Geosyncline of South Australia and its significance in Neoproterozoic
1340 continental reconstruction', *Precambrian Research*, vol. 100, no. 1-3, pp. 21-63.
1341 doi:10.1016/S0301-9268(99)00068-6.
- 1342 Preiss, WV 2006, 'Old Boolcoomata Conglomerate Member of the Benda Siltstone', *MESA Journal*, vol. 41,
1343 pp. 15-23.
1344 [https://sarigbasis.pir.sa.gov.au/WebtopEw/ws/samref/sarig1/wci/Record?r=0&m=1&w=catno=2025](https://sarigbasis.pir.sa.gov.au/WebtopEw/ws/samref/sarig1/wci/Record?r=0&m=1&w=catno=2025262)
1345 [262](https://sarigbasis.pir.sa.gov.au/WebtopEw/ws/samref/sarig1/wci/Record?r=0&m=1&w=catno=2025262).
- 1346 Preiss, WV 2014, *Geology and mineral resources of Bimbowrie Conservation Park – the MacDonald Corridor*
1347 *and adjacent parts of the Palaeo- to Mesoproterozoic basement*, Report Book, no. 2014/00003,
1348 Geological Survey of South Australia, I Department for Manufacturing, Trade, Resources and Energy,
1349 South Australia,
1350 <[https://sarigbasis.pir.sa.gov.au/WebtopEw/ws/samref/sarig1/wci/Record?r=0&m=1&w=catno=203](https://sarigbasis.pir.sa.gov.au/WebtopEw/ws/samref/sarig1/wci/Record?r=0&m=1&w=catno=2036052)
1351 [6052](https://sarigbasis.pir.sa.gov.au/WebtopEw/ws/samref/sarig1/wci/Record?r=0&m=1&w=catno=2036052)>.
- 1352 Preiss, WV, Alexander, EM, Cowley, WM & Schwarz, MP 2002, 'Towards defining South Australia's geological
1353 provinces and sedimentary basins', *MESA Journal*, vol. 27, pp. 39-52.
1354 [https://sarigbasis.pir.sa.gov.au/WebtopEw/ws/samref/sarig1/wci/Record?r=0&m=1&w=catno=2022](https://sarigbasis.pir.sa.gov.au/WebtopEw/ws/samref/sarig1/wci/Record?r=0&m=1&w=catno=2022981)
1355 [981](https://sarigbasis.pir.sa.gov.au/WebtopEw/ws/samref/sarig1/wci/Record?r=0&m=1&w=catno=2022981).
- 1356 Preiss, WV & Conon, CHH 2001, 'Origin and nomenclature of the Wilyama Inliers, Curnamona Province', *MESA*
1357 *Journal*, vol. 21, pp. 47-49.
1358 [https://sarigbasis.pir.sa.gov.au/WebtopEw/ws/samref/sarig1/wci/Record?r=0&m=1&w=catno=2022](https://sarigbasis.pir.sa.gov.au/WebtopEw/ws/samref/sarig1/wci/Record?r=0&m=1&w=catno=2022263)
1359 [263](https://sarigbasis.pir.sa.gov.au/WebtopEw/ws/samref/sarig1/wci/Record?r=0&m=1&w=catno=2022263).
- 1360 Preiss, WV, Dyson, IA, Reid, PW & Cowley, WM 1998, 'Revision of lithostratigraphic classification of the
1361 Umberatana Group', *MESA Journal*, vol. 9, pp. 36-42.
1362 [https://sarigbasis.pir.sa.gov.au/WebtopEw/ws/samref/sarig1/wci/Record?r=0&m=1&w=catno=202](https://sarigbasis.pir.sa.gov.au/WebtopEw/ws/samref/sarig1/wci/Record?r=0&m=1&w=catno=2025009)
1363 [5009](https://sarigbasis.pir.sa.gov.au/WebtopEw/ws/samref/sarig1/wci/Record?r=0&m=1&w=catno=2025009).
- 1364 Preiss, WV, Gostin, VA, McKirdy, DM, Ashley, PM, Williams, GE & Schmidt, PW 2011, 'The glacial succession
1365 of Sturtian age in South Australia: The Yudnamutana Subgroup', in E Arnaud, GP Halverson & GA
1366 Shields-Zhou (eds), *The Geological Record of Neoproterozoic Glaciations*, Geological Society, London,
1367 pp. 701-712.
- 1368 Preiss, WV, Walter, MR, Coats, RP & Wells, AT 1978, 'Lithological correlations of Adelaidean glaciogenic rocks
1369 in parts of the Amadeus, Ngalia, and Georgina Basins', *AGSO Journal of Australian Geology and*
1370 *Geophysics*, vol. 3, pp. 43-53. <http://pid.geoscience.gov.au/dataset/ga/80944>.
- 1371 Redaa, A, Farkaš, J, Gilbert, S, Collins, AS, Wade, B, Löhr, S, Zack, T & Garbe-Schönberg, D 2021,
1372 'Assessment of elemental fractionation and matrix effects during in situ Rb–Sr dating of phlogopite
1373 by LA-ICP-MS/MS: implications for the accuracy and precision of mineral ages', *Journal of Analytical*
1374 *Atomic Spectrometry*, vol. 36, no. 2, pp. 322-344. doi:10.1039/d0ja00299b.

- 1375 Reid, AJ, Halpin, JA & Dutch, RA 2019, 'Timing and style of high-temperature metamorphism across the
1376 Western Gawler Craton during the Paleo- to Mesoproterozoic', *Australian Journal of Earth Sciences*,
1377 vol. 66, no. 8, pp. 1085-1111. doi:10.1080/08120099.2019.1602565.
- 1378 Reid, AJ & Hand, M 2012, 'Mesoarchean to Mesoproterozoic evolution of the southern Gawler Craton, South
1379 Australia', *Episodes*, vol. 35, no. 1, pp. 216-225. doi:10.18814/epiiugs/2012/v35i1/021.
- 1380 Reid, AJ, Hand, M, Jagodzinski, EA, Kelsey, DE & Pearson, NJ 2008, 'Paleoproterozoic orogenesis in the
1381 southeastern Gawler Craton, South Australia', *Australian Journal of Earth Sciences*, vol. 55, no. 4, pp.
1382 449-471. doi:10.1080/08120090801888594.
- 1383 Reid, AJ, Jagodzinski, EA, Armit, RJ, Dutch, RA, Kirkland, CL, Betts, PG & Schaefer, BF 2014a, 'U-Pb and Hf
1384 isotopic evidence for Neoproterozoic and Paleoproterozoic basement in the buried northern Gawler
1385 Craton, South Australia', *Precambrian Research*, vol. 250, pp. 127-142.
1386 doi:10.1016/j.precamres.2014.05.019.
- 1387 Reid, AJ, Jagodzinski, EA, Fraser, GL & Pawley, MJ 2014b, 'SHRIMP U-Pb zircon age constraints on the
1388 tectonics of the Neoproterozoic to early Paleoproterozoic transition within the Mulgathing Complex,
1389 Gawler Craton, South Australia', *Precambrian Research*, vol. 250, pp. 27-49.
1390 doi:10.1016/j.precamres.2014.05.013.
- 1391 Reid, AJ, Jagodzinski, EA, Wade, CE, Payne, JL & Jourdan, F 2017, 'Recognition of c. 1780Ma magmatism
1392 and metamorphism in the buried northeastern Gawler Craton: Correlations with events of the Aileron
1393 Province', *Precambrian Research*, vol. 302, pp. 198-220. doi:10.1016/j.precamres.2017.09.010.
- 1394 Reid, AJ & Payne, JL 2017, 'Magmatic zircon Lu-Hf isotopic record of juvenile addition and crustal reworking
1395 in the Gawler Craton, Australia', *Lithos*, vol. 292-293, pp. 294-306.
1396 doi:10.1016/j.lithos.2017.08.010.
- 1397 Reid, AJ, Tiddy, C, Jagodzinski, E, Crowley, J, Conor, C, Brotodewo, A & Wade, C 2021, *Precise zircon U-Pb
1398 geochronology of Hiltaba Suite granites, Point Riley, Yorke Peninsula*, Report Book, no. 2021/00001,
1399 Geological Survey of South Australia, Department for Energy and Mining, South Australia.
- 1400 Romanov, M, Sovetov, JK, Vernikovskiy, VA, Rosenbaum, G, Wilde, SA, Vernikovskaya, AE, Matushkin, NY &
1401 Kadilnikov, PI 2021, 'Late Neoproterozoic evolution of the southwestern margin of the Siberian
1402 Craton: evidence from sedimentology, geochronology and detrital zircon analysis', *International
1403 Geology Review*, vol. 63, no. 13, pp. 1658-1681. doi:10.1080/00206814.2020.1790044.
- 1404 Rooney, AD, Chew, DM & Selby, D 2011, 'Re-Os geochronology of the Neoproterozoic-Cambrian Dalradian
1405 Supergroup of Scotland and Ireland: Implications for Neoproterozoic stratigraphy, glaciations and
1406 Re-Os systematics', *Precambrian Research*, vol. 185, no. 3-4, pp. 202-214.
1407 doi:10.1016/j.precamres.2011.01.009.
- 1408 Rooney, AD, Macdonald, FA, Strauss, JV, Dudas, FÖ, Hallmann, C & Selby, D 2014, 'Re-Os geochronology and
1409 coupled Os-Sr isotope constraints on the Sturtian snowball Earth', *Proceedings of the National
1410 Academy of Sciences of the United States of America*, vol. 111, no. 1, pp. 51-56.
1411 doi:10.1073/pnas.1317266110.
- 1412 Rooney, AD, Strauss, JV, Brandon, AD & Macdonald, FA 2015, 'A Cryogenian chronology: Two long-lasting
1413 synchronous Neoproterozoic glaciations', *Geology*, vol. 43, no. 5, pp. 459-462.
1414 doi:10.1130/G36511.1.
- 1415 Rooney, AD, Yang, C, Condon, DJ, Zhu, M & Macdonald, FA 2020, 'U-Pb and Re-Os geochronology tracks
1416 stratigraphic condensation in the Sturtian snowball Earth aftermath', *Geology*.
1417 doi:10.1130/G47246.1.

- 1418 Rose, CV, Maloof, AC, Schoene, B, Ewing, RC, Linnemann, U, Hofmann, M & Cottle, JM 2013, 'PAUL F.
1419 HOFFMAN SERIES The End-Cryogenian Glaciation of South Australia', *Geoscience Canada*, vol. 40,
1420 no. 4, pp. 256-293. doi:10.12789/geocanj.2013.40.019.
- 1421 Ross, GM & Villeneuve, J 1997, *U-Pb geochronology of stranger stones in Neoproterozoic diamictites,*
1422 *Canadian Cordillera: implications for provenance and ages of deposition*, Report, Geological Survey
1423 of Canada, Natural Resources Canada.
- 1424 Rubatto, D 2002, 'Zircon trace element geochemistry: partitioning with garnet and the link between U–Pb
1425 ages and metamorphism', *Chemical Geology*, vol. 184, no. 1, pp. 123-138. doi:10.1016/S0009-
1426 2541(01)00355-2.
- 1427 Rud`ko, S, Kuznetsov, N, Shatsillo, A, Rud`ko, D, Malyshev, S, Dubenskiy, A, Sheshukov, V, Kanygina, N &
1428 Romanyuk, T 2020, 'Sturtian glaciation in Siberia: Evidence of glacial origin and U-Pb dating of the
1429 diamictites of the Chivida Formation in the north of the Yenisei Ridge', *Precambrian Research*, vol.
1430 345. doi:10.1016/j.precamres.2020.105778.
- 1431 Schmitz, MD 2012, 'Radiometric ages used in GTS2012', in FM Gradstein, JG Ogg, MD Schmitz & GM Ogg
1432 (eds), *The Geologic Time Scale*, pp. 1045-1082.
- 1433 Segnit, RW 1939, *The Precambrian-Cambrian succession - The general and economic geology of these*
1434 *systems, in portions of South Australia*, Bulletin, 18, Department of Mines, Adelaide, South Australia.
- 1435 Shannon, RD 1976, 'Revised effective ionic radii and systematic studies of interatomic distances in halides
1436 and chalcogenides', *Acta Crystallographica Section A*, vol. 32, no. 5, pp. 751-767.
1437 doi:10.1107/S0567739476001551.
- 1438 Shields-Zhou, GA, Porter, SM & Halverson, GP 2016, 'A New Rock-Based Definition for the Cryogenian Period
1439 (Circa 720-635 Ma)', *Episodes*, vol. 39, no. 1. doi:10.18814/epiiugs/2016/v39i1/89231.
- 1440 Shields, GA, Halverson, GP & Porter, SM 2018, 'Descent into the Cryogenian', *Precambrian Research*, vol.
1441 319, pp. 1-5. doi:10.1016/j.precamres.2018.08.015.
- 1442 Shields, GA, Strachan, RA, Porter, SM, Halverson, GP, Macdonald, FA, Plumb, KA, de Alvarenga, CJ, Banerjee,
1443 DM, Bekker, A, Bleeker, W, Brasier, A, Chakraborty, PP, Collins, AS, Condie, K, Das, K, Evans, DAD,
1444 Ernst, R, Fallick, AE, Frimmel, H, Fuck, R, Hoffman, PF, Kamber, BS, Kuznetsov, AB, Mitchell, RN,
1445 Poiré, DG, Poulton, SW, Riding, R, Sharma, M, Storey, C, Stueeken, E, Tostevin, R, Turner, E, Xiao, S,
1446 Zhang, S, Zhou, Y & Zhu, M 2022, 'A template for an improved rock-based subdivision of the pre-
1447 Cryogenian timescale', *Journal of the Geological Society*, vol. 179, no. 1. doi:10.1144/jgs2020-222.
- 1448 Sláma, J & Košler, J 2012, 'Effects of sampling and mineral separation on accuracy of detrital zircon studies',
1449 *Geochemistry Geophysics Geosystems*, vol. 13, no. 5. doi:10.1029/2012gc004106.
- 1450 Sláma, J, Košler, J, Condon, DJ, Crowley, JL, Gerdes, A, Hanchar, JM, Horstwood, MSA, Morris, GA, Nasdala,
1451 L, Norberg, N, Schaltegger, U, Schoene, B, Tubrett, MN & Whitehouse, MJ 2008, 'Plešovice zircon – A
1452 new natural reference material for U–Pb and Hf isotopic microanalysis', *Chemical Geology*, vol. 249,
1453 no. 1, pp. 1-35. doi:10.1016/j.chemgeo.2007.11.005.
- 1454 Smithies, RH, Howard, HM, Evins, PM, Kirkland, CL, Bodorkos, S & Wingate, MTD 2008, *The west Musgrave*
1455 *Complex - new geological insights from recent mapping, geochronology, and geochemical studies*,
1456 Record, no. 2008/19, Geological Survey of Western Australia, Department of Industry and
1457 Resources, <[http://dmpbookshop.eruditetechnologies.com.au/product/the-west-musgrave-
1458 complex-new-geological-insights-from-recent-mapping-geochronology-and-geochemical-
1459 studies.do](http://dmpbookshop.eruditetechnologies.com.au/product/the-west-musgrave-complex-new-geological-insights-from-recent-mapping-geochronology-and-geochemical-studies.do)>.

- 1460 Smithies, RH, Howard, HM, Evins, PM, Kirkland, CL, Kelsey, DE, Hand, M, Wingate, MTD, Collins, AS &
1461 Belousova, EA 2011, 'High-Temperature Granite Magmatism, Crust–Mantle Interaction and the
1462 Mesoproterozoic Intracontinental Evolution of the Musgrave Province, Central Australia', *Journal of*
1463 *Petrology*, vol. 52, no. 5, pp. 931-958. doi:10.1093/petrology/egr010.
- 1464 Smits, RG, Collins, WJ, Hand, M, Dutch, R & Payne, J 2014, 'A Proterozoic Wilson cycle identified by Hf
1465 isotopes in central Australia: Implications for the assembly of Proterozoic Australia and Rodinia',
1466 *Geology*, vol. 42, no. 3, pp. 231-234. doi:10.1130/g35112.1.
- 1467 Song, G, Wang, X, Shi, X & Jiang, G 2017, 'New U-Pb age constraints on the upper Banxi Group and
1468 synchrony of the Sturtian glaciation in South China', *Geoscience Frontiers*, vol. 8, no. 5, pp. 1161-
1469 1173. doi:10.1016/j.gsf.2016.11.012.
- 1470 Sprigg, RC 1952, 'Sedimentation in the Adelaide Geosyncline and the formation of the continental terrace', in
1471 MF Glaessner & RC Sprigg (eds), *Sir Douglas Mawson Anniversary Volume*, The University of Adelaide,
1472 South Australia, pp. 153-159.
- 1473 Środoń, J, Gerdes, A, Kramers, J & Bojanowski, MJ 2022, 'Age constraints of the Sturtian glaciation on
1474 western Baltica based on U-Pb and Ar-Ar dating of the Lapichi Svita', *Precambrian Research*, vol. 371.
1475 doi:10.1016/j.precamres.2022.106595.
- 1476 Stevens, BPJ, Page, RW & Crooks†, A 2008, 'Geochronology of Willyama Supergroup metavolcanics,
1477 metasediments and contemporaneous intrusions, Broken Hill, Australia', *Australian Journal of Earth*
1478 *Sciences*, vol. 55, no. 3, pp. 301-330. doi:10.1080/08120090701769456.
- 1479 Strauss, JV, Rooney, AD, Macdonald, FA, Brandon, AD & Knoll, AH 2014, '740 Ma vase-shaped microfossils
1480 from Yukon, Canada: Implications for Neoproterozoic chronology and biostratigraphy', *Geology*, vol.
1481 42, no. 8, pp. 659-662. doi:10.1130/G35736.1.
- 1482 Subarkah, D, Blades, ML, Collins, AS, Farkaš, J, Gilbert, S, Löhr, SC, Redaa, A, Cassidy, E & Zack, T 2021,
1483 'Unraveling the histories of Proterozoic shales through in situ Rb-Sr dating and trace element laser
1484 ablation analysis', *Geology*. doi:10.1130/G49187.1.
- 1485 Subarkah, D, Nixon, AL, Jimenez, M, Collins, AS, Blades, ML, Farkaš, J, Gilbert, SE, Holford, S & Jarrett, A
1486 2022, 'Constraining the geothermal parameters of in situ Rb–Sr dating on Proterozoic shales and
1487 their subsequent applications', *Geochronology*, vol. 4, no. 2, pp. 577-600. doi:10.5194/gchron-4-
1488 577-2022.
- 1489 Swain, G, Woodhouse, A, Hand, M, Barovich, K, Schwarz, M & Fanning, CM 2005, 'Provenance and tectonic
1490 development of the late Archaean Gawler Craton, Australia; U–Pb zircon, geochemical and Sm–Nd
1491 isotopic implications', *Precambrian Research*, vol. 141, no. 3, pp. 106-136.
1492 doi:10.1016/j.precamres.2005.08.004.
- 1493 Thomson, BP, Coats, RP, Mirams, RC, Forbes, BG, Dalgarno, CR & Johnson, JE 1964, 'Precambrian Rock
1494 Groups in the Adelaide Geosyncline: A new subdivision', *Quarterly Geological Notes*, vol. 9, pp. 1-20.
- 1495 Tostevin, R & Mills, BJW 2020, 'Reconciling proxy records and models of Earth's oxygenation during the
1496 Neoproterozoic and Palaeozoic', *Interface Focus*, vol. 10, no. 4, p. 20190137.
1497 doi:10.1098/rsfs.2019.0137.
- 1498 van der Wolff, EJ 2020, 'Detrital Provenance and Geochronology of the Burra, Umberatana and Wilpena
1499 Groups in the Mount Lofty Ranges', Department of Earth Sciences, Honours Thesis, Bachelor of
1500 Science (Honours), University of Adelaide, Adelaide, South Australia.
- 1501 Verdel, C, Campbell, MJ & Allen, CM 2021, 'Detrital zircon petrochronology of central Australia, and
1502 implications for the secular record of zircon trace element composition', *Geosphere*.
1503 doi:10.1130/ges02300.1.

- 1504 Vermeesch, P 2018, 'IsoplotR: a free and open toolbox for geochronology', *Geoscience Frontiers*, vol. 9, no. 5.
1505 doi:10.1016/j.gsf.2018.04.001.
- 1506 Vermeesch, P, Resentini, A & Garzanti, E 2016, 'An R package for statistical provenance analysis',
1507 *Sedimentary Geology*, vol. 336, pp. 14-25. doi:10.1016/j.sedgeo.2016.01.009.
- 1508 Villa, IM, De Bièvre, P, Holden, NE & Renne, PR 2015, 'IUPAC-IUGS recommendation on the half life of ⁸⁷Rb',
1509 *Geochimica et Cosmochimica Acta*, vol. 164, pp. 382-385. doi:10.1016/j.gca.2015.05.025.
- 1510 Virgo, GM, Collins, AS, Amos, KJ, Farkaš, J, Blades, ML & Subarkah, D 2021, 'Descending into the “snowball”:
1511 High resolution sedimentological and geochemical analysis across the Tonian to Cryogenian
1512 boundary in South Australia', *Precambrian Research*, vol. 367.
1513 doi:10.1016/j.precamres.2021.106449.
- 1514 Wade, BP, Kelsey, DE, Hand, M & Barovich, KM 2008, 'The Musgrave Province: Stitching north, west and
1515 south Australia', *Precambrian Research*, vol. 166, no. 1, pp. 370-386.
1516 doi:10.1016/j.precamres.2007.05.007.
- 1517 Wade, CE 2011, 'Definition of the Mesoproterozoic Ninnerie Supersuite, Curnamona Province, South
1518 Australia', *MESA Journal*, vol. 62, pp. 25-42.
- 1519 Wallace, MW, Hood, Av, Shuster, A, Greig, A, Planavsky, NJ & Reed, CP 2017, 'Oxygenation history of the
1520 Neoproterozoic to early Phanerozoic and the rise of land plants', *Earth and Planetary Science Letters*,
1521 vol. 466, pp. 12-19. doi:10.1016/j.epsl.2017.02.046.
- 1522 Wallace, MW, Hood, AvS, Woon, EMS, Giddings, JA & Fromhold, TA 2015, 'The Cryogenian Balcanoona reef
1523 complexes of the Northern Flinders Ranges: Implications for Neoproterozoic ocean chemistry',
1524 *Palaeogeography, Palaeoclimatology, Palaeoecology*, vol. 417, pp. 320-336.
1525 doi:10.1016/j.palaeo.2014.09.028.
- 1526 Wang, D, Zhu, X-K, Zhao, N, Yan, B, Li, X-H, Shi, F & Zhang, F 2019, 'Timing of the termination of Sturtian
1527 glaciation: SIMS U-Pb zircon dating from South China', *Journal of Asian Earth Sciences*, vol. 177, pp.
1528 287-294. doi:10.1016/j.jseaes.2019.03.015.
- 1529 Webb, AW 1980, *Geochronology of stratigraphically significant rocks from South Australia. Progress Report*
1530 *No. 30*, no. Env 01689, Amdel Ltd, South Australia,
1531 <[https://sarigbasis.pir.sa.gov.au/WebtopEw/ws/samref/sarig1/wcir/Record?r=0&m=1&w=catno=20](https://sarigbasis.pir.sa.gov.au/WebtopEw/ws/samref/sarig1/wcir/Record?r=0&m=1&w=catno=2021979)
1532 [21979](https://sarigbasis.pir.sa.gov.au/WebtopEw/ws/samref/sarig1/wcir/Record?r=0&m=1&w=catno=2021979)>.
- 1533 Webb, AW, Coats, RP, Fanning, CM & Flint, RB 1983, 'Geochronological Framework of the Adelaide
1534 Geosyncline', in *Adelaide Geosyncline Sedimentary Environments and Tectonics Settings Symposium*,
1535 Geological Society of Australia, Sydney, New South Wales, pp. 7-9.
- 1536 Wiedenbeck, M, Allé, P, Corfu, F, Griffin, WL, Meier, M, Oberli, F, Quadt, AV, Roddick, JC & Spiegel, W 1995,
1537 'Three Natural Zircon Standards for U-Th-Pb, Lu-Hf, Trace Element and REE Analyses', *Geostandards*
1538 *Newsletter*, vol. 19, no. 1, pp. 1-23. doi:10.1111/j.1751-908X.1995.tb00147.x.
- 1539 Wiedenbeck, M, Hanchar, JM, Peck, WH, Sylvester, P, Valley, J, Whitehouse, M, Kronz, A, Morishita, Y,
1540 Nasdala, L, Fiebig, J, Franchi, I, Girard, JP, Greenwood, RC, Hinton, R, Kita, N, Mason, PRD, Norman,
1541 M, Ogasawara, M, Piccoli, PM, Rhede, D, Satoh, H, Schulz-Dobrick, B, Skår, O, Spicuzza, MJ, Terada,
1542 K, Tindle, A, Togashi, S, Vennemann, T, Xie, Q & Zheng, YF 2004, 'Further Characterisation of the
1543 91500 Zircon Crystal', *Geostandards and Geoanalytical Research*, vol. 28, no. 1, pp. 9-39.
1544 doi:10.1111/j.1751-908X.2004.tb01041.x.
- 1545 Williams, GE & Gostin, VA 2019, 'Late Cryogenian glaciation in South Australia: Fluctuating ice margin and no
1546 extreme or rapid post-glacial sea-level rise', *Geoscience Frontiers*. doi:10.1016/j.gsf.2019.02.002.

- 1547 Wu, L, Guan, S, Ren, R, Zhang, C & Feng, X 2019, 'Neoproterozoic glaciations and rift evolution in the
1548 northwest Tarim Craton, China: new constraints from geochronological, geochemical, and
1549 geophysical data', *International Geology Review*, pp. 1-20. doi:10.1080/00206814.2019.1700399.
- 1550 Wysoczanski, RJ & Allibone, AH 2004, 'Age, Correlation, and Provenance of the Neoproterozoic Skelton
1551 Group, Antarctica: Grenville Age Detritus on the Margin of East Antarctica', *Journal of Geology*, vol.
1552 112, no. 4, pp. 401-416. doi:10.1086/421071.
- 1553 Xiao, W, Cao, J, Luo, B, He, Y, Zhou, G, Zuo, Z, Xiao, D & Hu, K 2020, 'Marinoan glacial aftermath in South
1554 China: Paleo-environmental evolution and organic carbon accumulation in the Doushantuo shales',
1555 *Chemical Geology*, vol. 555, p. 119838. doi:10.1016/j.chemgeo.2020.119838.
- 1556 Xu, B, Xiao, S, Zou, H, Chen, Y, Li, Z-X, Song, B, Liu, D, Zhou, C & Yuan, X 2009, 'SHRIMP zircon U–Pb age
1557 constraints on Neoproterozoic Quruqtagh diamictites in NW China', *Precambrian Research*, vol. 168,
1558 no. 3, pp. 247-258. doi:10.1016/j.precamres.2008.10.008.
- 1559 Young, GM & Gostin, VA 1989a, 'Depositional environment and regional stratigraphic significance of the Serle
1560 Conglomerate: A Late Proterozoic submarine fan complex, South Australia', *Palaeogeography,
1561 Palaeoclimatology, Palaeoecology*, vol. 71, no. 3, pp. 237-252. doi:10.1016/0031-0182(89)90052-
1562 7.
- 1563 Young, GM & Gostin, VA 1989b, 'An exceptionally thick upper Proterozoic (Sturtian) glacial succession in the
1564 Mount Painter area, South Australia', *Geological Society of America Bulletin*, vol. 101, no. 6, pp. 834-
1565 845. doi:10.1130/0016-7606(1989)101<0834:Aetups>2.3.Co;2.
- 1566 Young, GM & Gostin, VA 1991, 'Late Proterozoic (Sturtian) succession of the North Flinders Basin, South
1567 Australia; An example of temperate glaciation in an active rift setting', in JB Anderson & GM Ashley
1568 (eds), *Glacial marine sedimentation; Paleoclimatic significance*, vol. 261, Geological Society of
1569 America, pp. 207–222.
- 1570 Zaitseva, TS, Kuznetsov, AB, Gorozhanin, VM, Gorokhov, IM, Ivanovskaya, TA & Konstantinova, GV 2019, 'The
1571 Lower Boundary of the Vendian in the Southern Urals as Evidenced by the Rb–Sr Age of Glauconites
1572 of the Bakeevo Formation', *Stratigraphy and Geological Correlation*, vol. 27, no. 5, pp. 573-587.
1573 doi:10.1134/s0869593819050083.
- 1574 Zhang, Q-R, Chu, X-L & Feng, L-J 2011, 'Neoproterozoic glacial records in the Yangtze Region, China', in E
1575 Arnaud, GP Halverson & GA Shields-Zhou (eds), *The Geological Record of Neoproterozoic Glaciations*,
1576 Geological Society, London, pp. 357-366.
- 1577 Zhang, Q-R, Li, X-H, Feng, L-J, Huang, J & Song, B 2008, 'A New Age Constraint on the Onset of the
1578 Neoproterozoic Glaciations in the Yangtze Platform, South China', *The Journal of Geology*, vol. 116,
1579 no. 4, pp. 423-429. doi:10.1086/589312.
- 1580 Zhang, S, Jiang, G, Zhang, J, Song, B, Kennedy, MJ & Christie-Blick, N 2005, 'U-Pb sensitive high-resolution
1581 ion microprobe ages from the Doushantuo Formation in south China: Constraints on late
1582 Neoproterozoic glaciations', *Geology*, vol. 33, no. 6. doi:10.1130/g21418.1.
- 1583 Zhou, C-M, Huyskens, MH, Xiao, S & Yin, Q-Z 2020, 'Refining the termination age of the Cryogenian Sturtian
1584 glaciation in South China', *Palaeoworld*, vol. 29, no. 3, pp. 462-468.
1585 doi:10.1016/j.palwor.2020.04.002.
- 1586 Zhou, C, Huyskens, MH, Lang, X, Xiao, S & Yin, Q-Z 2019, 'Calibrating the terminations of Cryogenian global
1587 glaciations', *Geology*, vol. 47, no. 3, pp. 251-254. doi:10.1130/g45719.1.
- 1588 Zhou, C, Tucker, R, Xiao, S, Peng, Z, Yuan, X & Chen, Z 2004, 'New constraints on the ages of Neoproterozoic
1589 glaciations in south China', *Geology*, vol. 32, no. 5, pp. 437-440. doi:10.1130/G20286.1.

1590 Zhu, M & Wang, H 2011, 'Neoproterozoic glaciogenic diamictites of the Tarim Block, NW China', in E Arnaud,
1591 GP Halverson & GA Shields-Zhou (eds), *The Geological Record of Neoproterozoic Glaciations*,
1592 Geological Society, London, pp. 367-378.

Appendix 1—DEFINITION CARD

NAME OF UNIT ¹ : Sturt Formation	STATE(S) ¹ : South Australia
STATUS OF UNIT : Redefinition	RANK : Formation
PROPOSER : Jarred C. Lloyd, Wolfgang V. Preiss, Georgina M. Virgo	DATE : 2022-03-31
RESERVED IN STRATIGRAPHIC UNITS DATABASE : YES	
PROPOSED PUBLICATION : Lloyd, JC, Preiss, WV, Collins, AS, Virgo, GM, Blades, ML & Amos, KJ [submitted to Geological Magazine], 'Geochronology and formal stratigraphy of the Sturtian Glaciation in the Adelaide Superbasin', (EarthArXiv preprint doi:10.31223/X50G9N)	

DERIVATION OF NAME ¹ : Sturt River/Warriparri, South Australia
<p>SYNONYMY, UNIT NAME HISTORY (if any) ¹:</p> <p>Sturt Tillite, Appila Tillite, Pualco Tillite, Merinjina Tillite, Bolla Bollana Tillite, Calthorinna Tillite, Hansborough Tillite (abandoned)</p> <p>Originally named the Sturtian Tillite (Howchin, 1920)</p>
CONSTITUENT UNITS ³ : Braemar ironstone facies (informal lithofacies)
PARENT UNIT : Yudnamutana Subgroup
<p>TYPE LOCALITY (including Lat. & Long.) ²:</p> <p>CRS for all coordinates is EPSG:7844 (GDA2020); estimations use historical data and modern remote sensing imagery and GIS data to provide locations that are as accurate as possible.</p> <p>Primary type: SW of Mount Harris, through MacDonnell Creek – base: 139.357, -30.095, top: 139.34021, -30.07363 (GDA2020)</p> <p>Reference sections:</p> <ul style="list-style-type: none"> • Sturt Gorge Recreation Park — base: 138.59633, -35.03398, top: 138.57289, -35.03947 (GDA2020, composite section, estimated from georeferenced map of Link 1977 and current boundaries shown on 100K surface) • Appila Gorge — base: 138.48247, -33.00312, top: 138.48458, -33.00341 (GDA2020, estimated based on section map from Segnit 1939) • Pualco Hill — base: 139.64033, -32.97827, top: 139.60483, -32.95732 (GDA2020, composite section, estimated location from map and detail in QGN 60) • NW of Copley — base: 138.38933, -30.56145, top: 138.39032, -30.5592 (GDA2020) • Termination Hill — base: 138.01746, -30.21562, top: 138.01387, -30.21756 (GDA2020) • Yankaninna Station — base: 138.94295, -30.28636, top: 138.9431, -30.28593, (GDA2020, northern section); base: 138.99635, -30.36184, top: 138.9976, -30.36354 (GDA2020, southern section) • Davenport and Denison Ranges — base: 135.94206, -28.68947, top: 135.93648, -28.70065 (GDA2020, estimated from Ambrose et al. 1981) • Tillite Gorge, Arkaroola – base: 139.43277, -30.33123, top: 139.40406, -30.34282 (GDA2020)
CONFIDENTIAL TYPE LOCALITY? : No
<p>DESCRIPTION AT TYPE LOCALITY ²:</p> <p>The Sturt Formation is comprised of (boulder) diamictites showing evidence for glaciogenic origin, and numerous subsidiary lithologies including poorly sorted sandstones/conglomerates through to finely laminated shales containing a wide variety of limestones and dropstones.</p>

LITHOLOGY ²:

The lithology of the Sturt Formation at its type section defined here is further detailed in Belperio (1973) and Young & Gostin (1989). It is subdivided into four generalised lithofacies:

Lithofacies 1: Very poorly sorted conglomerates with sandy matrix to diamictites with muddy, silty and even very fine sandy matrix. Clasts ranging up to boulder size (largest observed: 1 m); minor interbeds of laminated siltstone. A higher concentration of larger clasts is present in the lower sections.

Lithofacies 2: Interbedded, well laminated shales and sandy micaceous siltstones. Minor pebbly lenses and silty arenites, cross-bedding present, and ripple marked.

Lithofacies 3: Crudely stratified diamictite (lithic wacke, muddy to silty matrix) with clasts ranging up to boulder size (max. observed: 90 cm). Minor interbeds of calcareous shale, and thick interbeds of massive diamictite.

Lithofacies 4: Similar to unit 3, however has a higher mud content in matrix and is mostly massive diamictite. Greater number and size of clasts, ranging up to 1.25 m (observed).

THICKNESS ²: ~1,470 m at primary type section

FOSSILS: N/A

DIASTEMS OR HIATUSES (if relevant): N/A

RELATIONSHIPS & BOUNDARY CRITERIA ²:

Most commonly overlies Burra Group, less commonly Callanna Group or pre-Neoproterozoic basement. Conformably overlain by Holowilena Ironstone, Benda Siltstone, Wilyerpa Formation, and Lyndhurst Formation. Disconformably overlain by Tapley Hill Formation where Wilyerpa Formation is absent, e.g. Sturt Gorge.

DISTINGUISHING OR IDENTIFYING FEATURES ¹:

Poorly sorted, massive diamictite with clasts ranging up to extremely large boulders. These significantly differ lithologically from the over- and underlying strata. Evidence for glaciogenic origin (dropstones in laminated rocks [lonestones that warp and/or puncture the underlying laminae]; glacial striae and scouring of underlying rock; presence of polished, faceted, striated and grooved clasts) can often be found in outcrop; one glaciated pavement near Merinjina Well.

AGE & EVIDENCE ²:

Minimum: 663.03 ± 0.76 Ma (Tuff near base of overlying Wilyerpa Formation, Cox et al. 2018)

Detrital zircon max depositional age (upper Sturt Formation):

- 667 ± 6 Ma (Pichi Richi Pass, Keeman et al. 2020; data reinterpreted in Lloyd et al. 2020)
- 666 ± 25 Ma (Copley, Lloyd et al. 2022a [pre-print])
- 673 ± 19 Ma (Willouran Ranges, Lloyd et al. 2020)

Maximum age: constrained to younger than 731 ± 34 Ma by detrital zircon in the underlying Gilbert Range Quartzite (Keeman et al. 2020; data reinterpreted in Lloyd et al. 2020) and corroborated by detrital zircon in the Mitcham Quartzite, 734 ± 42 Ma (Lloyd et al. 2022b [pre-print]).

CORRELATION WITH OTHER UNITS ²:

Stratigraphic correlative of the Chambers Bluff Tillite (Officer Basin), Areyonga Formation (Amadeus Basin), Naburula Formation (Ngalia Basin), Yardida Tillite (Georgina Basin), and lower units of the Yancowinna Subgroup (NSW). Potential correlatives in Tasmania are the Julius River Member, Red Rock Member, Cotcase Creek Formation, and middle Port Sorrel Formation. Parts of the Benda Siltstone and Holowilena Ironstone may be correlative of the upper part of the Sturt Formation.

REGIONAL ASPECTS/GENERAL GEOLOGICAL DESCRIPTION:

General lithologic sequence common throughout the basin in complete, or near complete successions of the Sturt Formation is:

- poorly sorted, gravel to boulder conglomerate (diamictite in some areas) with generally sandy matrix; scoured bases are common in areas where the Fitton Formation is not present
- Interbedded fine laminated siltstones and shales to cross-bedded sandstones with few lonestones/dropstones
- boulder diamictite (both massive and stratified)

Regionally, the size, composition, and percentage of clasts in the diamictite lithologies varies. Mega-clasts, ranging up to 1.25 km have been described in the MacDonald corridor north of Olary (Conor & Preiss, 2019).

Arkosic, poorly sorted immature sandstones, and cross-bedded sandstones are predominant in some areas. Iron-rich sections are present in the Sturt Formation underlying the Benda Siltstone and Holowilena Ironstone in the Nackara Arc/South Flinders Ranges.

EXTENT:

Deposited across the entire Adelaide Rift Complex within the Adelaide Superbasin; local areas of non-deposition or subsequent erosion. Deposition on the Stuart Shelf appears to be limited to the eastern most areas and deposition on the Coombalarnie Platform is not known.

GEOMORPHIC EXPRESSION:

THICKNESS VARIATIONS: Thickness varies greatly because of palaeotopography, palaeotectonic activity, and erosion.

Minimum: 9 m, ~2.5 km to the NW of Tower Hill (Mount Lyndhurst station)

Maximum: 3,300 m at Pualco Hill.

STRUCTURE AND METAMORPHISM: Ranging from undeformed to strongly sheared. Locally metamorphosed up to amphibolite grade.

ALTERATION AND MINERALISATION: Iron rich facies present in the Nackara Arc; Talc, Au, Cu, Pb mineralised zones have also been found.

GEOPHYSICAL EXPRESSION:

Iron rich facies show strong anomaly on TMI where the original hematite (as in the Holowilena Ironstone) has been metamorphosed to magnetite (as in Braemar ironstone facies of the Benda Siltstone and the Pualco Range outcrops of the Sturt Formation).

Surface exposure can be readily identified using false colour remote sensing imagery, for LANDSAT 8 specifically using channels 7-5-2 and 5-6-7 for R-G-B.

GEOCHEMISTRY:

GENESIS/DEPOSITIONAL ENVIRONMENT:

Deposited under general glaciogenic conditions: dropstones, lonestones, glacial striae, mega-clasts. Exact environment is dependent on location but encompasses the full range of sub-glacial to pro-glacial terrestrial and glacio-marine sedimentary environments. Mostly massive but contains lithologies showing planar stratification, cross stratification, reverse graded bedding, scour structures, and ripple laminations. The cast of a glaciated pavement is preserved near Merinjina Well where the Sturt Formation disconformably overlies the Wooltana Volcanics.

COMMENTS:

The "Tillite" portion of the name has been dropped in favour for "Formation" in contrast to the reasoning outlined in Coats & Preiss (1987). This change is done to better reflect the diversity in lithologies present throughout the Sturt Formation. The most prominent of these are the diamictites, many of which are shown to be true tillites, however the formation varies from sub-glacial to grounded ice-margin and glacio-marine facies.

The exact (chrono)stratigraphic relationship of the Holowilena Ironstone and Benda Siltstone to the entirety of the Sturt Formation is uncertain. They may be upper members of the Sturt Formation, or an intervening sequence between the Sturt and Wilyerpa formations.

REFERENCES (if any) ¹: **This is not exhaustive, as many are already in ASUD. These are the key resources for this definition card.**

- Ambrose, GJ, Flint, RB & Webb, AW 1981, 'Precambrian and Palaeozoic Geology of the Peake and Denison Ranges', *Bulletin* (50), Geological Survey of South Australia
- Belperio, AP 1973, 'The stratigraphy and facies of the Late Precambrian Lower Glacial sequence, Mt Painter, South Australia', Department of Geology, Honours Thesis, Bachelor of Science (Honours), University of Adelaide, Adelaide, South Australia, <https://hdl.handle.net/2440/131123>
- Coats RP & Preiss WV 1987, 'Stratigraphy of the Umberatana Group', IN: WV Preiss (compiler), 'The Adelaide Geosyncline – Later Proterozoic Stratigraphy, Sedimentation, Palaeontology and Tectonics', *Bulletin* (53), pp. 125–210, Geological Survey of South Australia
- Conor, CHH & Preiss, WV 2019, 'Cryogenian glaciomarine megaclasts of the MacDonald Corridor, Bimbowrie Conservation Park, Olary Region, South Australia', *Australian Journal of Earth Sciences*, vol. 67 (6), pp. 857-872. doi:10.1080/08120099.2018.1553206
- Cox, GM, Isakson, V, Hoffman, PF, Gernon, TM, Schmitz, MD, Shahin, S, Collins, AS, Preiss, WV, Blades, ML, Mitchell, RN & Nordsvan, A 2018, 'South Australian U-Pb zircon (CA-ID-TIMS) age supports globally synchronous Sturtian deglaciation', *Precambrian Research*, vol. 315, pp. 257-263. doi:10.1016/j.precamres.2018.07.007
- Forbes, BG & Cooper RS 1976, 'The Pualco Tillite of the Olary Region, South Australia', *Quarterly Geological Notes*, vol. 60, pp. 2–5, Geological Survey of South Australia
- Howchin, W 1920, 'Past Glacial Action in Australia', IN: Year Book (13), Australian Bureau of Statistics, Australia, pp. 1133-1146
- Keeman, J, Turner, S, Haines, PW, Belousova, E, Ireland, T, Brouwer, P, Foden, J & Wörner, G 2020, 'New UPb, Hf and O isotope constraints on the provenance of sediments from the Adelaide Rift Complex – Documenting the key Neoproterozoic to early Cambrian succession', *Gondwana Research*, vol. 83, pp. 248-278. doi:10.1016/j.j.gr.2020.02.005
- Link, PK 1977, 'Facies and palaeogeography of Late Precambrian Sturtian glacial sediments, Copley area, northern Flinders Ranges and in the Sturt Gorge near Adelaide, South Australia', Honours Thesis, University of Adelaide, <https://hdl.handle.net/2440/131122>
- Lloyd, JC, Blades, ML, Counts, JW, Collins, AS, Amos, KJ, Wade, BP, Hall, JW, Hore, S, Ball, AL, Shahin, S & Drabsch, M 2020, 'Neoproterozoic geochronology and provenance of the Adelaide Superbasin', *Precambrian Research*, vol. 350, p. 105849. doi:10.1016/j.precamres.2020.105849.
- [Pre-print] Lloyd, JC, Preiss WV, Collins, AS, Virgo, GM, Blades, ML, Gilbert, SE & Amos, KJ 2022a, 'Geochronology and formal stratigraphy of the Sturtian Glaciation in the Adelaide Superbasin', *EarthArXiv*, doi:10.31223/X50G9N
- [Pre-print] Lloyd, JC, Collins, AS, Blades, ML, Gilbert, SE & Amos, KJ 2022b, 'Late Tonian development of the Adelaide Superbasin', *EarthArXiv*, doi:10.31223/X5N63H
- Segnit, RW 1939, 'The Precambrian-Cambrian succession — The general and economic geology of these systems, in portions of South Australia', *Bulletin* (18), Geological Survey of South Australia

Young, GM & Gostin, VA 1989, 'An exceptionally thick upper Proterozoic (Sturtian) glacial succession in the Mount Painter area, South Australia', *Geological Society of America Bulletin*, vol. 101 (6), ppp. 834-845.
doi:10.1130/0016-7606(1989)101<0834:Aetups>2.3.Co;2

(for subcommittee use only)

Definition approved by:

Mario Werner

SA Stratigraphy Subcommission

(delete where inapplicable)

Date: 31/03/2022

(for registry use only)

Name first published by:

Definition by:

